UC San Diego

UC San Diego Electronic Theses and Dissertations

Title

Dissecting centromeric DNA-microtubule interactions In vitro uncovers a mechanism that ensures proper connection of chromosomes to the mitotic spindle

Permalink

https://escholarship.org/uc/item/22x96121

Author

Sandall, Sharsti L.

Publication Date

2008

Peer reviewed|Thesis/dissertation

eScholarship.org Powered by the California Digital Library
University of California

UNIVERSITY OF CALIFORNIA, SAN DIEGO

Dissecting Centromeric DNA-Microtubule Interactions *In Vitro* Uncovers a Mechanism that Ensures Proper Connection of Chromosomes to the Mitotic Spindle

A dissertation submitted in partial satisfaction of the

requirements for the degree Doctor of Philosophy

in

Biomedical Sciences

by

Sharsti L. Sandall

Committee in charge:

Professor Arshad Desai, Chair
Professor Don W. Cleveland
Professor Randy Hampton
Professor Richard Kolodner
Professor Karen Oegema

2008

Copyright

Sharsti L. Sandall, 2008

All rights reserved.

The dissertation of Sharsti L. Sandall is approved, and it is acceptable in quality and form for publication of microfilm and electronically:

_____

_____

_____

_____

_____

Chair

University of California, San Diego

2008

Table of Contents

SIGNATURE PAGE..... iii

TABLE OF CONTENTS..... iv

LIST OF FIGURES..... viii

LIST OF TABLES..... x

ACKNOWLEDGEMENTS..... xi

VITA..... xiii

ABSTRACT OF THE DISSERTATION..... xiv

CHAPTER 1: INTRODUCTION 1

1.1 CHROMOSOME SEGREGATION AND THE KINETOCHORE 1

1.1.1 Overview of kinetochores 2

1.1.1.1 The budding yeast kinetochore 3

1.1.2 Formation of kinetochores on centromeric DNA 4

1.1.2.1 Specification of centromeres 5

1.1.2.2 Budding yeast centromeres 6

1.1.2.3 The CBF3 complex 9

1.1.3 Microtubule binding components of the kinetochore 11

1.1.4 Kinetochore capture by microtubules 15

1.1.4.1 Initial lateral attachment 15

1.1.4.2 Switch to end on attachments: Biorientation 16

1.1.4.3 Coupling attachments to microtubule dynamics 18

1.1.4.4 Mechanisms that promote biorientation: geometry and tension 19

1.1.5 Mechanisms to Ensure Proper Segregation 21

1.1.5.1 The spindle checkpoint 22

1.1.5.2 Regulation of microtubule attachments 23

1.2 THE CHROMOSOMAL PASSENGER COMPLEX 24

1.2.1 Components of the CPC *25*

1.2.2 The budding yeast CPC *26*

1.2.3 Functions of the CPC *27*

1.2.3.1 Regulation of chromosome and spindle dynamics 27

1.2.3.2 Regulation of chromosome microtubule interactions 29

1.2.3.3 Role in cytokinesis 31

1.2.4 Localization to centromeres *33*

1.2.5 Localization to the spindle midzone in anaphase/cytokinesis *35*

1.2.6 Activation of Aurora B kinase/Ipl1 ..... *36*

1.2.7 The INCENP family of proteins *37*

1.2.7.1 Previously characterized Sli15 domains 38

1.2.7.2 Conserved microtubule binding activity 39

1.3 CHROMOSOME SEGREGATION ERRORS 40

1.3.1 Aneuploidy and its link to cancer and birth defects *40*

1.3.2 The CPC and its relationship to cancer *40*

CHAPTER 2: A BIR1-SLI15 COMPLEX CONNECTS CENTROMERES TO MICROTUBULES AND IS REQUIRED TO SENSE KINETOCHORE TENSION 42

2.1 SUMMARY 42

2.2 INTRODUCTION 43

2.3 RESULTS 45

2.3.1 A Quantitative In Vitro Assay for the Interaction of CBF3-Bound CEN DNA with Microtubules *45*

2.3.2 A Conventional Purification Strategy Identifies Bir1 as a Candidate for the Activity that Links CBF3-Bound CEN DNA to Microtubules *46*

2.3.3 Bir1 Is an Essential Component of the CBF3-Complementing Activity *48*

2.3.4 Sli15 and Bir1, but Not Ipl1, Are Required for the CBF3-Complementing Activity . *49*

2.3.5 A Purified Endogenous Bir1-Sli15 Complex Complements CBF3 and bir1Δ Extracts *51*

2.3.6 Shutting Off Sli15 or Deleting Its Microtubule-Binding Domain Eliminates the Linkage between CEN DNA and Microtubules In Vitro *53*

2.3.7 Both the Sli15 Shutoff and the Sli15 Microtubule-Binding Domain Deletion Mutant Phenocopy Ipl1 Kinase Activation Mutants In Vivo *55*

2.4 DISCUSSION 57

2.4.1 A Complex of Bir1-Sli15 Links CBF3-CEN DNA to Microtubules In Vitro *57*

2.4.2 Ipl1 Kinase Regulates, but Is Not Required for, the CEN DNA-Microtubule Linkage In Vitro *58*

2.4.3 In Vivo Function of the Bir1-Sli15-Mediated Linkage Between CBF3-Bound CEN DNA and Microtubules *59*

2.4.4 A Speculative Model for Tension-Regulated Ipl1 Activation by Bir1-Sli15 ..... *60*

2.4.5 Significance to Metazoan Chromosome Segregation *62*

2.5 METHODS 63

2.5.1 Strains and Extract Preparation *63*

2.5.2 Partial Purification of CBF3 ..... *63*

2.5.3 In Vitro CEN DNA-Microtubule Interaction Assay *64*

2.5.4 Enrichment of the CBF3-Complementing Activity and Mass Spectrometry *65*

2.5.5 HA Immunodepletions, TAP Purifications, and Antibody Production *66*

2.6 ACKNOWLEDGMENTS 66

CHAPTER 3: MOLECULAR CHARACTERIZATION OF THE BIR1-SLI15 CONNECTION BETWEEN CEN-DNA AND MICROTUBULES 88

3.1 INTRODUCTION 88

3.2 RESULTS 91

3.2.1 A region of 290 amino acids contributes to the microtubule binding activity of Sli15 91

3.2.1.1 Microtubule binding and bundling activity of Sli15 fragments 92

3.2.1.2 Localization of Sli15 microtubule binding domain to centromeres and the mitotic spindle 95

3.2.2 Eliminating any portion of Sli15 from amino acids 227-559 results in cell death.... 96

3.2.3 Ipl1 prevents the Bir1-Sli15 mediated link between CEN-DNA and microtubules from forming, but has less effect on the linkage after initial formation..... 97

3.2.4 Ipl1 weakens the interaction between CEN-DNA, CBF3 complex, Bir1-Sli15, and microtubules 99

3.2.4.1 ATP addition makes Bir1-Sli15 mediated CEN-DNA microtubule attachments weaker 100

3.2.4.2 Mutant extracts of Sli15 and Ipl1 that lack Ipl1 activity have similar rupture forces with and without ATP 102

3.3 DISCUSSION 102

3.3.1 Over one-third of Sli15 can bind microtubules and is essential for viability 102

3.3.2 A 42 amino acid fragment that links the microtubule binding region to the conserved IN box is essential for Sli15 function 105

3.3.3 Ipl1 controls the Bir1-Sli15 mediated connection between CEN-DNA and microtubules at multiple levels 106

3.3.4 Using the optical trap and flow to test how tension affects Ipl1 activity..... 108

3.4 METHODS 109

3.4.1 Strains, plasmids & protein purification 109

3.4.2 Microtubule co-sedimentation assays..... 111

3.4.3 Microscopy and CEN-DNA Optical Trap Assays 112

3.5 ACKNOWLEDGEMENTS 113

CHAPTER 4: CONCLUSIONS AND FUTURE DIRECTIONS 123

4.1 CONCLUSIONS 123

4.2 FUTURE DIRECTIONS 126

REFERENCES 130

List of Figures

FIGURE 2.1 A QUANTITATIVE IN VITRO ASSAY FOR THE BINDING OF BUDDING YEAST CEN DNA TO MICROTUBULES 68

FIGURE 2.2 CONVENTIONAL PURIFICATION OF AN ACTIVITY THAT COMPLEMENTS CBF3 IN THE IN VITRO ASSAY 69

FIGURE 2.3 (A-C) BIR1 IS REQUIRED FOR LINKING CEN DNA TO MICROTUBULES IN VITRO 70

FIGURE 2.3 (D,E) BIR1 IS REQUIRED FOR LINKING CEN DNA TO MICROTUBULES IN VITRO 71

FIGURE 2.4 SLI15, BUT NOT IPL1, IS REQUIRED FOR THE COMPLEMENTING ACTIVITY 72

FIGURE 2.5 (A-D) SLI15 MUTANTS THAT ELIMINATE CEN DNA-MICROTUBULE INTERACTIONS IN VITRO PHENOCOPY IPL1 KINASE ACTIVATION MUTANTS IN VIVO 73

FIGURE 2.5 (E-G) SLI15 MUTANTS THAT ELIMINATE CEN DNA-MICROTUBULE INTERACTIONS IN VITRO PHENOCOPY IPL1 KINASE ACTIVATION MUTANTS IN VIVO 74

FIGURE 2.6 A MODEL FOR TENSION-REGULATED IPL1 ACTIVATION BY THE BIR1-SLI15-MEDIATED LINKAGE BETWEEN CENTROMERES AND MICROTUBULES 75

FIGURE S2.1 THE CBF3 COMPLEMENTING ACTIVITY IS SENSITIVE TO PROTEASE TREATMENT. 76

FIGURE S2.2 THE BIR1-SLI15 MEDIATED IN VITRO LINKAGE BETWEEN CEN DNA AND SPINDLE MICROTUBULES DOES NOT SPECIFICALLY REFLECT ACTIVITY OF ANAPHASE DEPHOSPHORYLATED SLI15. 77

FIGURE S2.3 *SLI15-3* ENCODES A MUTANT PROTEIN SPECIFICALLY DEFECTIVE IN IPL1 ACTIVATION. 78

FIGURE S2.4 REPRESSING SLI15 EXPRESSION CAUSES RAPID LOSS OF CELL VIABILITY. 79

FIGURE S2.5 THE SLI15-MTBΔ MUTANT FAILS TO SUPPORT CELL VIABILITY BUT RETAINS THE ABILITY TO INTERACT WITH BIR1. 80

FIGURE 3.1 ALL SLI15-MTB GST FRAGMENTS, EXCEPT THE CONSERVED REGION FROM AMINO ACIDS 517-559, BIND MICROTUBULES WITH VARYING AFFINITY. 114

FIGURE 3.2 (A-C) ANALYSIS OF MICROTUBULE BINDING AND BUNDLING AFFINITY OF SLI15-MTB PROTEINS. 115

FIGURE 3.3 IN VIVO LOCALIZATION OF SLI15-MTB:GFP FRAGMENTS. 116

FIGURE 3.4 BIR1-SLI15 MEDIATED BINDING OF CEN-DNA AND MICROTUBULES IS INSENSITIVE TO IPL1/ATP REGULATION AFTER INITIAL BINDING, BUT ATTACHMENTS MADE IN THE PRESENCE OF ATP ARE WEAKER. 117

FIGURE S3.1 SLI15 CONSERVATION AMONG *SACCHAROMYCES* SPECIES. 118

FIGURE S3.2 GEL FILTRATION ANALYSIS OF SLI15 MICROTUBULE FRAGMENTS 119

List of Tables

TABLE 2.1 CANDIDATES TESTED IN THE IN VITRO CEN DNA-MICROTUBULE INTERACTION ASSAY USING MUTANTS / IMMUNODEPLETIONS 81

TABLE 2.2 COMPOSITION OF MONOS POOL 82

TABLE 2.3 COMPOSITION OF (PP)CBF3 84

TABLE 2.4 YEAST STRAINS USED IN THIS STUDY 85

TABLE 3.1 DISRUPTING ANY PORTION OF THE SLI15 MICROTUBULE BINDING DOMAIN RESULTS IN CELL LETHALITY 120

TABLE 3.2 PLASMIDS AND YEAST STRAINS USED IN THIS STUDY 121

Acknowledgements

I would first like to acknowledge my advisor, Arshad Desai, for providing me with the opportunity to be a part of the incredible intellectual environment of his lab where I have developed and matured as a scientist. I have learned so many lessons from Arshad that I will carry with me in all aspects of my scientific career, and yes, I can finally say that I am grateful for his “school of hard-knocks”. I feel privileged and lucky to have completed my doctoral dissertation in his lab.

I also want to acknowledge the tremendous support I received from all Desai & Oegema lab members over the many years. From science, to life, to the life of science, there is not a single member of the lab who ever hesitated to take the time to discuss anything I wanted, and provide encouragement when things were rough. Thanks especially to the kinetochore crew, and in particular Iain Cheeseman and Paul Maddox, both of who went out of their way to guide me through the scientific process. The original OD lab members, including Jon Audya, Amy Maddox, and Alexander Dammerman were also a large influence in shaping my scientific mind. I would also like to thank my fellow classmate, Joost Monen, for being a great friend and support as we helped each other survive as the “firsts”. And of course I must give credit to the other OD lab graduate students, Nathan Portier, Lindsay Lewellyn, Anthony Essex, and Molly Bush, for making graduate school not only bearable, but fun!

In addition, I am indebted to my family for their continuous support of all my decisions and providing me with a base of curiosity and determination that led me to pursue science. My parents have always believed I could achieve anything. This confidence they instilled in me is one of the key attributes of my success in both life and science. Lastly, but by no means least, I want to thank my husband, Caleb Wilkinson, for always listening to my problems and offering advice, support, and distractions. I couldn't possibly have completed my dissertation without him. He has made a huge number of sacrifices to see that I fulfill my dreams, and for this I am immensely grateful.

Chapter 2, in full, was published under the following citation: *Cell*, 2006(127):1179-1191, Sandall, S., Severin, F., McLeod, I., Yates, J.R., Oegema, K., Hyman, A.A., and Desai, A. The dissertation author was the primary researcher and author of this paper.

Vita

2002 BS, Microbiology, California State University, Long Beach

2008 PhD, Biomedical Sciences, University of California, San Diego

Publications

Sandall S., Desai, A. *When it comes to couple(r)s, do opposites attract?* Nature Structural & Molecular Biology, 2007 (14):790-792.

Sandall S., Severin F., McLeod, I., Yates, J.R., Oegema, K., Hyman, A.A., Desai, A. *A Sli15-Bir1 complex connects centromeres to microtubules and is the likely tension sensor controlling Aurora B activation.* Cell, 2006 (127):1179-1191.

Saitoh, A.*, Singh, K.K.*, **Sandall, S**.*, Powell, C.A., Fenton, T., Fletcher, C.V., Hsia, K., Spector, S.A. (2006). *Association of CD4(+) T-lymphocyte counts and new thymic emigrants in HIV-infected children during successful highly active antiretroviral therapy.* J. Allergy Clin Immunol, 2006 (117):909-915. (*Equal Contribution)

Kline-Smith S.L., **Sandall, S**., Desai, A. *Kinetochore-spindle microtubule interactions during mitosis.* Curr. Opin. Cell Biol., 2005 (17):35-46.

Alaniz, R.C., **Sandall, S**., Thomas, E.K., and Wilson, C.B. *Increased dendritic cell numbers impair protective immunity to intracellular bacteria despite augmenting antigen-specific CD8+ T lymphocyte responses.* J. Immunol., 2004 (172):3725-3735.

ABSTRACT OF THE DISSERTATION

Dissecting Centromeric DNA-Microtubule Interactions *In Vitro* Uncovers a Mechanism that Ensures Proper Connection of Chromosomes to the Mitotic Spindle

by

Sharsti L. Sandall

Doctor of Philosophy in Biomedical Sciences

University of California, San Diego, 2008

Professor Arshad Desai, Chair

Mitosis is the period of the cell cycle during which the duplicated genome is equally partitioned into two daughter cells. Cells accomplish this feat by condensing their chromosomes into compact units that are aligned and segregated by the cytoskeleton. This process requires correct attachment of sister chromatids to the dynamic mitotic spindle. Attachment errors have

severe consequences and can lead to developmental defects, cell death, and cancer.

The molecular machine responsible for making attachments between chromosomes and the mitotic spindle is the kinetochore. Composed of over 60 proteins, the kinetochore serves as the attachment interface between chromosomes and microtubules and monitors its' own attachment status. The coupling of these two functions provides a mechanism to delay cell division until all sister chromatids are properly attached to the mitotic spindle, ensuring their correct segregation. While the functions of the kinetochore have long been appreciated, the underlying molecular mechanisms have remained elusive.

Studies presented here, which utilize the biochemical and genetic amenability of budding yeast, *Saccharomyces cerevisiae*, reveal a specific attachment between the centromeric DNA and microtubules that is mediated by two conserved proteins Bir1/Survivin, and Sli15/INCENP. These proteins are of particular interest for their multiple roles in cell division and their potential use as cancer therapy targets since both are over-expressed in several types of cancer. The Bir1/Survivin-Sli15/INCENP mediated attachment is not responsible for making "core attachments" between kinetochores and microtubules, but instead functions to regulate the conserved kinase, Ipl1/Aurora B. Ipl1/Aurora B, Sli15/INCENP, and Bir1/Survivin are known collectively as the chromosomal passenger complex

(CPC) and over a decade of work has revealed that they are important for regulating kinetochore attachments, presumably by recognizing the amount of tension felt by sister chromatids when they are correctly attached to the mitotic spindle. The discoveries described in Chapter 2 has led to the hypothesis that this Bir1/Survivin-Sli15/INCENP mediated attachment is sensing tension directly to regulate Aurora B/Ipl1, which in turn regulates attachments. This model forms the basis for work presented in Chapter 3, which explores the molecular mechanisms of how the Bir1/Survivin-Sli15/INCENP mediated CEN-DNA linkage regulates and is regulated by Ipl1/Aurora B.

Chapter 1: Introduction

1.1 Chromosome Segregation and the Kinetochore

Cell division is a highly conserved symphony of events that culminates in an exact duplication of the original cell. This fundamental biological event has been appreciated and studied by scientists for over a century. Perhaps the most cytologically distinct phase of the cell division cycle is when the chromosomes, which comprise the genetic material of the cell, are replicated, compacted, and equally segregated into the two resulting daughter cells. This phase was first documented using light microscopy by Walther Flemming and termed “mitosis”, from the Greek word for thread based on the threadlike appearance of the mitotic spindle (Flemming, 1882). Since this initial discovery, scientists have made great strides in understanding how the chromosomes are segregated in a precise manner during each and every cell division.

The major cellular components responsible for chromosome segregation are now defined and largely consist of the cytoskeletal protein tubulin, which dynamically assembles and disassembles into noncovalent microtubule polymers in order to facilitate cellular functions. While being structurally robust, it is these dynamic properties that facilitate microtubule function, a characteristic obvious to early cytologists who documented the

rapid rearrangement these “linear elements” undergo throughout the cell cycle (Wilson, 1928). In the context of mitosis, microtubule polymers, which consist of α–and β–tubulin heterodimers, connect to the chromosomes via a specialized, proteinaceous structure termed the kinetochore. This mechanics of this connection have been difficult to understand, primarily because the microtubules at the site of connection are still undergoing polymerization, a characteristic that facilitates chromosome alignment at the metaphase plate by providing a pushing force. During anaphase the dynamic property switches to favor depolymerization, which results in pulling forces that act to segregate the chromosomes (Inoué and Salmon, 1995). This non-equilibrium dynamic, termed dynamic instability, works primarily because β–tubulin hydrolyzes GTP during polymerization, providing an energy input (Mitchison and Kirschner, 1984). Microtubule dynamics are essential for cell division as evidenced by the many naturally occurring drugs utilized in cancer therapy that either suppress or alter the dynamics to favor depolymerization (reviewed in (Desai and Mitchison, 1997)).

1.1.1 Overview of kinetochores

Rather than being a simple attachment site for the connection of chromosomes and microtubules, the kinetochore is a highly specialized machine that influences and harnesses microtubule polymer dynamics and serves as a signaling hub that monitors and controls its very own attachments. By relaying the status of its attachments to the cell cycle machinery, the

kinetochore ensures that chromosome segregation is inhibited until all chromosomes are attached and properly aligned at the metaphase plate. Kinetochores are made up of over 60 proteins that assemble into several discrete complexes (Cheeseman, 2004; De Wulf, 2003; Foltz et al., 2006; Okada et al., 2006; Wigge et al., 1998; Wigge and Kilmartin, 2001). Many of these proteins are conserved from yeast to humans despite the fact that the size and specificity of the underlying DNA on which the kinetochores form varies widely (Cleveland et al., 2003). Electron microscopy has revealed that vertebrate kinetochores form a trilaminar structure, an inner layer that binds the chromosomes, a linker layer, and an outermost layer into which the ends of spindle microtubules are embedded (Brinkley and Stubblefield, 1966; Dong et al., 2007; McEwen et al., 2007).

1.1.1.1 The budding yeast kinetochore

The simple unicellular budding yeast, *Saccharomyces cerevisiae,* has proven invaluable for studying the molecular architecture of the kinetochore. This is largely due to the ease of genetic and biochemical techniques in budding yeast, but is enhanced by two features of budding yeast kinetochores. The first is that, unlike kinetochores of higher eukaryotes, which attach to multiple microtubules (kinetochore fibers), budding yeast kinetochores attach to a single microtubule. This was first observed when tomographic reconstruction revealed the budding yeast half spindle was composed of 16 kinetochore microtubules (King et al., 1982a, b; Peterson and Ris, 1976;

Winey et al., 1995), corresponding to the number of chromosomes in budding yeast. The second convenient feature of budding yeast kinetochores is that the centromeric DNA on which they form is short (125 base pairs) and has a sequence specific element that directs formation (point centromeres, (Meraldi et al., 2006)). This is in contrast to higher eukaryotes where centromeric DNA can span 20-5000 kilobases (regional centromeres, (Cleveland et al., 2003)) and where centromere identity is epigenetically marked (see section below for further discussion (Karpen and Allshire, 1997)). The sum of these features has resulted in the budding yeast centromere being the best described and hence the most amenable to biochemical reconstitution.

Recent imaging studies have quantified the number of each protein complex at a single budding yeast kinetochore (Joglekar et al., 2006). Expanding this work to fission yeast, which have a regional centromere more similar to higher eukaryotes, revealed that the number of kinetochore components correlates with the number of microtubule attachments at each kinetochore (Joglekar et al., 2008). These findings suggest that the budding yeast kinetochore architecture represents a simple unit that is repeated in higher eukaryotes to facilitate more than one microtubule attachment.

1.1.2 Formation of kinetochores on centromeric DNA

In order for kinetochores to faithfully segregate chromosomes, it is essential that they assemble at a designated site along the DNA. Attaching at multiple sites would result in spindle forces acting inappropriately and

potentially causing higher frequencies of chromosome fragmentation once anaphase onset occurs. Cells avoid this problem by designating either one precise location (monocentric centromere), which is the case in both budding yeast and most vertebrates, or by forming kinetochores along the entire length of the chromosome (holocentric centromere, (Maddox et al., 2004)), a strategy utilized by the nematode *C. elegans* as well as other insects and plants. In each case this ensures that sister chromatids are attached to spindle microtubules emanating from opposite spindle poles.

1.1.2.1 Specification of centromeres

One of the key questions being investigated in the mitosis field is how cells specify centromeres. Budding yeast centromeres are exceptional in that a specific DNA sequence directs centromere specification. In other eukaryotes, the prevailing hypothesis is that a conserved histone variant, CENP-A replaces canonical histone H3 at centromeric sites, serving as an epigenetic mark that directs kinetochore formation (Blower et al., 2002). CENP-A is essential for kinetochore formation in all organisms studied to date, including monocentric, holocentric, and even budding yeast (Collins et al., 2005; Howman et al., 2000; Kalitsis et al., 1998; Meluh et al., 1998; Oegema et al., 2001; Sullivan et al., 2001; Takahashi et al., 2000). How CENP-A targeting is specified and limited to the centromeric location is currently being actively studied. As mentioned previously, most eukaryotic centromeres have no sequence specific element, however in humans, centromeres are

composed of tandem arrays of A/T rich α-satellite DNA. Although α-satellite DNA is essential for the formation of de-novo centromeres on artificial chromosomes, there are examples in human patients where neocentromeres have formed spontaneously on regions of the chromosome that do not contain α-satellite DNA (Ohzeki et al., 2002). The conclusion from analysis in humans is that α–satellite DNA is neither necessary nor sufficient for centromere specification (Amor and Choo, 2002).

Work in the past five years has greatly advanced our understanding of how CENP-A gets loaded into chromatin. Several proteins have been discovered that are required for the centromeric localization of CENP-A (Camahort et al., 2007; Fujita et al., 2007; Furuyama et al., 2006; Goshima et al., 2007; Hayashi, 2004; Maddox et al., 2007; Mizuguchi et al., 2007; Okada et al., 2006; Stoler et al., 2007; Takahashi et al., 2000). Interestingly, in human cells these proteins transiently localize to centromeres during telophase and early G1 of the new cell cycle, which is coincident with new CENP-A loading (Jansen et al., 2007; Maddox et al., 2007; Schuh et al., 2007). Nevertheless, since no direct biochemical interaction has been observed for these proteins with CENP-A, the mechanism by which they are affecting CENP-A loading is still poorly understood.

1.1.2.2 Budding yeast centromeres

Centromeres of budding yeast are simple 125 base pair sequences that can be divided into three regions, termed CDEI, CDEII, and CDEIII (Cottarel et

al., 1989; Fitzgerald-Hayes et al., 1982). The CDEI region contains the binding domain of the conserved yet non-essential protein CBF1 (Mellor et al., 1990), which is the putative CENP-B homologue and shows DNA bending activity (Niedenthal et al., 1993). CDEII is the region where the budding yeast CENP-A homologue, Cse4p binds, and may be more analogous to the α-satellite DNA of higher eukaryotic centromeres as it is highly A/T rich (Stoler et al., 1995). The CDEIII region contains sequence specific information that is required for a four-protein complex, the CBF3 complex to bind specifically to the DNA (discussed in detail below). Mutational analysis of these three regions suggests that the CDEIII region is essential for kinetochore formation and centromere activity (McGrew et al., 1986; Ng et al., 1986). If just 3 base pairs are mutated in this region, then kinetochores will not form in vivo (Ng et al., 1986). Unlike the essential CDEIII region, kinetochores form when CDEI is deleted, albeit it does lead to a 10-fold increase in chromosome loss rate (Baker et al., 1989; Cai and Davis, 1990). Mutations in CDEII don't render the centromere totally inactive, but do decrease its function, while complete deletion of CDEII, like CDEIII, abolishes kinetochore formation (Gaudet and Fitzgerald-Hayes, 1987; Murphy et al., 1991). While the sequence of CDEIII is palindromic, it is inherently asymmetric as inverting the sequence relative to CDEII results in failure to form a centromere in vivo even though CBF3 binding is retained (Murphy et al., 1991). These results suggest that the CDEII and

CDEIII regions cooperate to form a functional centromere and that while not essential, the CDEI region helps fine tune the structure.

One popular hypothesis is that the simple budding yeast centromeric sequence is wrapped around one nucleosome, where Cse4 replaces Histone H3, providing the platform for other kinetochore proteins to bind (Keith and Fitzgerald-Hayes, 2000; Meluh et al., 1998). In this scenario both the N-terminal tails of Cse4 and the CBF3 complex would cooperate to help bend the ends of the nucleosome, forcing the centromeric nucleosome to face proximal to the plus end of the kinetochore microtubule (Pietrasanta et al., 1999). Since the diameter of the nucleosome (~20nm) would be very similar to the diameter of a microtubule (~25nm), this model is very attractive (De Wulf, 2003). An alternative model is based on the observation that Ndc10 dimers can bind to the CDEII region of the centromere and when these binding sites are mutated result in similar chromosome loss rates similar to those observed when CDEII is replaced with plasmid DNA (Espelin et al., 2003). This model proposes that it is the CBF3 complex that forms the core-binding platform on the centromeric DNA and that a Cse4 containing nucleosome flanks this region.

A recent study has shed new light on the structure of the budding yeast centromere (Yeh et al., 2008). Localization of cohesion, a molecule responsible for holding sister chromatids together until anaphase onset, combined with crosslinking studies indicates that approximately 20 kilobases

of pericentric DNA surrounding the budding yeast point centromere is enriched in cohesion and forms an intramolecular loop. This loop may provide mechanical support to the budding yeast spindle and explains why sister kinetochores are stretched great distances, up to 800 nm, in a budding yeast spindle. Kinetochore formation is essential for this loop to form, suggesting that the CBF3 complex and perhaps Cse4 do indeed bend the DNA in a manner that allows for intramolecular pairing between DNA proximal to the core centromere sequence. In addition to elucidating centromere structure, this study also adds weight to the hypothesis that the budding yeast centromere/kinetochore is indeed analogous to a simple unit that is repeated in higher eukaryotes. If one considers this pericentric DNA as an integral part of the centromeric DNA, then 20 KB of DNA per microtubule attachment scales nicely with the approximate size and microtubule number of a vertebrate kinetochore.

1.1.2.3 The CBF3 complex

Made up of four proteins, Ndc10, Cep3, Ctf13, and Skp1, the CBF3 complex binds in a sequence specific manner to the CDEIII region of budding yeast centromeric DNA and is absolutely essential for all known kinetochore proteins to localize (Goh and Kilmartin, 1993; Ortiz et al., 1999; Sorger et al., 1994). All four genes are essential and when mutated result in high incidence of chromosome loss. The CBF3 complex was first identified as a 240 kd multi subunit complex by conventional biochemical purification of CEN-DNA binding

activity (Lechner and Carbon, 1991). Work since this initial discovery has elucidated a mechanism for how CBF3 gets loaded into centromeric DNA, which includes the cooperation of the chaperone protein Hsp90 (Bansal et al., 2004; Lingelbach and Kaplan, 2004; Rodrigo-Brenni et al., 2004; Stemmann et al., 2002) as well as the conserved protein Sgt1 (Bansal et al., 2004; Kitagawa et al., 1999; Lee et al., 2004; Steensgaard et al., 2004). The direct DNA binding element appears to be comprised primarily of the zinc finger protein Cep3 (Espelin et al., 1997), however recent evidence also suggests that Ndc10 contains a DNA binding domain (Espelin et al., 2003).

For many years it was thought that while CBF3 was essential for Cse4/CENP-A to bind centromeric DNA, the converse was not true. However, this observation was based on studies using a temperature sensitive allele of *cse4* (Measday et al., 2002). New studies using a heat inducible degron allele, which leads to degradation of Cse4, revealed that Cse4/CENP-A is indeed essential for CBF3 localization (Collins et al., 2005). Considering that a direct interaction between CBF3 and Cse4/CENP-A had never been observed, the mechanism for how these two influence one another was unclear. The recent identification of a new centromere protein, Scm3, has shed some light on this problem. Scm3 co-purifies with both Cse4/CENP-A and Ndc10 and is required for both to localize, suggesting it may link the two core budding yeast kinetochore components (Camahort et al., 2007). Biochemical studies have led to a speculative model that Scm3 binds to a

tetramer of Cse4/CENP-A and Histone H4, replacing histones H2A and H2B, to form the core nucleosome structure that then binds to the Ndc10 subunit of CBF3 (Camahort et al., 2007; Mizuguchi et al., 2007; Stoler et al., 2007). While this advance is quite exciting for explaining how point centromeres may be formed, it is important to note that functional homologues for CBF3 complex or Scm3 have not been identified outside of fungi (Meraldi et al., 2006).

1.1.3 Microtubule binding components of the kinetochore

The inner kinetochore scaffold of the CBF3 complex and Cse4/CENP-A provide a platform for the rest of the 60 plus kinetochore proteins to assemble. Biochemical analysis in budding yeast as well us localization experiments in yeast and other model organisms have greatly advanced our understanding of how kinetochore sub-complexes fit together. There appears to be a linker layer of proteins that serve to bridge proteins that are making direct contact with either the DNA or microtubules. In budding yeast, these linker proteins include Mif2/CENP-C, the Mtw1/Mis12 complex, Ctf19/CENP-H/I complex, and Spc105/KNL-1 (Westermann et al., 2007). It should be noted, however that the function of these linker proteins is still rather unclear and some of them have been shown to participate in both Cse4/CENP-A deposition, such as Chl4 of the Ctf19 complex (Mythreye, 2003), and microtubule binding, as is the case with KNL-1 in *Caenorhabditis elegans* (Cheeseman et al., 2006).

Proteins making direct contact with microtubules rely on the linker proteins to localize properly, and some do so in a microtubule dependent manner. In fact it is still unclear if these microtubule associated proteins first bind to microtubules, forming one half of a sandwich that is only completed when it finds the other half on the DNA side, or if they assemble at the kinetochore and are stabilized upon microtubule binding. Nevertheless, the last five years have greatly advanced our understanding of the important proteins making direct contact with the microtubule interface. In budding yeast there appear to be two major complexes that are accomplishing this task, the Ndc80 complex and the Dam1 complex. Both of these complexes show a dependency on inner and linker kinetochore proteins in order to localize to kinetochores and depletions of either complex have no effect on the kinetochore scaffold of the inner and linker proteins.

The Ndc80 complex is made up of four subunits, is conserved in all eukaryotes, and in all species studied appears to be essential for connecting the microtubule interface to the kinetochore (Cheeseman and Desai, 2008; Ciferri et al., 2007; Kline-Smith et al., 2005). Structural analysis of this complex has shed light on how it is binding to microtubules and indicates it is a long rod with globular domains on either end, which provide the binding sites for linker proteins on one end and microtubules on the other (Cheeseman et al., 2006; Ciferri et al., 2008; Wei et al., 2007). Biochemical analysis of the microtubule binding activity of the *C. elegans* recombinant complex has

revealed a weak affinity for microtubules that synergistically increases when combined with Spc105/KNL-1, which also has a weak affinity for microtubules, and the Mtw1/Mis12 complex (Cheeseman et al., 2006). This has led to the model that Ndc80 and Spc105/KNL-1 contact the microtubule surface at multiple low affinity sites and that when bound to the linker layer can cooperatively achieve a stable connection to the microtubule. This type of an attachment site correlates nicely with electron microscopy images of the human outer kinetochore where several fibrillar attachments are seen binding to the microtubule (Dong et al., 2007). Furthermore, it has also been shown in budding yeast that there are 8 copies of the Ndc80 complex per microtubule (Joglekar et al., 2006), further supporting this type of a model. This observation suggests that the interface between the microtubule and kinetochore is similar to velcro, where attachments can easily be modulated without entirely disconnecting from a microtubule. By keeping the kinetochore partially attached, this may avoid a scenario where complete detachment and re-attachment is necessary.

The Dam1 complex is also clearly important for coupling the kinetochore to the microtubule in budding yeast (Enquist-Newman et al., 2001; Hofmann et al., 1998; Janke et al., 2002; Jones et al., 2001; Miranda et al., 2007; Westermann et al., 2005). However, no clear homologues of this complex have been identified outside of fungi and in fission yeast the complex is not essential (Sanchez-Perez et al., 2005). Elegant structural and

biophysical studies have demonstrated that this 10-subunit complex forms rings around microtubules and is capable of coupling load to microtubule depolymerization in vitro, providing an example of how a microtubule-coupling device may be working in vivo (Asbury et al., 2006; Franck et al., 2007; Miranda et al., 2007; Wang et al., 2007; Westermann et al., 2006).

In addition to the Ndc80 and Dam1 complexes, there are several motor proteins that also localize to the kinetochore microtubule interface and affect microtubule dynamics. The kinesin 14 family member Kar3, although not essential in yeast, has been shown to be required for initial kinetochore capture and transport to the metaphase plate (see lateral attachment below (Tanaka et al., 2007; Tanaka et al., 2005a)). Other MAPs that localize to the budding yeast kinetochore include three plus end microtubule-tracking proteins (+TIPs) Stu2, Bim1 and Bik1 (Westermann et al., 2007). These may be important in the extension and stabilization of microtubules extending from the spindle pole bodies and in turn help facilitate kinetochore capture. Of these three proteins only Stu2 is essential in haploid budding yeast, and evidence suggests that Bim1 and Bik1 may have redundant roles in regulating kinetochore microtubules. Stu2 has the dual ability to rescue and stabilize microtubules that have kinetochores attached to them and to also promote depolymerization once biorientation is achieved (Al-Bassam et al., 2006; Pearson et al., 2003; Tanaka et al., 2005a; van Breugel et al., 2003).

1.1.4 Kinetochore capture by microtubules

1.1.4.1 Initial lateral attachment

Unlike higher eukaryotes, yeast cells undergo mitosis without breaking down the nuclear membrane (closed mitosis). Throughout the cell cycle, kinetochores stay in close proximity to the spindle pole bodies where they remain attached to nuclear microtubules except for a brief interlude in S-phase when centromere replication occurs (Kitamura et al., 2007). Higher eukaryotic kinetochores, which don't encounter microtubules until the nuclear envelope breaks down, are initially captured by microtubules in a lateral fashion, on the side of the microtubule surface, transported towards the centrosomes, and then positioned on the metaphase plate once biorientation is achieved (Rieder and Alexander, 1990). Until recently it was not clear that budding yeast displayed a similar mechanism. Elegant imaging studies have established that yeast kinetochores also undergo an initial lateral attachment followed by biorientation (Tanaka et al., 2005a). Extensive analysis of kinetochore mutants demonstrated that the majority of kinetochore components were required for this initial capture and that the movement on the lateral microtubule surface was primarily due to sliding promoted by Kar3 and end-on pulling promoted by the Dam1 complex (Kitamura et al., 2007).

1.1.4.2 Switch to end on attachments: Biorientation

Newly replicated sister centromeres have to biorient on the spindle. Biorienting sister chromatids correctly on the mitotic spindle is perhaps the least understood aspect of kinetochore function. The mechanism of how kinetochores switch from lateral to correct end-on binding is still unclear. The Dam1 complex and an instrumental kinetochore regulatory kinase, Ipl1/Aurora B and its' activating partner Sli15/INCENP are the only kinetochore proteins specifically required for the switch to biorientation (Tanaka et al., 2005a). When sister centromeres are replicated, the recently duplicated spindle pole body is not yet mature to bind to the new sister centromere, presenting a situation where one sister kinetochore is attached to the spindle pole body and the newly replicated sister is either unattached (monotelic attachment), or attached to the same spindle pole body as its sister (syntelic attachment). In either case, these attachments must be converted into bioriented (amphitelic) attachments.

Over a decade worth of experiments has demonstrated that the Ipl1/Aurora B kinase complex plays a central role in biorientation, which is a conserved function from yeast to humans (Tanaka, 2008; Tanaka and Desai, 2008). This complex, made up of Sli15/INCENP, Bir1/Survivin, and Ipl1/Aurora B in budding yeast (see the chromosomal passenger section below) is essential for biorientation as mutations of these proteins result in a high incidence of syntellic attachments that are not resolved leading to sister

kinetochores segregating together. Another mitotic kinase, Mps1, initially discovered for its role in spindle pole body duplication, has recently been shown to also play a major role in biorientation (Maure, 2007). While the mutant phenotype of *mps1* has an identical biorientation phenotype to *ipl1* mutants, it has not been elucidated if the two kinases cooperate or influence biorientation using independent pathways.

It is becoming more apparent that the mechanism for how Ipl1/Aurora B is promoting biorientation is by regulating targets of the microtubule interface through phosphorylation to modulate attachments. Several lines of evidence point to the Ndc80 complex as being a key target of Ipl1/Aurora B. Phosphorylation of Ipl1/Aurora B residues in the globular microtubule-binding domain of the both the human and *C. elegans* Ndc80 complex result in a decreased microtubule binding affinity (Cheeseman et al., 2006; Ciferri et al., 2008). Furthermore, mutations of these phosphorylation sites in human cells cause an increase in merotelic attachments (where one sister kinetochore is attached to microtubules from both spindle poles) and chromosome segregation defects reminiscent of errors caused when members of the Ip1l/Aurora B complex are inhibited (DeLuca et al., 2006).

In budding yeast it is clear that the Dam1 complex is also a key target of the Ipl1/Aurora B complex instrumental in promoting biorientation (Cheeseman et al., 2002; Wang et al., 2007). Like Ndc80, the Dam1 complex is phosphorylated by Ipl1/Aurora B in vitro, however it is unclear if this

phosphorylation results in a decrease in microtubule affinity, or rather affects the dynamics of ring assembly (Wang et al., 2007). Nevertheless, when Ipl1/Aurora B sites are mutated in Dam1 to a non-phosphorylatable form it mimicks Ipl1/Aurora B biorientation defects. Conversely, Dam1 phosphomimic mutants partially suppress Ipl1/Aurora B mutants (Cheeseman et al., 2002).

1.1.4.3 Coupling attachments to microtubule dynamics

An important feature of the kinetochore microtubule interface is the ability to couple and harness microtubule dynamics such that chromosomes can be moved. It has been demonstrated that the disassembly of microtubules provides enough energy to move isolated chromosomes in vitro (Koshland et al., 1988; Mitchison and Kirschner, 1985a, b). Since both polymerization, depolymerization, and kinetochore attachment occur at the plus ends of microtubules it has remained a mystery how the kinetochore can stay attached to and harness this energy. A theoretical model, the Hill-Sleeve, was proposed in 1985 by T. Hill that attempts to explain how the kinetochore might facilitate this function (Hill, 1985). The model proposes that a sleeve-like structure would allow for microtubule dynamics to occur in the “sleeve space” while the actual microtubule binding surface would be made up of the “sleeve end” which would be on the lateral surface of the microtubule polymer. As the microtubule depolymerizes the sleeve could slide along the lateral surface effectively coupling the kinetochore to the dynamic microtubule. Both the Dam1 complex, which forms an asymmetric ring around microtubules in vitro,

as well as multiple complexes of the Ndc80 rod complex fit well into the Hill-Sleeve model and are attractive molecular candidates that could ultimately validate the Hill-Sleeve concept.

1.1.4.4 Mechanisms that promote biorientation: geometry and tension

Two primary mechanisms have been proposed for how biorientation is achieved, one based on the geometry of sister kinetochores and the other based on the tension that results from proper biorientation (Ault and Rieder, 1992; Tanaka et al., 2005b). The geometry based mechanism assumes that sister chromatids have an inherent configuration that would make it difficult for each sister to face the same spindle pole, inherently discouraging syntelic attachments. The weakness of this model is that it doesn't explain how kinetochores that do end up attached to the same spindle pole, a situation known to occur in vivo, are corrected. The tension-based mechanism addresses the correction issue, however, it too cannot account for all properties of biorientation, suggesting that both mechanisms contribute to biorientation, although the extent of contribution each are making has been widely debated (Ault and Rieder, 1992).

The tension model has its origins from ingenious experiments performed by Nicklas and colleagues in the late 1960s using a meiotic spindle model, grasshopper oocytes (Nicklas and Koch, 1969). They elegantly demonstrated that until biorientation is achieved, chromosome microtubule attachments are continuously forming and detaching and that applying tension

on the chromosomes using a microneedle resulted in the stabilization of attachments. The model is based on the principle that correctly bioriented attachments will be stretched at the attachment site, which is opposed by the cohesion linking sister chomatids together and the end result is tension across the sister centromeres, a situation artificially created in the grasshopper experiments. In the case where attachments are syntelic, a significant reduction in tension would result since the spindle pulling forces would be on the same side. Since syntelic attachments have microtubules attached to both sister kinetochores, the difference in tension would be an ideal way for the cell to distinguish syntelic and bioriented attachments independently from the mere occupancy of microtubules.

Experiments in budding yeast using a dicentric plasmid has supported this model and suggested that independent of geometry, tension across centromeres is sufficient for their biorientation (Dewar et al., 2004). Nevertheless, the tension model does not account for how the cell discriminates between a monotelic attachment and a syntelic attachment. While there could be subtle changes in tension in these two cases, it is unclear if tension is playing a role in promoting biorientation from a monotelic attachment. Furthermore, the experiment using the dicentric chromosome does not rule out a redundant role for a geometry-based mechanism (Indjeian and Murray, 2007).

1.1.5 Mechanisms to Ensure Proper Segregation

Making attachments between kinetochores and microtubules is key to proper chromosome segregation; however, inevitably errors are made during the process. Cells have evolved mechanisms to monitor attachments and communicate the status back to the cell cycle such that cell division will halt until all sister chromatids are properly connected. This error correction process has been coined the spindle checkpoint and is made up of a set of conserved proteins that use the kinetochore as a signaling platform to produce a “wait anaphase” signal (Musacchio and Salmon, 2007). While it is clear that the spindle checkpoint recognizes kinetochores that lack microtubule occupancy, it is less clear how the spindle checkpoint coordinates the recognition and correction of kinetochores that have microtubules present, albeit incorrectly as in the case of syntelic and merotelic attachments and has given rise to an intense debate over the role of tension in the spindle checkpoint (Pinsky and Biggins, 2005). While this debate is far from settled, it is clear in budding yeast that Ipl1/Aurora B detects attachment defects and promotes their detachment, thus indirectly signaling to the spindle checkpoint. This was elucidated from a study where it was observed that kinetochore mutants that have many chromosomes detached from the mitotic spindle have restored, albeit weakened attachments, when crossed with *ipl1* mutants (Pinsky et al., 2006b).

1.1.5.1 The spindle checkpoint

The ultimate goal of the spindle checkpoint is to delay anaphase until chromosomes are correctly attached to the mitotic spindle. It achieves this by inhibiting Cdc20, a specificity factor for the Anaphase Promoting Complex (APC), which is an E3 ubiquitin ligase that targets several proteins for degradation. The APC target, whose degradation results in anaphase onset, is securin, which inhibits the protease separase. Once separase is no longer inhibited, it cleaves the cohesion that it is holding sister chromatids together. The most conserved and well-studied spindle checkpoint components were originally identified in budding yeast. Two screens uncovered three Mad (Mitotic Arrest Deficient) proteins, Mad1, Mad2, and Mad3/BubR1 (Li and Murray, 1991), and two Bub (Budding Uninhibited by Benzamidazole), Bub1 and Bub3 proteins (Hoyt et al., 1991). Additionally, the Mps1 kinase is required for the spindle checkpoint and its over-expression ectopically activates the checkpoint (Hardwick et al., 1996). These proteins all localize transiently to the kinetochore and depend on outer kinetochore proteins to target correctly.

As productive kinetochore microtubule attachments are made, the Mad proteins are depleted from the kinetochore. A popular model proposes that the kinetochore catalyzes the formation of a diffusible signal made up of the potent mitotic checkpoint complex (Mad3/BubR1, Mad2, Bub3, and Cdc20), which then diffuses away to inhibit the APC (Musacchio and Salmon, 2007).

However, a recently updated model proposes that microtubule-binding proteins such as Ndc80 and KNL-1 recruit spindle checkpoint proteins to kinetochores limiting checkpoint signaling to unattached kinetochores (Burke and Stukenberg, 2008). The checkpoint is more complex in higher eukaryotes where there are additional components involved such as the RZZ complex (Rod, Zwilch, and Zeste-White 10), the kinesin CENP-E, kinases p38 MAP, Nek2A, Tao1, and Prp4 (Cheeseman and Desai, 2008).

1.1.5.2 Regulation of microtubule attachments

Multiple post-translational modifications help modulate and regulate kinetochore microtubule interactions. These primarily include phosphorylation, which is carried out by six mitotic kinases, Aurora B/Ipl1 (Ruchaud et al., 2007), Polo-like kinase 1 (PLK1) (Sumara et al., 2004), cycklin dependent kinase-1 (CDK-1), and the spindle checkpoint kinases Mps1 (Jones et al., 2005; Schmidt et al., 2005), BubR1 (Lampson and Kapoor, 2005), and Bub1 (Johnson et al., 2004; Meraldi and Sorger, 2005). These kinases are opposed by Protein phosphatase-1 (opposes Aurora B function (Pinsky et al., 2006a; Trinkle-Mulcahy et al., 2003)) and Protein Phosphatase-2A (PP2A), which gets targeted to inner centromeres by the conserved protein Shugoshin-1 (Sgo1) where it helps prevent the proteolytic cleavage of cohesion (Kitajima et al., 2006; Riedel et al., 2006; Tang et al., 2006). Other modifications regulating kinetochore proteins include sumoylation (Montpetit, 2006), ubiquitylation (Vong et al., 2005), and potentially methylation, as the Set1 methyltransferase

seems to oppose Ipl1 function in budding yeast (Zhang et al., 2005). The level of post-translational modification at the kinetochore is likely to be complex and dynamic. Future work will undoubtedly be focused on understanding how these modifications contribute to regulating kinetochore assembly and function.

1.2 The Chromosomal Passenger Complex

The chromosomal passenger complex is a well-conserved complex that derives its name from its unique and dynamic mitotic localization pattern. In early prophase the complex can be seen localizing throughout the chromatin and focusing at centromeres by late prometaphase. At anaphase onset the complex leaves the centromeres and "passages" to the spindle midzone where it plays an essential role in cytokinesis. The multiple mitotic functions of the CPC include control of both chromosome and spindle structure, regulation of kinetochore-microtubule attachments, and completion of cytokinesis. All of these functions rely on the dynamic localization pattern of the CPC (Ruchaud et al., 2007). Despite decades of work and hundreds of manuscripts, the mechanisms by which the CPC is functioning throughout mitosis are not very well understood. Recent advances, however, are starting to shed light on some of the mechanisms governing CPC localization and function.

1.2.1 Components of the CPC

In almost all organisms the CPC complex is made up of four subunits: the Aurora B/Ipl1 Kinase (Terada et al., 1998), and three non-enzymatic components, INCENP/Sli15 (Adams et al., 2000; Cooke et al., 1987), Survivin/Bir1, and Borealin/Dasra-B (Gassmann et al., 2004; Honda et al., 2003; Klein et al., 2006; Sampath et al., 2004). Thus far a Borealin subunit has not been identified in budding or fission yeast. The complex is dependent on each member to function properly and depletions or mutations of either subunit results in identical mitotic phenotypes in all organisms analyzed, which include chromosome segregation errors and cytokinesis failure.

INCENP (inner centromere protein), the founding member of the complex was first discovered in 1987 when a monoclonal antibody was isolated that labeled the space between the two centromeres (Cooke et al., 1987). It is the presumptive scaffold of the CPC (Adams et al., 2000; Chen et al., 2003; Gassmann et al., 2004; Kim et al., 1999; Wheatley et al., 2001) and its conserved C-terminus is responsible for activating Aurora B kinase (Adams et al., 2000; Kang et al., 2001). In humans there are three Ser/Thr Aurora Kinases, A, B, and C and all have distinct localization patterns and tissue expression (Carmena and Earnshaw, 2003). Aurora A, although related has a distinct activation mechanism, unique binding partners, and localizes to the centrosomes. And while Aurora C can bind to other CPC members, its localization and function seem to be limited to the testis (Kimura et al., 1999;

Sasai et al., 2004; Yan et al., 2005). Survivin, a member of the IAP (inhibitor of apoptosis) family of proteins contains a BIR (baculovirus IAP domain) in its N-terminus, which has led to a long-standing debate over whether Survivin has a dual function in the apoptotic pathway (Altieri, 2006; Lens et al., 2006). Borealin was simultaneously discovered a few years ago in both *X. laevis* and humans in screens for novel mitosis proteins (Gassmann et al., 2004; Sampath et al., 2004). Although they share very little sequence conservation, Borealin/Dasra B is most likely the functional homologue of the *C. elegans* protein CSC-1 (Romano, 2003).

1.2.2 The budding yeast CPC

Ipl1, is the sole Aurora kinase in budding yeast and was the first member of the CPC to be identified in this organism. In a screen for Increase in Ploidy (IPL) mutants, several alleles of *ipl1* were isolated, hinting at its essential role in chromosome segregation (Chan and Botstein, 1993). Sli15/INCENP was subsequently identified after performing a Synthetically Lethal with Ipl1 (SLI) screen (Kim et al., 1999), however it was only with advances in bioinformatics that it was realized that Sli15 was the INCENP homologue, as sequence conservation between the two proteins is primarily limited to the C-terminal IN box, which is responsible for activating Aurora B/Ipl1 (Kang et al., 2001). While Survivin/Bir1 was identified in budding yeast last, it had been characterized well before it was recognized as the third budding yeast CPC component (Uren et al., 1999; Yoon and Carbon, 1999).

Its participation in the CPC wasn't realized until immunopurifications of Sli15, followed by mass spectrometry, revealed it was in a complex with Sli15/INCENP and Ipl1/Aurora B (Cheeseman et al., 2002). Like Survivin, Bir1 contains two BIR domains in its N-terminus, however these domains are not essential for the yeast function of Bir1 (Widlund et al., 2006).

1.2.3 Functions of the CPC

1.2.3.1 Regulation of chromosome and spindle dynamics

In as early as G2 of the cell cycle, Aurora B phosphorylation of Histone H3 on Ser10 and Ser28 can be detected near centromeres (Crosio et al., 2002; Giet and Glover, 2001; Hsu et al., 2000; Murnion et al., 2001). This characteristic phosphorylation mark spreads over the arms of chromosomes as they begin to condense in prophase (Monier et al., 2007). While often used as an indicator of Aurora B kinase activity, the function of this phosphorylation event, however, has remained unclear (Adams et al., 2001b; Goto et al., 2006; Hsu et al., 2000). In the same cell cycle phase, there is also a potential link between the CPC and proper loading of the condensin complex onto chromatin, however this function has not been consistent in various model organisms (Giet and Glover, 2001; Hagstrom et al., 2002; Lipp et al., 2007; MacCallum et al., 2002; Takemoto et al., 2007). So while it appears that the CPC is in the right place at the right time to affect chromosome structure and is clearly active at this time, what exactly it is doing is poorly understood.

The CPC contribution to spindle assembly regulation is more evident, however also seems to be variable amongst organisms. Mitotic spindle assembly has been shown to be controlled from both ends, the canonical pathway of centrosome microtubule nucleation and chromosome capture, and a second pathway, clearly relevant in meiotic systems that lack centrosomes, initiated by the chromosomes in which cytosolic microtubules are stabilized near the vicinity of centromeres and focused into the spindle pole by motor proteins (Wadsworth and Khodjakov, 2004). In human cells it seems like the CPC has some effect on the canonical spindle formation pathway as Borealin inhibition leads to the initial assembly of the bi-polar spindle which is not maintained in metaphase and ultimately leads to ectopic spindle poles (Gassmann et al., 2004). In Drosophila S2 cells mitotic spindle assembly is similar disrupted in the absence of CPC function (Adams et al., 2001b).

In a system devoid of centrosomes, *X. laevis* ooctye extracts, the CPC has also been shown to be essential for bi-polar spindle formation, suggesting that it is important for both mechanisms of spindle assembly (Gadea and Ruderman, 2006; Sampath et al., 2004). In this system, the CPC is likely controlling spindle assembly by Aurora B phosphorylation of two key targets, stathmanin/OP18, a microtubule de-stabilizing protein (Andersen et al., 1997; Gadea and Ruderman, 2006; Kelly et al., 2007) and MCAK, a kinesin-13 microtubule depolymerase (Ohi et al., 2004; Sampath et al., 2004; Tulu et al., 2006), which is also a target of Aurora B in regulating kinetochore microtubule

attachments during chromosome biorientation (see the following section for further details). In budding yeast, it was also recently demonstrated that Ipl1/Aurora B regulates centrosome dependent spindle assembly. Although its function may be redundant with two BimC motor proteins, Cin8 and Kip3, it is clear that in the absence of Cin8, Ipl1, presumably via regulation of the microtubule bundling protein Ase1, becomes essential for spindle assembly (Kotwaliwale et al., 2007).

1.2.3.2 Regulation of chromosome microtubule interactions

An undisputed, universal role for the CPC in all species studied is its function in regulating chromosome biorientation. Studies in budding yeast were the first to reveal that Aurora B/Ipl1 is accomplishing this by promoting turnover of kinetochore microtubule interactions (Pinsky et al., 2006b) . Presumably the CPC is able to carry out this function by monitoring the status of kinetochore-microtubule interactions and detecting incorrect ones via tension (see section 1.1.4.4). A potential mechanism for how the CPC senses tension, which relies on an intrinsic function of the CPC itself, is discussed in Chapter 2 of this thesis, however an alternative tension sensor in mammalian cells was proposed to be the Snf2 family protein PICH (Baumann et al., 2007). While it is less clear how the CPC recognizes attachments with less tension, a picture of how it subsequently regulates attachments is emerging and involves phosphorlyation of outer kinetochore components to promote the turnover of attachments. The Ipl1/Aurora B targets important for this function include both

the Dam1 complex in budding yeast (Cheeseman et al., 2002) and the Ndc80 complex in higher eukaryotes (Cheeseman et al., 2006; DeLuca et al., 2006), although it is also likely that Ndc80 is also a major target in budding yeast (Cheeseman et al., 2002). Another target of Aurora B that has been demonstrated to be important in regulating kinetochore microtubule attachments is MCAK, which is only found in higher eukaryotes. In *X. laevis*, Aurora B phosphorylates MCAK on Ser196, which leads to an inhibition of depolymerization (Andrews et al., 2004; Lan et al., 2004). This result coupled with the observation that the CPC is enriched at sites of merotelic and unattached kinetochores has led to the hypothesis that the CPC regulates attachments at these sites by controlling the localization and function of MCAK. However, since MCAK is not conserved in budding or fission yeast, unlike the Ndc80 complex, it is unlikely to be a universal mechanism for how the CPC functions to regulate biorientation. Furthermore, one might hypothesize that Aurora B activity would promote microtubule depolymerization as a way to increase the turnover of incorrect attachments. But, since phosphorylation of MCAK by Aurora B results in decreased depolymerization rates (Andrews et al., 2004; Lan et al., 2004), it is hard to reconcile how this activity would promote biorientation and lead to the correction of merotelic attachments.

Since there is still controversy over whether the spindle checkpoint recognizes lack of tension in addition to lack of attachments, it is difficult to

assess if the CPC has a direct versus indirect role in the spindle checkpoint (see section 1.1.5). Nevertheless, in higher eukaryotes it is clear that the CPC is required for the spindle checkpoint only when tension is reduced, not when attachments are lacking. All CPC components are required to sustain a checkpoint arrest when cells are treated with the spindle poison taxol, which dampers microtubule dynamics and leads to a lack of tension at attachment sites (Carvalho et al., 2003; Ditchfield et al., 2003; Hauf et al., 2003; Kallio et al., 2002; Lens and Medema, 2003; Vader et al., 2006). Additionally, the CPC is been shown to recruit the spindle checkpoint protein BubR1 to the kinetochore (Carvalho et al., 2003; Lens and Medema, 2003; Vader et al., 2006), and Aurora B may also function with Bub1 to maintain an interaction between BubR1 and the APC (Morrow, 2005). A recent report implicates the coiled coil domain of INCENP as having a direct role in checkpoint function (Vader et al., 2007). When this region is deleted in an INCENP null background chromosome biorientation and Aurora B centromere localization and activation are unperturbed, but cells still can't maintain a checkpoint arrest induced by taxol treatment (Vader et al., 2007).

1.2.3.3 Role in cytokinesis

The CPC performs an essential role in cytokinesis following chromosome segregation. Although the complex is localized to the spindle midzone directly following chromosome separation, the CPC does not seem to be required for furrow initiation (Mackay et al., 1998). However, in the

absence of the CPC furrow ingression fails, resulting in furrow regression (Adams et al., 2001b; Carvalho et al., 2003; Gassmann et al., 2004; Honda et al., 2003; Schumacher et al., 1998; Tatsuka et al., 1998; Terada et al., 1998). The CPC may be functioning either in cooperation or in a distinct pathway with a complex termed centralspindlin (Mishima et al., 2002), made up of the mitotic kinesin-like protein-1 (MKLP-1), or ZEN-4 in *C. elegans*, and a Rac GTPase activating protein MgcRacGAP/Cyk4. There have been reports that Aurora B phosphorylates MgcRacGAP/Cyk4 and knockdown studies of Aurora B also implicate it as regulating the localization of the centralspindilin complex (Guse et al., 2005; Minoshima et al., 2003).

Since budding yeast undergo a closed mitosis, cytokinesis involves the pinching off of both the cytoplasmic and nuclear membranes and may involve mechanism quite distinct from organisms that undergo open mitosis. Infact, in budding yeast the cytokinesis role of the CPC seems to be inhibitory, primarily by regulating spindle length and dynamics. In a pathway termed NoCut, it was found that Ipl1/Aurora B was controlling the localization of the anillin-like proteins, which play a role in preventing cytokinesis onset until chromosomes are segregated (Norden et al., 2006). There may also be an indirect role for the CPC in organizing the septins during the final stages of cytokinesis, via an anaphase/telophase interaction with members of the CBF3 complex (Bouck and Bloom, 2005; Gillis, 2005; Widlund et al., 2006). Furthermore, it has also

been reported that Ipl1 plays an essential role in spindle disassembly in budding yeast (Buvelot et al., 2003).

1.2.4 Localization to centromeres

From prometaphase to metaphase of the cell cycle, the CPC is concentrated from the arms of the chromosomes to the centromeres. While a wealth of information has been collected on what components of the CPC itself are important for targeting the complex, it is unclear if other proteins are directing the CPC or if it is an intrinsic property of the CPC to localize to the centromere. In higher eukaryotes, it may be that Survivin helps target the complex to the centromeres, presumably through the interaction of the INCENP N-terminus (Klein et al., 2006; Vader et al., 2006). In fact, a chimera of Survivin and INCENP in which Survivin replaced the first 47 amino acids of INCENP was able to localize properly to centromeres in the absence of endogenous INCENP and Survivin (Vader et al., 2006). However, Borealin also binds to the N-terminus of INCENP and a new study in which a crystal structure of the 1:1:1 complex of full length Survivin, $INCENP_{1-57}$, and $Borealin_{10-109}$ was solved to a resolution of 1.4Å revealing that the entire ternary complex may be important for centromere targeting (Jeyaprakash et al., 2007). This contradicts the finding that the INCENP/Survivin chimera could localize in the absence of Borealin. Additionally, Survivin, Aurora B, and INCENP are very dynamic at the centromere (Ahonen et al., 2008; Beardmore et al., 2004; Murata-Hori and Wang, 2002). An additional level of complexity

involves ubiquitylation of Survivin, which has been shown to be important for the centromere turnover of Survivin (Vong et al., 2005). Taking these results together it is likely that the centromere targeting of the CPC is an extremely dynamic process with the three non-enzymatic components intricately controlling and influencing Aurora B localization and activity.

Other centromere proteins that have been implicated in CPC centromere targeting, include the histone variants CENP-A and H2A.Z. Although the results are contradictory (Klein et al., 2006), some groups have found that Aurora A phosphorylation of CENP-A in prophase promotes the relocalization of Aurora B to the inner centromere (Kunitoku et al., 2003; Zeitlin et al., 2001). H2A.Z appears to have a role in the formation of the inner centromere structure and has been found to bind to INCENP (Greaves et al., 2007; Rangasamy et al., 2003). In addition, knock down studies of H2A.Z reveal a similar phenotype to that of the CPC members, hinting that it is playing a part in CPC targeting, although this has not been demonstrated directly (Greaves et al., 2007; Rangasamy et al., 2003). Bir1 in budding yeast has been shown to interact with the Ndc10 subunit of the CBF3 complex, suggesting it may function to localize the complex, but this has not been rigorously tested. Furthermore, in fission yeast the shugoshin protein Sgo2 has been shown to be required for maintaining CPC localization on centromeres during spindle checkpoint activation (Kawashima et al., 2007; Vanoosthuyse and Hardwick, 2005).

1.2.5 Localization to the spindle midzone in anaphase/cytokinesis

A dramatic re-localization of the CPC occurs after the onset of anaphase when they move from the inner centromere to the spindle microtubules that form between the segregating DNA. This transition also marks a change in the dynamics of the complex, as it goes from being highly dynamic to mostly static (Ahonen et al., 2008; Beardmore et al., 2004; Murata-Hori and Wang, 2002). Two mechanisms have been proposed for how the CPC is transferred to the spindle midzone. The first involves the de-phosphorylation of INCENP at Cdk sites by the phosphatase Cdc14, which is triggered by the activation of separase (Pereira, 2003). This has been demonstrated in budding yeast, but remains to be determined if other species also utilize this to re-localize the CPC. In vertebrates, MKLP-2 has been shown to be required for the localization of both the CPC and Cdc14 to the spindle midzone (Gruneberg et al., 2004), and the MKLP-2 homologue, Subito, has been reported to interact with INCENP and Aurora B in Drosophila (Cesario et al., 2006). While it is possible that the motor activity of MKLP-2 is responsible for the re-localization, since Cdc14 is also present, this could be an indirect consequence of the phosphatase activity. The crystal structure of the ternary complex also suggests that there is an acidic stretch in INCENP and a basic stretch in Survivin that are critical for the entire CPC to localize to the spindle midzone, however dispensable for centromere targeting (Jeyaprakash et al., 2007).

1.2.6 Activation of Aurora B kinase/Ipl1

Recent advances have started to shed light on the mechanism for how Aurora B/Ipl1 gets activated, however it is still an area that is still not fully understood and generates wide interest. The most concrete and universal evidence points to the conserved IN box of Sli15/INCENP being instrumental for full Ipl1/Aurora B activation. It has been demonstrated that Ipl1/Aurora B first phosphorylates Sli15/INCENP at a conserved Thr-Ser-Ser (TSS) motif near the C-terminus, which in turn fully activates the kinase (Bishop and Schumacher, 2002; Bolton et al., 2002; Honda et al., 2003). The crystal structure of the *X. laevis* Aurora B in contact with both the IN box of INCENP and hesperadin, a specific Aurora B inhibitor, demonstrated that the binding of INCENP to Aurora B allosterically promotes the active conformation of the kinase (Sessa et al., 2005). Survivin has also been implicated as both a substrate and activator of Aurora B (Bolton et al., 2002). A recent study also demonstrated that a putative CPC member, telophase disk-60kDa (TD-60) and microtubules activate Aurora B (Rosasco-Nitcher et al., 2008). Furthermore, this study provided some evidence that Aurora B substrates can inhibit Aurora B activation, which can be reversed by phosphorylation by two other mitotic centromeric kinases, Plk1 and Haspin (Rosasco-Nitcher et al., 2008).

1.2.7 The INCENP family of proteins

Recent experiments have begun to shed some light into some of the structural features of INCENP proteins. The most conserved domain of the protein, the IN box, resides in the C-terminus and is responsible for activating Aurora B/Ipl1 (Adams et al., 2001b). The *X. laveis* IN box domain was crystallized bound to Ipl1 revealing that it formed three alpha helices which form a molecular crown around the Aurora B/Ipl1 (Sessa et al., 2005). Additionally, the first 58 amino acids of human INCENP were recently crystallized in complex with full-length Survivin, and Borealin$_{10\text{-}109}$ (Jeyaprakash et al., 2007). Within the ternary complex, INCENP residues 8-46 comprise a single α-helix 10 turns long that packs up in a parallel fashion to an the Survivin α-helix, which in turn binds to an α-helix of Borealin making up a 3-helix bundle that is responsible for targeting the complex to centromeres and re-localizing them to the spindle midzone. While the primary sequence of this stretch of amino acids is well-conserved in human, mouse, chicken, and frogs, the sequence is quite divergent even in flies and shows little conservation with budding yeast Sli15. Furthermore, deletion of the Sli15 N-terminal region is able to support cell viability in budding yeast (data not shown), suggesting that this may not be the primary or sole centromere targeting region in budding yeast and leaves open the question of how conserved this domain actually is within the INCENP family. The remainder of Sli15 is a structural mystery with the exception of a coiled-coil domain in the

middle of the protein. This coiled-coil is highly variable amongst each species and ranges from just 28 amino acids in the fungus *A. gossypii* to over 250 in the human INCENP (this study). While it was originally predicted that Sli15 contained a coiled-coil as well comprised of 42 amino acids, I have since determined that this is not a real coil, but rather contains an unusual charge distribution (this study, Chapter 3).

1.2.7.1 Previously characterized Sli15 domains

A very general domain analysis of Sli15 in budding yeast has been carried out to determine what regions are important for 1) association with Ipl1 as a kinase activator and substrate 2) microtubule binding, 3) localization to the centromere and mitotic spindle, and 4) interaction with Dam1. By expressing Sli15 as three domains compromising amino acids 1-227, 228-559, and 560-698, some general conclusions were made about what portion is contributing to Sli15 function. The N-terminus partially localized to the mitotic spindle but did not interact with Ipl1 or the Dam1 complex nor could it bind microtubules. The middle portion, which includes the region once predicted to be a coiled coil, is a weak substrate of Ipl1/Aurora B, binds microtubules, localizes to the mitotic spindle, and interacts with Dam1 via yeast two-hybrid and immunoprecipitation. The C-terminus, which includes the IN-box does not bind microtubules but is responsible for the interaction and activation of Ipl1 and is subsequently phosphorylated by Ipl1. This region also showed a partial interaction with Dam1 when immunoprecipitated from yeast extracts (Kang et

al., 2001). While it has been demonstrated by yeast two hybrid that the N-terminus of Sli15 interacts with Bir1 (Thomas and Kaplan, 2007), it has not been confirmed in vivo, nor has the N-terminal deletion been assessed to see if it retains the ability to interact with Bir1 in a different region of the protein.

1.2.7.2 Conserved microtubule binding activity

Although the length and/or presence of the coiled coil in INCENP proteins is variable, it has been demonstrated to be important for binding to microtubules in vitro in both chicken and budding yeast (Kang et al., 2001; Wheatley, 2001). Other groups have also assessed the role of the INCENP region of microtubule binding activity and found in budding yeast that the region is regulated by Cdk and that an opposing phosphatase, Cdc14, is required to de-phosphorylate Sli15 and transfer it to the spindle midzone in anaphase (Pereira, 2003). Recently it was found in human cells that the region might be playing a role in the checkpoint that is independent of its function in chromosome biorientation (Vader et al., 2007). In these same studies Aurora B targeting and activation appeared to be normal when this region was deleted. Additionally, no other CPC members bind to the coiled-coil region of human INCENP (Klein et al., 2006).

1.3 Chromosome Segregation Errors

1.3.1 Aneuploidy and its link to cancer and birth defects

When chromosomes fail to segregate properly genetic material is either lost or gained in the resulting daughter cells. This leads to aneuploidy, an abnormal number of chromosomes. The consequences of this type of mistake can be disastrous for both a developing organism as well as a fully formed one. Aneuploidy remains a hallmark of many cancer cells and in fact, over 100 years ago Boveri proposed that aneuploidy could cause cancer. Furthermore, mouse models heterozygous for several mitotic checkpoint proteins show increased rates of spontaneous and chemically induced cancers. Boveri's hypothesis was recently directly tested by utilizing a heterozygous mouse model of the centromeric motor protein CENP-E and it was found that aneuploidy can indeed act oncogenically in certain situations and ironically can suppress cancer formation in other instances (Weaver and Cleveland, 2007; Weaver et al., 2007). These studies highlight the important, yet still largely understood link, between cancer and aneuploidy, a direct consequence of chromosome missegregation.

1.3.2 The CPC and its relationship to cancer

While the reasons why are still unclear, what is clear is that INCENP, Survivin, and Aurora B are all over-expressed in several different cancer types (Adams et al., 2001a; Altieri, 2008; Nguyen and Ravid, 2006). This has led to

much excitement and investigation into the promise of these proteins as cancer therapy targets. An Aurora B inhibitor is now being studied in a phase two clinical trials and Survivin is often utilized as a marker in cancer detection and progression (Altieri, 2008; Mountzios et al., 2008; Nguyen and Ravid, 2006). Furthermore, a gastric ulcer drug, rebamipide, has been shown to be effective against gastric cancer, presumably by decreasing Survivin expression. It is currently in clinical use in Japan and validates the chromosomal passenger proteins as promising, effective cancer therapy targets (Tarnawski et al., 2005).

Chapter 2: A Bir1-Sli15 Complex Connects Centromeres to Microtubules and is Required to Sense Kinetochore Tension

2.1 Summary

Proper connections between centromeres and spindle microtubules are of critical importance in ensuring accurate segregation of the genome during cell division. Using an in vitro approach based on the sequence-specific budding yeast centromere, we identified a complex of the chromosomal passenger proteins Bir1 and Sli15 (Survivin and INCENP) that links centromeres to microtubules. This linkage does not require Ipl1/Aurora B kinase, whose targeting and activation are controlled by Bir1 and Sli15. Ipl1 is the tension-dependent regulator of centromere-microtubule interactions that ensures chromosome biorientation on the spindle. Elimination of the linkage between centromeres and microtubules mediated by Bir1-Sli15 phenocopies mutations that selectively cripple Ipl1 kinase activation. These findings lead us to propose that the Bir1-Sli15-mediated linkage, which bridges centromeres and microtubules and includes the Aurora kinase-activating domain of INCENP family proteins, is the tension sensor that relays the mechanical state of centromere-microtubule attachments into local control of Ipl1 kinase activity.

2.2 Introduction

During mitosis, kinetochores assemble on the centromeric regions of each sister chromatid to act as the primary chromosomal attachment sites for spindle microtubules (Cleveland et al., 2003; Kline-Smith et al., 2005 p00291; Maiato et al., 2004). Kinetochores exhibit both end-on and lateral interactions with microtubules. End-on connections between the outer kinetochore and microtubule plus ends couple chromosome motility to changes in the polymerization and depolymerization of bound microtubules (Inoué and Salmon, 1995). Lateral interactions between kinetochores and spindle microtubules are associated with poleward as well as equatorial chromosome movements that facilitate the establishment of stable end-on connections (Kapoor et al., 2006; Rieder and Alexander, 1990; Tanaka et al., 2005a).

In addition to their mechanical role in segregation, kinetochores serve as signaling hubs that inhibit anaphase onset until every chromosome in the cell is properly connected. The kinetochore-based mitotic checkpoint pathway relays the presence of any unattached kinetochores into inhibition of the ubiquitin protein ligase that triggers sister chromatid separation and mitotic exit (Cleveland et al., 2003; Nasmyth, 2005; Pinsky and Biggins, 2005). Classic micromanipulation studies in insect spermactocytes as well as recent work using chromosome engineering in budding yeast have highlighted the importance of tension in selectively stabilizing correctly bioriented chromatid pairs (Dewar et al., 2004; Li and Nicklas, 1995; Nicklas and Koch, 1969; Stern

and Murray, 2001). Biorientation places kinetochore-microtubule connections under tension, whereas incorrect syntelic attachments, where the kinetochores on both sisters are connected to the same spindle pole, do not. The conserved Aurora B kinase is required to eliminate syntelic attachments, facilitating new connection attempts until the correct configuration is achieved (Biggins, 2001; Dewar et al., 2004; Ditchfield et al., 2003; Hauf et al., 2003; Kallio et al., 2002; Lampson et al., 2004; Pinsky et al., 2003; Tanaka et al., 2002). The action of Aurora B generates unoccupied kinetochores that in turn signal via the mitotic checkpoint pathway to prevent anaphase onset (Pinsky et al., 2006b). Thus, the choreography of chromosome segregation is comprised of an intimate feedback between the mechanics of kinetochore-microtubule connections and localized signaling pathways.

Efforts to reconstitute the mechanical and regulatory functions of kinetochores in vitro have been limited by the complexity of the underlying centromeric DNA (Cleveland et al., 2003). An exception to this complexity is budding yeast, where centromeres consist of a well-defined 125 base-pair region (Clarke, 1998; Mcainsh et al., 2003). The biochemical identification of CBF3, the protein complex that directly binds the key cis-acting CDEIII domain (Lechner and Carbon, 1991), provided further impetus for analyzing kinetochore-microtubule interactions in vitro. Previous studies have demonstrated that budding yeast centromeric (CEN) DNA will bind to microtubules following incubation in a cell extract (Hyman et al., 1992;

Kingsbury and Koshland, 1991; Severin et al., 1997; Sorger et al., 1994). This interaction requires the CBF3 complex and is subject to regulation by Ipl1, the budding yeast Aurora B kinase, and the counteracting phosphatase PP1/Glc7 (Biggins et al., 1999; Sassoon et al., 1999). However, CBF3 is not sufficient, indicating that other factor or factors are necessary to link CBF3-CEN DNA to microtubules (Sorger et al., 1994). Here, we extend this in vitro approach to biochemically identify the missing factor(s). Our results reveal that a complex of two chromosomal passenger proteins, Bir1/Survivin and Sli15/INCENP, connects CBF3-CEN DNA to microtubules in vitro. This connection is independent of Ipl1, whose activation and targeting are controlled by Bir1 and Sli15. In vivo analysis of Sli15 mutants that eliminate the in vitro activity leads us to propose that the Bir1-Sli15-mediated linkage between CBF3-CEN DNA and microtubules acts as a tension sensor that activates Ipl1 in the vicinity of incorrect syntelic attachments.

2.3 Results

2.3.1 A Quantitative In Vitro Assay for the Interaction of CBF3-Bound CEN DNA with Microtubules

In the presence of a yeast cell extract, fluorescent beads coupled to CEN DNA will bind to immobilized microtubules adsorbed to a coverslip surface. Although required, CBF3 is not sufficient for binding, indicating the presence of additional factor or factors in the extract that connect CBF3-bound

CEN DNA to microtubules (Sorger et al., 1994). To identify these factor(s), we adapted the bead assay to enable rapid, reproducible testing of column fractions (Figure 2.1A). As expected, beads coated with CEN DNA exhibited robust microtubule binding in the presence of wild-type extract, whereas beads coated with a mutant CEN DNA that renders it nonfunctional in vivo failed to bind (Figure 2.1B). To generate a source of CBF3 for in vitro complementation assays, we optimized a partial purification using CEN DNA band shift to monitor CBF3 activity (Figure 2.1C). This procedure yielded 50-fold partially purified (PP)CBF3 that exhibited a robust band shift (Figure 2.1C) but did not support binding of CEN DNA beads to microtubules on its own (Figure 2.1D). Extracts prepared from strains harboring mutations in CBF3 lacked CEN DNA band shift but complemented (PP)CBF3 in the bead-microtubule-binding assay (data not shown, (Sorger et al., 1994)). Trypsin treatment indicated that the complementing activity is protease sensitive (see Figure S2.1). Taken together, these results confirmed the existence of an unknown factor that connects CBF3-bound CEN DNA to microtubules in vitro and established a robust assay that could be used for its identification.

2.3.2 A Conventional Purification Strategy Identifies Bir1 as a Candidate for the Activity that Links CBF3-Bound CEN DNA to Microtubules

To identify the protein or proteins that connect CBF3-bound CEN DNA to microtubules, we utilized two strategies. First, we tested CBF3-complementing activity in extracts either prepared from mutant strains or

immunodepleted of candidate kinetochore-localized or microtubule-binding proteins. At the budding yeast kinetochore, the Dam1 ring complex plays an important role in bioriented microtubule attachments and the Mis12, Ctf19, and Ndc80 complexes are suggested to direct assembly of the microtubule-binding interface (reviewed in (De Wulf, 2003; Mcainsh et al., 2003; Tanaka et al., 2005b)). However, neither mutations in nor immunodepletions of these complexes perturbed the in vitro linkage between CEN DNA and microtubules (Table 2.1). Other candidates, including motor and nonmotor microtubule binding proteins, were similarly excluded. These results indicated the presence of a CBF3-dependent linkage between CEN DNA and microtubules that did not involve any of the obvious candidates suggested by prior studies. Parallel to the candidate analysis, we pursued an unbiased conventional purification, using the quantitative in vitro assay (Figure 2.2A). Complementing activity was measured relative to a standard curve generated by serially diluting the starting material for the purification step into a constant amount of (PP)CBF3 (Figures 2.2B and 2.2C). Negative controls in which mutant CEN DNA beads were used, or (PP)CBF3 was omitted, verified the specificity of binding. By combining three purification steps in series, we enriched the complementing activity 400-fold (Figure 2.2D). However, attempts at additional purification resulted in a significant loss of specific activity that did not appear to be due to separation of different components. Since the purification did not achieve sufficient enrichment to directly correlate complementing activity with

copurifying proteins, we identified candidates that could be functionally tested by performing mass spectrometry (Washburn et al., 2001) on the highest specific activity material—the Mono S cation-exchange pool (Figures 2.2E and 2.2F). This approach identified 247 polypeptides with greater than 10% sequence coverage in the Mono S pool (Table 2.2). Database functional annotations identified a single protein within this large set previously implicated in centromere function (Figure 2.2G; Table 2.2). This protein was Bir1, the budding yeast homolog of the Survivin subunit of the chromosomal passenger complex. This finding led us to focus on Bir1 as a candidate for the CBF3-complementing activity.

2.3.3 Bir1 Is an Essential Component of the CBF3-Complementing Activity

To test whether Bir1 is required to link CEN DNA to microtubules in vitro, we generated a strain in which bir1 was deleted. Sporulation of heterozygous diploids yielded two wild-type and two apparently inviable spores (n =105 tetrads), as expected for an essential gene. However, consistent with previous conflicting studies describing *bir1* as both essential (Li et al., 2000; Widlund et al., 2006) and nonessential (Uren et al., 1999; Yoon and Carbon, 1999), 10% of *bir1Δ* spores formed tiny colonies after extended incubation. The *bir1Δ* cells derived from these colonies grew but had aberrant, polyploid DNA content (data not shown). Similar aberrant cells are obtained if the deletion is covered with a centromeric plasmid expressing Bir1 and the

plasmid is removed from the deleted haploid using negative selection after tetrad dissection, indicating that neither passage through meiosis nor haploinsufficiency in the diploid state is required for the observed phenotype. Immunoblotting using an affinity-purified anti-Bir1 antibody confirmed that a series of bands present in wild-type extracts, likely reflecting differentially phosphorylated forms of Bir1, is absent in *bir1Δ* extracts (Figure 2.3A). Extracts prepared from *bir1Δ* cells exhibit no activity in the in vitro CEN DNA microtubule interaction assay (Figure 2.3B), whereas the ability of the CBF3 to bind CEN DNA was unaffected (Figure 2.3C). Addition of (PP)CBF3 to *birΔ* extracts failed to restore CEN DNA-microtubule binding activity (data not shown). Transformation with a plasmid encoding Bir1 under control of its endogenous promoter fully restored activity in the assay (Figure 2.3B) as well as the bands detected in the Bir1 molecular weight range in immunoblots (Figure 2.3A). We conclude that Bir1, a candidate identified by mass spectrometry of a fraction enriched for the complementing activity by conventional purification, is an essential component of the link between CBF3-bound CEN DNA and microtubules in vitro.

2.3.4 Sli15 and Bir1, but Not Ipl1, Are Required for the CBF3-Complementing Activity

Bir1, like its homolog Survivin in higher eukaryotes, is a subunit of the chromosomal passenger complex. In budding yeast, this complex includes Ipl1, the single Aurora family kinase in budding yeast, and Sli15, the homolog

of the Aurora B activator and targeting subunit INCENP (Adams et al., 2000; Cheeseman et al., 2002; Kim et al., 1999). Since the complexity of the Mono S fraction could have prevented identification of the other two subunits by mass spectrometry, we repeated the purification and monitored the fate of each subunit. Bir1 and Sli15 showed a fractionation profile that was similar to the activity throughout the purification (Figures 2.3D and 2.3E). In contrast, the majority of Ipl1 fractionated away from Bir1-Sli15 into a distinct pool of smaller hydrodynamic radius during the gel filtration step (Figure 2.3D). The fractionation analysis suggested that a complex containing Bir1 and Sli15 is responsible for the in vitro complementing activity, and that Ipl1 might be dispensable. Since Sli15 and Ipl1 are essential genes, and the available conditional alleles do not affect protein levels (see below), we tested this by immunodepleting >90% of Sli15 or Ipl1, each tagged with six copies of the hemagglutinin (HA) epitope (Figure 2.4A). Consistent with their fate during purification, depletion of Sli15 dramatically reduced activity whereas depletion of Ipl1 had no effect (Figure 2.4A). The assays were performed without ATP addition, and normal binding was observed at all tested dilutions, arguing against the catalytic activity of residual Ipl1 kinase accounting for the difference between extracts depleted of Sli15 and Ipl1. Although Ipl1 does not appear to be required to connect CEN DNA to microtubules in vitro, its kinase activity regulates this linkage (Biggins et al., 1999). Addition of ATP to wild-type extracts severely inhibits binding of CEN DNA beads to microtubules

(Figure 2.4B; (Biggins et al., 1999). Sensitivity to ATP addition is lost in extracts prepared from ipl1 mutants with compromised kinase activity but can be restored following addition of purified Ipl1 protein (Figure 2.4B). This result predicts that if Ipl1 is absent from fractions enriched for the complementing activity, they should be insensitive to ATP. We tested this prediction using the Mono S pool (Figures 2.2E and 2.2F). The binding observed in mixtures of the Mono S pool and (PP)CBF3 is insensitive to ATP but becomes sensitive following addition of purified Ipl1 protein (Figure 2.4B). These results suggest that the CBF3-complementing activity is comprised of a complex containing Bir1-Sli15 that is independent of Ipl1 but subject to regulation by its kinase activity.

2.3.5 A Purified Endogenous Bir1-Sli15 Complex Complements CBF3 and bir1Δ Extracts

To determine whether a purified Bir1-Sli15 complex complements (PP)CBF3, we generated extracts from a strain expressing tandem affinity purification (TAP)-tagged Bir1. Following incubation with IgG resin, the Bir1-TAP complex was eluted by cleavage with TEV protease. A fraction of the elution was subjected to the second affinity purification step and analyzed by mass spectrometry; the rest of the elution was used for in vitro experiments (Figure 2.4C). Both immunoblotting and mass spectrometry indicated that the TAP prep of Bir1 contains Sli15 (Figure 2.4D), but not Ipl1, as expected from a previous study (Widlund et al., 2006). Neither protein was detectable in the

(PP)CBF3 fraction (Table 2.3). The purified Bir1-Sli15 complex had no activity on its own but exhibited robust activity when mixed with (PP)CBF3 (Figure 2.4E). Mass spectrometry of (PP)CBF3 indicated that no other known kinetochore proteins were present in this fraction (Table 2.3). Addition of Bir1-Sli15 also complemented the activity loss in *bir1Δ* extracts (Figure 2.4F). These findings strongly suggest that a complex containing Bir1 and Sli15 directly connects CBF3-bound CEN DNA to microtubules in vitro. This conclusion is supported by previous work documenting an interaction between Bir1 and the Ndc10 subunit of CBF3 (Bouck and Bloom, 2005; Gillis, 2005; Yoon and Carbon, 1999) and direct binding of Sli15 to microtubules (Kang et al., 2001).

Bir1-Sli15 and Ipl1 are chromosomal passenger proteins that localize prominently to the anaphase spindle. Dephosphorylation of Sli15 by the phosphatase Cdc14 is required for this localization (Pereira, 2003). Recent work has shown that the CBF3 complex also localizes to the anaphase spindle (Bouck and Bloom, 2005; Gillis, 2005). These observations raised the possibility that the in vitro CEN DNA-microtubule linkage assay is detecting microtubule-binding activity of the pool of Bir1-Sli15 present in anaphase. To test this, we analyzed *cdc14-1* and *cdc15-2*, two mutants in which Sli15 anaphase spindle localization is not observed (Pereira, 2003; Stoepel et al., 2005). Extracts prepared from these mutants exhibited wild-type CEN DNA-microtubule linkage (Figure S2.2A). Linkage activity is also low in G1, when

Sli15 is dephosphorylated, but high in mitosis, when Sli15 is hyperphosphorylated (Figure S2.2B). Together with the in vivo analysis described below, these results support the conclusion that the CEN DNA-microtubule linkage mediated by Bir1-Sli15 is of critical importance during chromosome segregation.

2.3.6 Shutting Off Sli15 or Deleting Its Microtubule-Binding Domain Eliminates the Linkage between CEN DNA and Microtubules In Vitro

To investigate the physiological role of the Bir1-Sli15-mediated linkage between CBF3-CEN DNA and microtubules, we focused our efforts on Sli15 because of the abnormal polyploidy observed in *bir1* mutants. Extracts prepared from strains harboring the only previously characterized mutant allele of *SLI15*, *sli15-3* (Kim et al., 1999), exhibited normal CEN DNA-microtubule binding but were insensitive to the addition of ATP (Figure 2.5A). *sli15-3* extracts are therefore similar to extracts prepared from *ipl1* mutants but distinct from extracts immunodepleted of Sli15 (see Figure 2.4A). This difference was explained by sequencing *sli15-3*, which revealed that the critical mutation is within the IN box domain that binds to and activates Ipl1 kinase (Figures S2.3A and S2.3B; (Sessa et al., 2005). Thus, the mutant protein encoded by the *sli15-3* allele, while defective in Ipl1 activation, is present at normal levels (Figure S2.3C) and capable of linking CEN DNA to microtubules in vitro.

Since *sli15-3* encodes a protein that retains the ability to link CEN DNA

to microtubules, a new mutant was needed to investigate the in vivo role of the Bir1-Sli15 mediated linkage. To obtain such a mutant, we generated a strain where the galactose promoter is integrated upstream of the *SLI15* coding region (*pGAL-SLI15*). Sli15 is overexpressed when this mutant is grown in galactose ($SLI15^{ON}$; Figure 2.5C and Figure S2.4A), but this does not result in a significant phenotype. Switching this strain to glucose medium ($SLI15^{OFF}$) causes a dramatic loss in Sli15 protein levels (Figure 2.5C and Figure S2.4A). Importantly, in agreement with results obtained from immunodepleting Sli15, no CEN DNA-microtubule linkage activity was detected in $SLI15^{OFF}$ extracts (Figure 2.5D).

The Sli15 shutoff mutant offered the opportunity to directly test the role of the Sli15 microtubule-binding domain in the in vitro linkage. Sli15 is a multidomain protein with a centrally located microtubule-binding domain (Kang et al., 2001). The C terminus of Sli15, like all INCENP family proteins, contains the Aurora-activating IN box which binds to and activates Aurora B (Kang et al., 2001; Sessa et al., 2005). To test the function of the microtubule-binding domain, we integrated a mutant (Sli15-MTBΔ; Figure 2.5B) into the URA3 locus of the strain harboring the *pGAL-SLI15* shutoff allele. Wild-type Sli15 coding sequence was integrated in parallel as a control. Both the mutant and wild-type coding regions were under control of the endogenous *SLI15* promoter.

Immunoblots confirmed expression of Sli15-MTBΔ before and after

shutting off pGAL-SLI15 (Figure 2.5C) and the mutant protein retained the ability to interact with Bir1 (Figure S2.5B), indicating that it is not misfolded. When expression of wild-type Sli15 was turned off, cells expressing the Sli15-MTBΔ mutant protein failed to survive, in contrast to controls expressing the wild-type protein, indicating that the microtubule-binding domain of Sli15 is essential for viability (Figure S2.5A). Analysis of nocodazole-arrested extracts prepared after shutting off *pGAL-SLI15* showed that the Sli15-MTBΔ mutant failed to support in vitro CEN DNA-microtubule linkage, in contrast to full length Sli15, which supported normal binding (Figure 2.5D). Thus, the linkage detected in vitro requires the microtubule-binding domain of Sli15.

2.3.7 Both the Sli15 Shutoff and the Sli15 Microtubule-Binding Domain Deletion Mutant Phenocopy Ipl1 Kinase Activation Mutants In Vivo

The Sli15 shutoff and the Sli15-MTBΔ mutant both eliminate the linkage between CEN DNA and microtubules in vitro. Analyzing the phenotype of these mutants would therefore make it feasible to distinguish between two potential models for the physiological role of this linkage. First, as anticipated during the initial development of the bead assay, the Bir1-Sli15 linkage could play an Ipl1-independent role in the force-transducing connection of centromeres to spindle microtubules, which we will refer to as the ‘‘core’’ attachment. Alternatively, the role of Sli15 as an activator of Ipl1 raised the attractive possibility that Bir1-Sli15 mediate a ‘‘tension-sensing’’ attachment that ensures chromosome biorientation by locally controlling Ipl1 kinase

activation.

To distinguish between these models, we used a GFP marked-chromosome to follow the segregation of sister chromatids. The failure to correct syntelic attachments in *ipl1* mutants results in sister chromatids cosegregating to the mother or the bud with roughly equal frequency (Figure 2.5E; (Biggins, 2001; Biggins et al., 1999; Tanaka et al., 2002). In both the *SLI15*^{OFF} and *SLI15*^{OFF}+Sli15-MTBΔ cells, the marked chromosome exhibited a missegregation pattern similar to *ipl1* kinase activity mutants (Figure 2.5F). This missegregation pattern is distinct from different classes of kinetochore mutants required for the core attachment (reviewed in (Biggins, 2003)). By contrast, the majority of sisters segregated properly in *SLI15*^{ON} and *SLI15*^{OFF}+Sli15 cells (Figure 2.5F). In *ipl1* mutants, despite a functional checkpoint and nearly 100% missegregation, the cell cycle is not delayed because core attachments, although incorrect, are present. This is in contrast to mutations that compromise the core attachment, which either delay in the cell cycle due to checkpoint activation or lack a functional checkpoint due to severe defects in kinetochore structure (Biggins, 2003). To determine whether cells lacking Sli15 have a functional checkpoint and/or experience a cell-cycle delay, we monitored the levels of securin (Pds1) after releasing *SLI15*^{OFF} cells from a G1 arrest in the presence or absence of nocodazole. *SLI15*^{OFF} mutants arrested normally in nocodazole, indicating the presence of a functional checkpoint (Figure 2.5G). However, in the absence of nocodazole, *SLI15*^{OFF}

cells did not exhibit a significant cell-cycle delay (Figure 2.5G) despite extensive missegregation of sister chromatids (Figure 2.5F). This high rate of missegregation was associated with a rapid loss of cell viability (Figure S2.4C). These results indicate that cells lacking Sli15 behave similarly to *ipl1* kinase activity mutants (*ipl1-321*, *ipl1-2*, and *sli15-3*) but distinctly from mutants in kinetochore proteins important for the core attachment. We conclude that the Bir1-Sli15-mediated linkage between CEN DNA and microtubules is not part of the core attachment. Instead, our results indicate that the Bir1-Sli15-mediated linkage is essential for the tension-dependent regulation of microtubule attachments by Ipl1 that ensures biorientation.

2.4 Discussion

2.4.1 A Complex of Bir1-Sli15 Links CBF3-CEN DNA to Microtubules In Vitro

The ability of budding yeast CEN DNA to interact with microtubules following incubation in a cell extract was first documented more than a decade ago. The importance of CBF3, the sequence-specific scaffold of the budding yeast kinetochore, was immediately apparent. However, the identity of an additional necessary component remained elusive. Here, we used a biochemical complementation assay to show that a complex of Bir1-Sli15 links CBF3-CEN DNA to microtubules in vitro. Bir1 directly interacts with the Ndc10 subunit of CBF3 (Bouck and Bloom, 2005; Gillis, 2005; Yoon and Carbon,

1999), and the central region of Sli15, required for the in vitro CEN DNA-microtubule linkage (this study), directly binds microtubules (Kang et al., 2001). Although a full reconstitution using recombinant proteins remains to be achieved, the evidence strongly suggests that the linkage observed in the in vitro assay can be accounted for by Bir1-Sli15 directly connecting CBF3-CEN DNA to microtubules.

It is interesting to note that the majority of proteins required for kinetochore assembly and function in vivo do not play a role in the in vitro linkage. This result was anticipated by the earlier finding that the CDEIII element of CEN DNA is sufficient in the in vitro assay but is not sufficient for centromere function in cells (Sorger et al., 1994). We suspect that the specialized chromatin domain on which kinetochores assemble, which includes nucleosomes containing the centromere-specific histone CENP-A, will be important for achieving in vitro reconstitution of the core attachment.

2.4.2 Ipl1 Kinase Regulates, but Is Not Required for, the CEN DNA-Microtubule Linkage In Vitro

Ipl1 kinase is dispensable for connecting CBF3-bound CEN DNA to microtubules but regulates this linkage (this study; (Biggins et al., 1999)). This observation raises the question as to what specific components are phosphorylated by Ipl1. In the original study describing Ipl1 regulation, the Ndc10 subunit of CBF3 was suggested to be the critical target (Biggins et al., 1999). Identification of Bir1-Sli15 as the linker between CBF3-CEN DNA and

microtubules raises the possibility that phosphorylation of these components may also be important. In particular, Sli15 is a well-established Ipl1 substrate in addition to being its activator (Cheeseman et al., 2002; Kang et al., 2001). The binding of CBF3 to CEN DNA is unaffected in *ipl1* kinase mutant or *bir1Δ* extracts (this study; (Biggins et al., 1999)). An important future direction will be to determine whether Ipl1 phosphorylation regulates the interaction between CBF3 and Bir1-Sli15, between Bir1 and Sli15, or between Bir1-Sli15 and microtubules.

2.4.3 In Vivo Function of the Bir1-Sli15-Mediated Linkage Between CBF3-Bound CEN DNA and Microtubules

In considering the in vivo role of the Bir1-Sli15-mediated linkage in chromosome segregation, we focused on the connection to Ipl1, which is known to play a central role in biorientation. In the bioriented state, sister chromatids are connected to opposite spindle poles, placing centromere-spindle attachments under tension. Improper syntellic attachments are detected and eliminated in an Ipl1-dependent manner, facilitating new connection attempts until all chromosomes are bioriented. This paradigm for the mechanism of biorientation raises the question as to how changes in tension at centromere-microtubule connections are relayed to control Ipl1 kinase activity. The centromeric cohesion protector Sgo1 has been suggested to act as a tension sensor (Indjeian et al., 2005), but this function appears to be distinct from the Ipl1-dependent mechanism (Pinsky et al., 2006b).

Our in vivo analysis indicates that the Bir1-Sli15-mediated linkage between CEN DNA and microtubules is required for Ipl1-dependent correction of core attachments lacking tension. One possibility to explain these findings is that the Bir1-Sli15 linkage facilitates recognition of Ipl1 substrates at syntelic attachments. Alternatively, this linkage, which includes the Aurora-activating IN box domain, may constitute the tension-sensitive activator of Ipl1. We favor the latter possibility and discuss it further below, although direct evidence for a tension-induced change in the Bir1-Sli15 linkage is necessary to distinguish between these alternatives.

2.4.4 A Speculative Model for Tension-Regulated Ipl1 Activation by Bir1-Sli15

The independent biorientation of multiple chromosomes on the same spindle poses a major challenge to understanding tension-regulated Ipl1 activation. We propose that Bir1-Sli15 links centromeres to microtubules in a manner that allows the IN box of Sli15 to locally activate Ipl1 when core attachments are not under tension (Figure 2.6). The finding that deletion of the microtubule-binding domain of Sli15 phenocopies ipl1 kinase mutants suggests that formation of the ternary complex between Bir1-Sli15, CBF3-CEN DNA, and microtubules is necessary for robust Ipl1 activation. Such a mechanism could contribute to restricting Ipl1 kinase activity to the vicinity of attachments lacking tension. A potentially intriguing mechanistic parallel exists with Aurora A, the other major Aurora kinase present in metazoans but absent

in fungi, that is activated by the TPX2 protein (Kufer et al., 2002; Tsai et al., 2003). Like INCENPs, TPX2 directly binds microtubules and the activation of Aurora A by TPX2 is strongly enhanced by microtubule binding (Tsai et al., 2003).

Ipl1 activated in the vicinity of syntelic attachments is predicted to phosphorylate components of both the core attachment and the tension-sensing attachment to release the centromere from the microtubule (Figure 2.6; (Cheeseman et al., 2002; Kang et al., 2001). Recent work suggests that one of the critical core attachment targets is the Ndc80 complex, which binds directly to microtubules and whose microtubule-binding affinity is reduce by Ipl1/Aurora B-directed phosphorylation (Cheeseman et al., 2006). Phosphorylation-triggered detachment of the tension-sensing attachment, presumably recapitulated in the in vitro assay when ATP is present, may reduce Ipl1 activation and promote dephosphorylation to allow new attachments to be formed.

Once a chromosome is bioriented and the core attachment is under tension, this in turn could modulate the tension-sensing attachment such that Sli15 is no longer able to activate Ipl1 (Figure 2.6). The modulation could occur by a tension-induced conformational change that buries the IN box, as depicted in Figure 2.6. Alternatively, tension may detach Bir1-Sli15 from the microtubule or from CBF3, preventing formation of the ternary complex that promotes activation (not depicted in Figure 2.6). Exploring potential tension

regulation will be facilitated by the in vitro CEN DNA bead-microtubule interaction assay, which is amenable to direct biophysical analysis.

2.4.5 Significance to Metazoan Chromosome Segregation

The role of Aurora B in correction of syntelic attachments and the activation of Aurora B by INCENP family proteins are widely conserved (reviewed in (Andrews et al., 2003; Meraldi et al., 2004; Vagnarelli and Earnshaw, 2004)). Drosophila and mammalian INCENPs directly bind to microtubules, indicating that this biochemical activity is also conserved (Adams et al., 2001b; Wheatley, 2001). Although the CBF3-Bir1/Survivin interaction is restricted to budding yeast, Survivin and another accessory subunit Borealin/Dasra target Aurora B to centromeres in metazoans (reviewed in (Vagnarelli and Earnshaw, 2004)). Thus, we suspect that the general principle of utilizing a direct connection between centromeres and spindle microtubules that includes the activator of Aurora B will be widely relevant for understanding how tension helps ensure the correct distribution of chromosomes.

In summary, our work highlights the existence of a direct linkage between centromeres and microtubules that includes the activating scaffold protein for Ipl1/Aurora B. Such a linkage provides the potential for mechanically sensitive control of kinase activation. The concept of kinase-activating scaffolds acting as local mechanical sensors controlling phosphorylation cascades is likely to also be significant in other cellular

contexts.

2.5 Methods

2.5.1 Strains and Extract Preparation

Strains are summarized in Table 2.4. For Pds1 blots, 1.5 ml culture was processed at each time point as described (Pinsky et al., 2006b). To test candidate mutants in the bead assay, 200–500 ml cultures were grown to mid-log phase. Cells were washed in water, resuspended in a volume equal to the cell pellet of 2X breakage buffer (100 mM Bis-Tris Propane, 200 mM β-glycerophosphate, 400 mM KCl, 10 mM EDTA, 10mM EGTA, 20% glycerol, and 1mM PMSF [pH 7.6]), frozen as drops in liquid nitrogen, and ground in a liquid nitrogen-cooled mortar and pestle. The crude lysate was centrifuged at 15,000 x g for 2 X 15min, and the supernatant was used for assays. Alpha factor was used at 1 mg/ml; nocodazole was used at 10 mg/ml.

2.5.2 Partial Purification of CBF3

CEN DNA band-shift assays were performed as described (Severin et al., 1999; Severin et al., 1997; Sorger et al., 1994). For the partial CBF3 purification, 50 ml extract was precipitated with 60% ammonium sulfate, resuspended in 40 ml BB150 (50 mM Bis-Tris Propane, 100 mM b-glycerophosphate, 150 mM KCl, 2 mM EDTA, 2 mM EGTA, 1 mM DTT, 10% glycerol, and protease inhibitors [pH 7.0]), dialyzed into BB150, loaded onto a 20 ml Poros HQ/20 column, and eluted with a KCl gradient. Fractions with

peak activity were pooled, flowed through a 5 ml HiTrap SP cation-exchange column, and concentrated on a 1.6 ml Poros HQ/20 column by elution with a KCl step gradient.

2.5.3 In Vitro CEN DNA-Microtubule Interaction Assay

The in vitro assay was performed as described (Severin et al., 1999), with the following modifications. Double-stick tape flow cells were constructed such that six samples could be analyzed on a single slide using a multichannel pipette. Taxol microtubules, polymerized using unlabeled, digoxigenin-labeled, and rhodamine-labeled tubulin (30:9:1), were adsorbed to anti-digoxigenin (10 mg/ml) antibody coated flow cell surfaces for 5 min. Unbound microtubules were washed out, and the chamber was blocked for 5 min in BRB80 (80 mM PIPES, 1 mM $MgCl_2$, and 1 mM EGTA [pH 6.8]) plus 10 mM taxol and 1.5 mg/ml casein. In parallel, 2 ml of 20 mg/ml yeast extracts was incubated in 15 ml reactions in binding buffer (10 mM HEPES [pH 8.0], 6 mM $MgCl_2$, 10% glycerol, and 120–140 mM KCl); 3 mg sheared salmon sperm DNA was added as a nonspecific competitor. For complementation assays, (PP)CBF3 was added to ~3X the band-shift activity present in a typical extract assay, casein was added to 0.3 mg/ml, and the final reaction included 15 mM Bis-Tris Propane, 30 mM b-glycerophosphate, 0.6 mM EGTA, and 0.6 mM EDTA [pH 7.0], in addition to the binding buffer components. After 45 min, an equal volume of reaction buffer plus 10 mM taxol was added and reactions were introduced into the flow cell with adsorbed microtubules. Fifteen minutes later,

unbound beads were washed out and ten fields of the coverslip surface per sample were photographed using a 20X, 0.7 NA objective. Bead binding was stable and did not change appreciably for 1 to 2 hr after the final wash. A custom macro was written to threshold and binarize each image and quantify bead number.

2.5.4 Enrichment of the CBF3-Complementing Activity and Mass Spectrometry

Conventional purification of the CBF3-complementing activity was performed using strain PS886. A fermenter was used to grow 100 liter cultures to mid-log phase. Cells were harvested using an ultrafiltration cassette followed by centrifugation. After a water wash, cell paste was directly extruded as fine vermicelli-like threads into liquid nitrogen using a compressor-driven caulk gun. Extracts were prepared by grinding the frozen cell paste threads in a liquid nitrogen-chilled stainless steel Waring blender. The fine cell powder was weighed and thawed by addition of an equivalent volume of 2X breakage buffer. Crude extract was clarified in two sequential 45,000 rpm spins (2 hr each, 4ºC) and frozen in 50 ml aliquots. For a standard prep, 125–150 ml extract was precipitated with 40% ammonium sulfate and the pellet was resuspended in 0.5X extract volume of BB300 and loaded onto a 1 liter S400HR gel filtration column volume (in BB300). Peak activity fractions were dialyzed into SB150 (100 mM Bis-Tris Propane, 150 mM KCl, 2 mM EDTA, 2 mM EGTA, 0.5 mM DTT, 10% glycerol, and protease inhibitors [pH 7.0]),

loaded onto a 1 ml Mono S column, and eluted with a 20 column volume SB150 to SB1000 gradient. TCA was added to a final concentration of 20% to 50 mg of the Mono S pool, and the sample was left overnight on ice. The precipitate was washed in cold acetone and analyzed by MudPIT mass spectrometry (Washburn et al., 2001).

2.5.5 HA Immunodepletions, TAP Purifications, and Antibody Production

For immunodepletions, extracts prepared from 6HA-tagged strains were diluted with an equal volume of extract dilution buffer (50 mM Bis-Tris Propane, 1mMEDTA, 1mMEGTA, and 5% glycerol, plus protease inhibitors) clarified by centrifugation at 80,000 rpm for 10 min at 4ºC in a TLA100.2 rotor and added to 25 ml anti-HA resin (Roche). The bead/extract mix was rotated at 4ºC for 2 hr, and the supernatant was used for assays and quantifying depletions. TAP tagging and purifications were carried out as described (Cheeseman et al., 2002). GST-Ipl1 (full length), GST-Sli15 (aa 558–698), and GST-Bir1 (aa 700–945) were used as antigens for injection into rabbits. Affinity purifications were performed using standard methods.

2.6 Acknowledgments

We are grateful to Sue Biggins and Iain Cheeseman for advice and encouragement, Paul Maddox for help with imaging, Scott Emr for use of his tetrad dissection scope, David Drechsel for help with the fermenter, and the yeast chromosome segregation community for its generosity, especially the

Biggins, Drubin, Barnes, Kilmartin, Nasmyth, and Murray labs. For comments on the manuscript, we thank Don Cleveland, Ben Black, Iain Cheeseman, and Reto Gassmann. This work was supported by a training grant from the National Cancer Institute (to S.S.), by a grant from the National Center for Research Resources, NIH to Trisha N. Davis (P41 RR11823), by grants from the Human Frontier Science Program and the NIH to A.D., and by the Max Planck Institute (to F.S. and A.H.). K.O. is a Pew Scholar in the Biomedical Sciences; A.D. is the Connie and Bob Lurie Scholar of the Damon Runyon Cancer Research Foundation (DRS 38-04). K.O. and A.D. receive salary and additional support from the Ludwig Institute for Cancer Research. This chapter has appeared in print under the following citation: Sandall S., Severin F., McLeod, I., Yates, J.R., Oegema, K., Hyman, A.A., Desai, A. *A Sli15-Bir1 complex connects centromeres to microtubules and is the likely tension sensor controlling Aurora B activation.* Cell, 2006 (127):1179-1191. The dissertation author was the primary author of this paper.

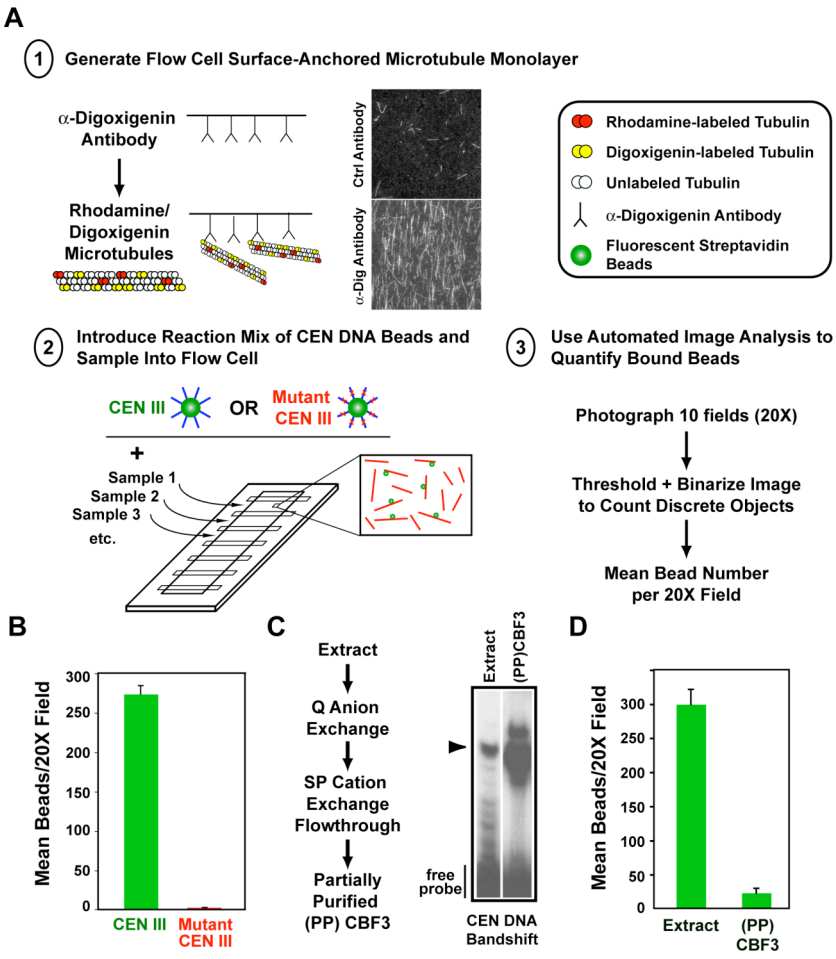


Figure 2.1 A Quantitative In Vitro Assay for the Binding of Budding Yeast CEN DNA to Microtubules

(A) Schematic of the in vitro assay. Adaptations to the original scheme important for quantitative biochemical analysis are emphasized here and include the following: (1) stable adsorption of microtubules using tubulin covalently modified with digoxigenin, (2) multiplexing of flow cells on a single slide, and (3) automated image analysis to measure number of bound beads. For quantification, 10 fields at 20X magnification are photographed and averaged.

(B) Linkage of beads to microtubules is observed with wild-type but not mutant CEN DNA. The mutant harbors a deletion of the central CCG in CDEIII that prevents binding of the CBF3 complex and abolishes centromere activity in vivo. Error bars show SD.

(C) Partial purification of CBF3 using a CEN DNA gel shift assay. The flow chart describes the chromatography steps, and the gel panel shows enrichment of the CEN DNA band shift relative to starting extract in the partially purified (PP) fraction. The arrowhead marks the CBF3-CEN DNA complex.

(D) Partially purified CBF3 does not link CEN DNA beads to microtubules. Note that the volume of starting extract used to prepare the CBF3 added to the (PP)CBF3 reaction is 25-fold greater than that assayed in the extract reaction. If equivalent extract volumes are assayed, no binding is observed with (PP)CBF3. Error bars show SD.

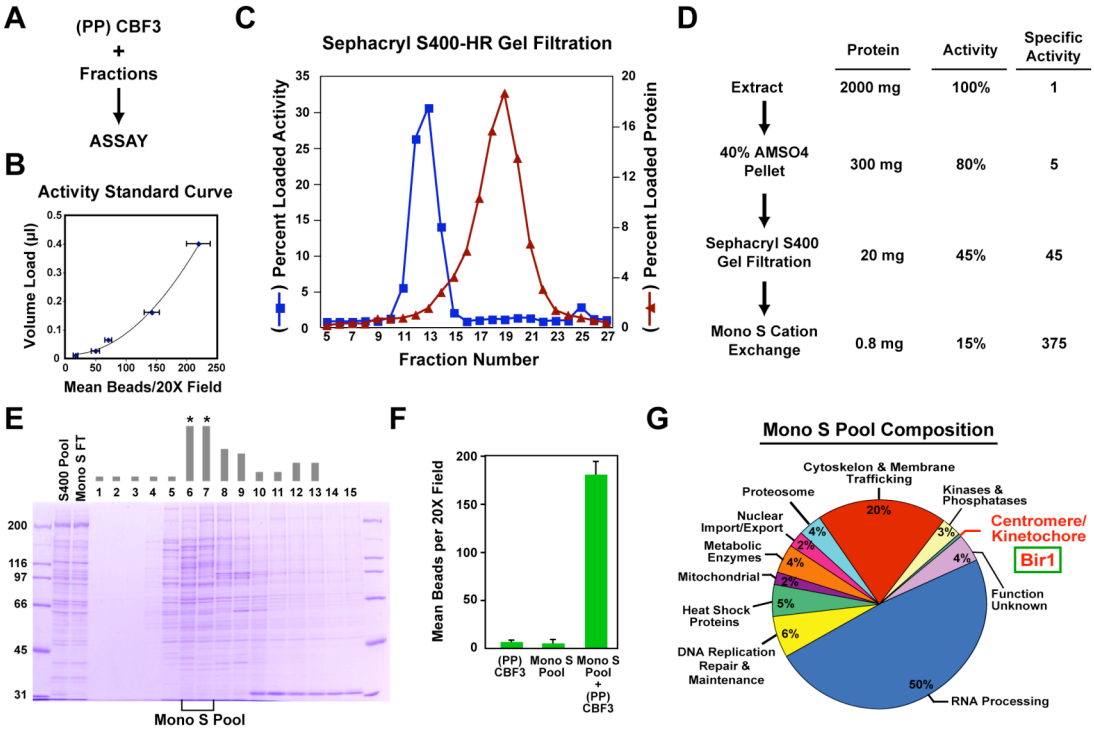


Figure 2.2 Conventional Purification of an Activity that Complements CBF3 in the In Vitro Assay

(A) Schematic of the in vitro complementation approach.

(B) Example of a standard curve used to quantitatively monitor fractionation of the complementing activity. The starting material, in this case the gel filtration load, is serially diluted into a constant amount of (PP)CBF3, and the points are fitted to a polynomial curve. Complementing activity in each fraction measured after adding the same amount of (PP)CBF3 is converted to a percentage of total loaded activity. Error bars show SD.

(C) Column profile of Sephacryl S400HR gel filtration. The percentage of loaded activity calculated from the standard curve and the percentage of total loaded protein are plotted for each fraction.

(D) Summary of the complementing-activity purification. The activity column lists the percentage yield, relative to the starting extract, after each step.

(E) Fractions from the Mono S gradient elution stained with Coomassie blue. The complementing activity is indicated with the gray bars above each fraction. No activity is detected in the column flow through. Asterisks denote the two fractions that constitute the Mono S Pool.

(F) The Mono S Pool complements (PP)CBF3. Error bars show SD.

(G) Annotation-based classification of proteins identified by mass spectrometry of the Mono S pool. The 247 proteins that showed >10% sequence coverage are represented in the pie chart (see also Table 2.2).

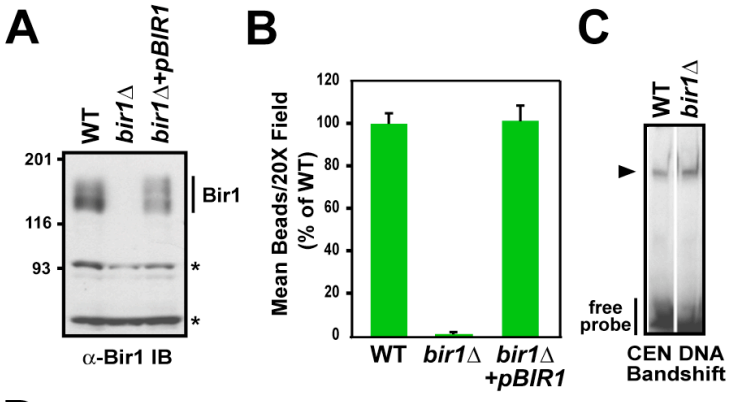


Figure 2.3 (A-C) Bir1 Is Required for Linking CEN DNA to Microtubules In Vitro

(A) *bir1Δ* cells lack Bir1 protein. Western blot of extracts prepared from wild-type (ODY49), bir1Δ (ODY65), and bir1Δ+pCEN-BIR1 (ODY114) strains probed with an anti-Bir1 antibody is shown. Asterisks indicate background bands that serve as loading controls.

(B) Bir1 is required for linking CEN DNA to microtubules. Extracts indicated in (A) were analyzed using the bead assay. Activity was normalized relative to the wild-type extract. Error bars show SD.

(C) Bir1 does not affect the ability of CBF3 to bind to CEN DNA. Arrowhead indicates position of the CBF3-CEN DNA complex.

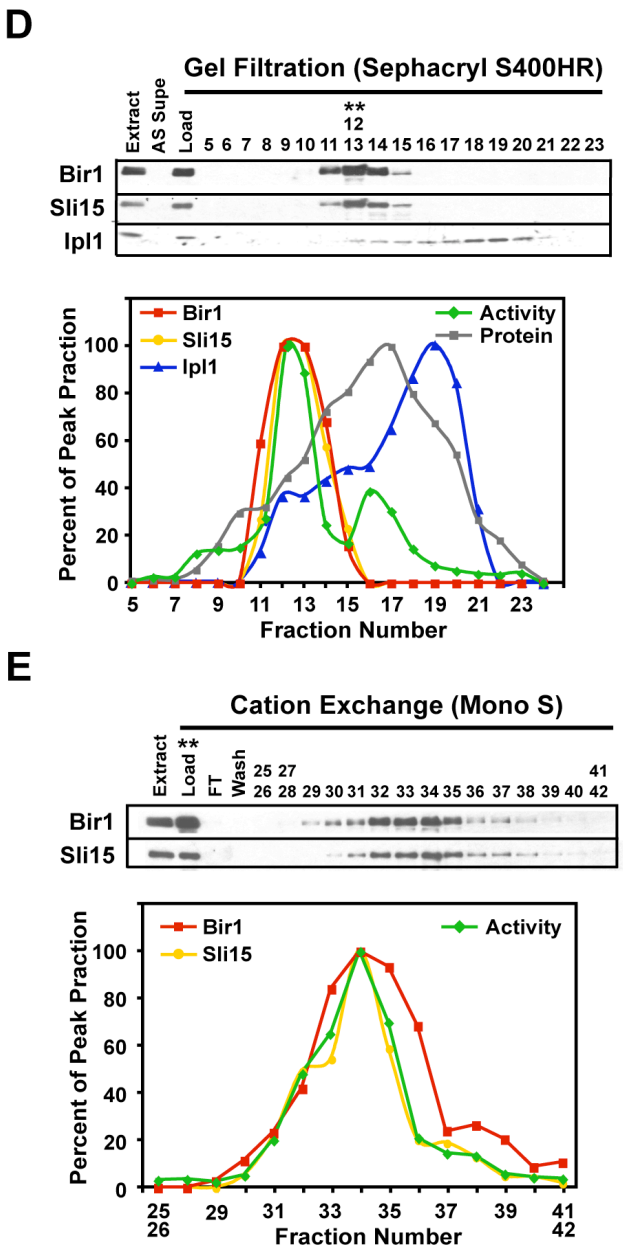


Figure 2.3 (D,E) Bir1 Is Required for Linking CEN DNA to Microtubules In Vitro

(D) Bir1 and Sli15, but not Ipl1, cofractionate with the complementing activity. Gel filtration fractions of extracts prepared from BIR1:6HA;SLI15:13Myc (ODY97) were analyzed by western blotting using anti-HA, anti-Myc, and anti-Ipl1 antibodies. The blot signal intensity for all three proteins, as well as activity in the bead assay, is plotted as a percentage of the respective peak fractions (12/13 for Sli15, Bir1, and activity; 18 for Ipl1).

(E) Bir1 and Sli15 continue to cofractionate with the complementing activity during the cation-exchange step. The activity peak from gel filtration (fractions 12/13 in [D]) was further fractionated using a Mono S cation-exchange column and analyzed as in (D)

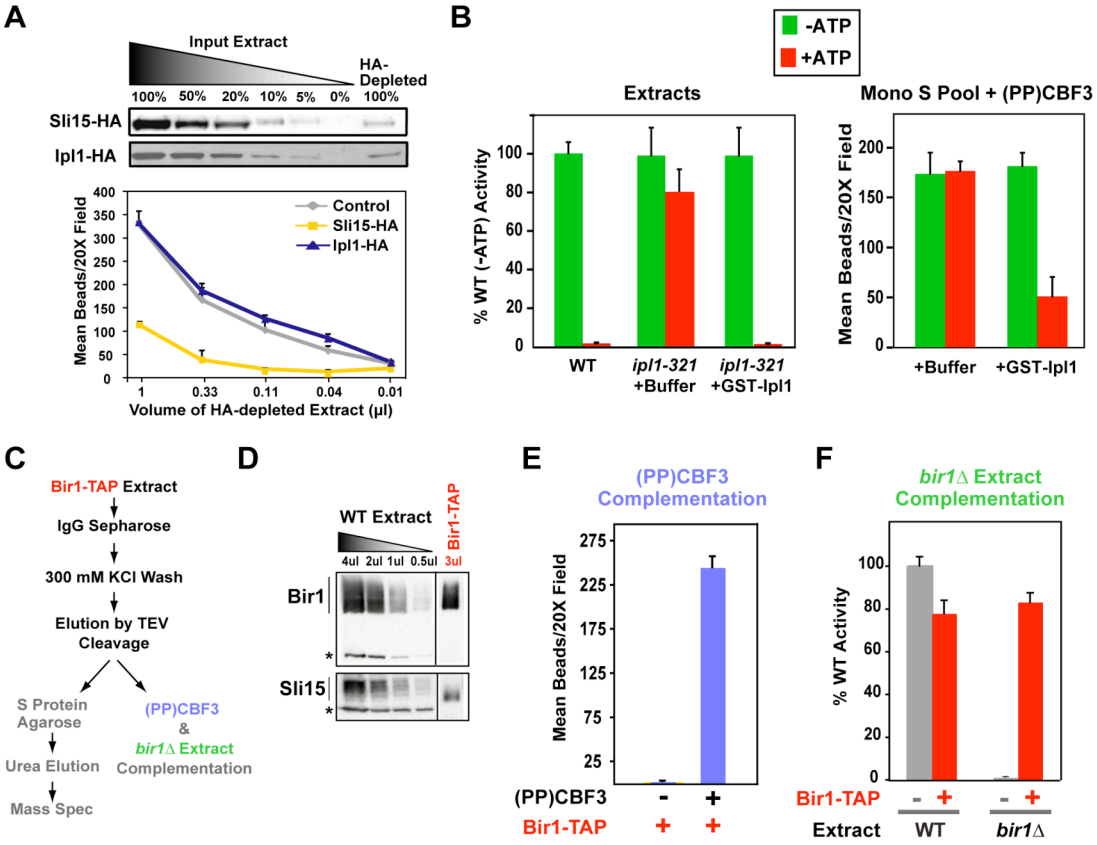


Figure 2.4 Sli15, but Not Ipl1, Is Required for the Complementing Activity

(A) Extracts prepared from SLI15:6HA (ODY54) and IPL1:6HA (ODY55) cells were immunodepleted using an anti-HA affinity resin. The depleted supernatants were serially diluted, and complementing activity was measured with constant (PP)CBF3. Comparing a standard curve of the input extract to the depleted extract using anti-HA immunoblotting assessed depletion efficiency. Both Sli15 and Ipl1 were successfully depleted by >90%, but only the Sli15 depletion resulted in a severe activity reduction. Error bars show SD.

(B) Ipl1 kinase activity regulates the binding observed in the in vitro assay. *ipl1-321* mutant extracts are insensitive to ATP addition, which is in contrast to wild-type extracts. Addition of purified GST-Ipl1 protein restores ATP sensitivity to the mutant extracts. The Mono S pool combined with (PP)CBF3 is ATP insensitive in the bead assay but becomes sensitive following addition of GST-Ipl1. Error bars show SD.

(C) Flow chart describing the purification and use of the Bir1-TAP complex.

(D) Immunoblot of Bir1-TAP after elution by TEV cleavage. Both Sli15 and Bir1 are present in the elution.

(E) Bir1-TAP complements (PP)CBF3. Error bars show SD.

(F) Bir1-TAP complements loss of activity in *bir1Δ* extracts. In both (E) and (F), the amount of Bir1-TAP added is similar to that present in 2 ml of extract, which is the standard amount analyzed in the bead assay (D). Error bars show SD.

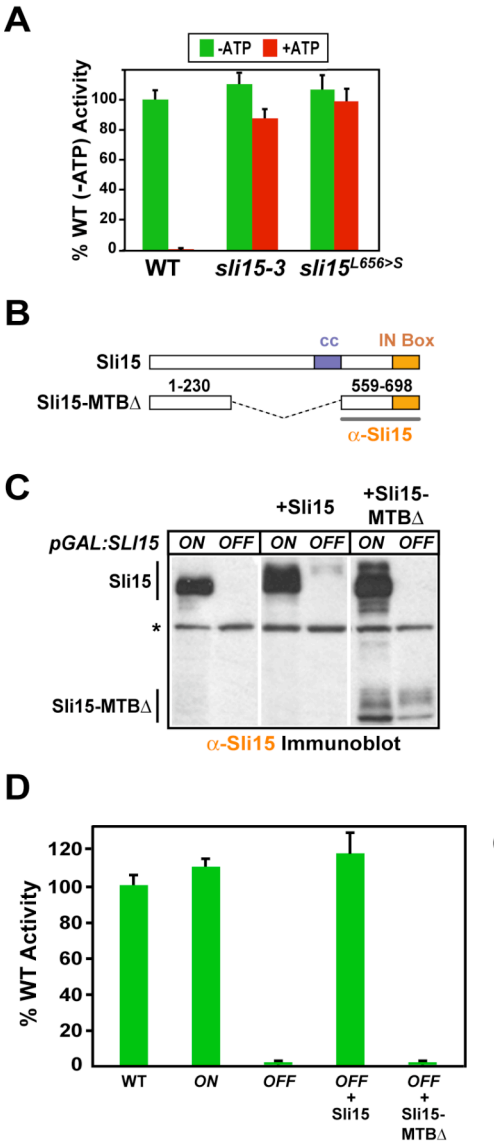


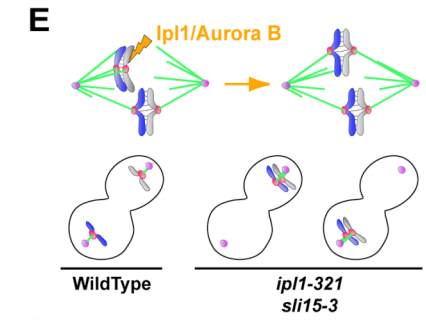
Figure 2.5 (A-D) Sli15 Mutants that Eliminate CEN DNA-Microtubule Interactions In Vitro Phenocopy Ipl1 Kinase Activation Mutants In Vivo

(A) *sli15-3* extracts behave similarly to *ipl1* kinase mutant extracts. *sli15*$^{L656>S}$ is an engineered mutant with the IN box amino acid change in *sli15-3* (see Figure S2.3). Error bars show SD.

(B) Schematic of Sli15 and the Sli15-MTBΔ mutant lacking the central microtubule-binding domain. The C-terminal region used to generate the anti-Sli15 antibody is underlined.

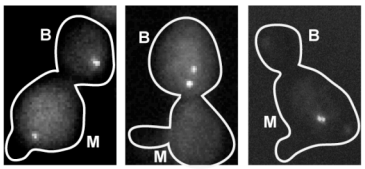
(C) Immunoblotting of ODY155 (pGAL-SLI15), ODY192 (pGAL-SLI15+Sli15), and ODY193 (pGAL-SLI15+Sli15-MTBΔ) in galactose (ON) or glucose (OFF) medium. All SLI15^{OFF} samples were prepared from cells arrested with nocodazole to maintain viability. Asterisk denotes the background band that serves as a loading control. See also Figures S2.4 and S2.5.

(D) Depletion of Sli15 or deletion of its microtubule-binding domain eliminates the CEN DNA-microtubule linkage in vitro. Error bars show SD.



F

B (bud), M (mother)



100%	0%	0%	WT
95.3%	4.7%	0%	*SLI15*^{ON}
7.1%	49.6%	43.3%	*SLI15*^{OFF}
97.6%	1.6%	0.8%	*SLI15*^{OFF} +Sli15
9%	48.4%	42.6%	*SLI15*^{OFF} +Sli15-MTBΔ

G

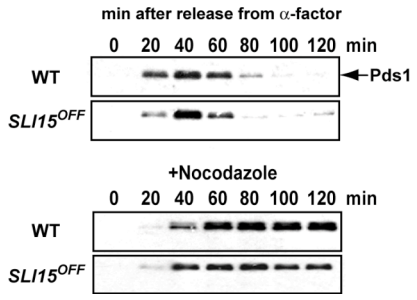


Figure 2.5 (E-G) Sli15 Mutants that Eliminate CEN DNA-Microtubule Interactions In Vitro Phenocopy Ipl1 Kinase Activation Mutants In Vivo

E) Ipl1/Aurora B is required for the correction of attachment errors where both sister chromatids are connected to the same spindle pole (syntellic attachment; upper panels). Mutants that perturb Ipl1 kinase activity (*ipl1-321*, *ipl1-2,* and *sli15-3*) fail to correct syntelic attachments, resulting in sister chromatid missegregation (lower panels).

(F) *SLI15*^{OFF} *and SLI15*^{OFF}*+Sli15-MTBΔ* both phenocopy ipl1 kinase activity mutants in vivo. Segregation of a marked Chr IV was monitored 120 min after release from α–factor arrest. Between 100 and 200 cells for each strain and growth condition were analyzed. The mother cell (M) was identified by residual a factor-induced shmoos (projections in cell outline).

(G) *SLI15*^{OFF} cells do not arrest in the cell cycle despite having a functional checkpoint. Wild-type (SBY818) and pGAL:SLI15 cells expressing Pds1-Myc18 (ODY181) were grown as described above. Nocodazole was added to one set of cultures at 10 mg/ml upon release from α-factor. Lysates were immunoblotted with an anti-Myc antibody.

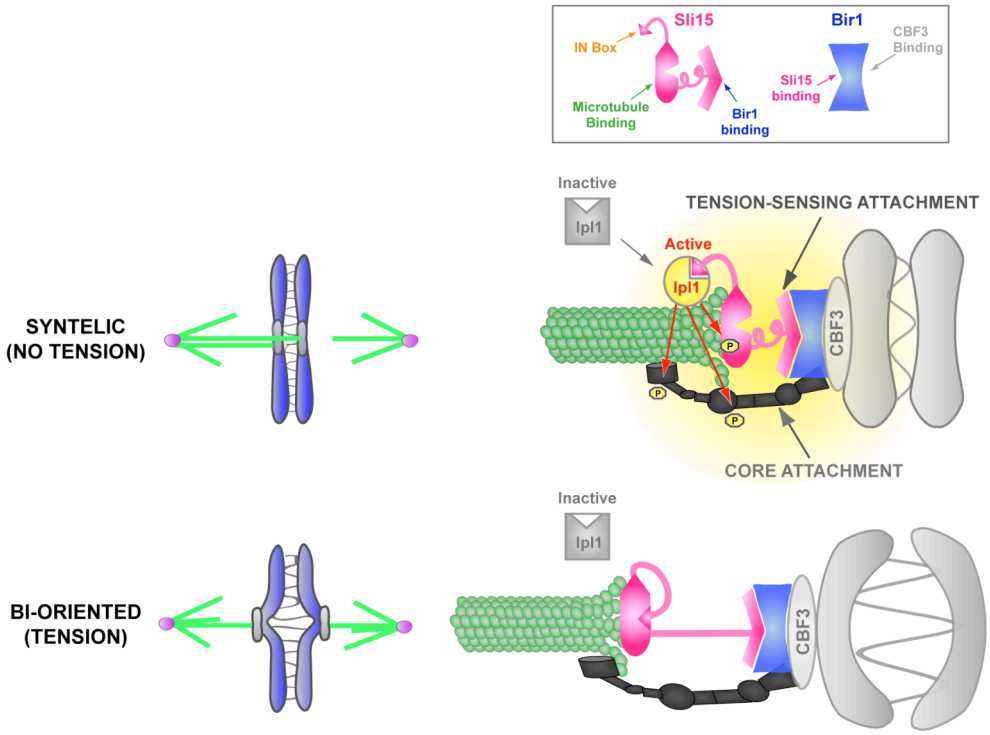


Figure 2.6 A Model for Tension-Regulated Ipl1 Activation by the Bir1-Sli15-Mediated Linkage between Centromeres and Microtubules

The central tenet of the model is based on the finding that the Bir1-Sli15-mediated linkage between CBF3-CEN DNA and microtubules is required for correction of syntely, but not for the core attachment between centromeres and microtubules in vivo. We propose that this linkage constitutes a tension-sensing attachment that is modulated by the primary force-generating (or force-transducing) core attachment such that syntely (no tension) promotes Ipl1 activation. Active Ipl1 phosphorylates multiple targets (red arrows) to dissociate the centromere from the microtubule. Biorientation (tension) silences Ipl1 activation, stabilizing the correct configuration.

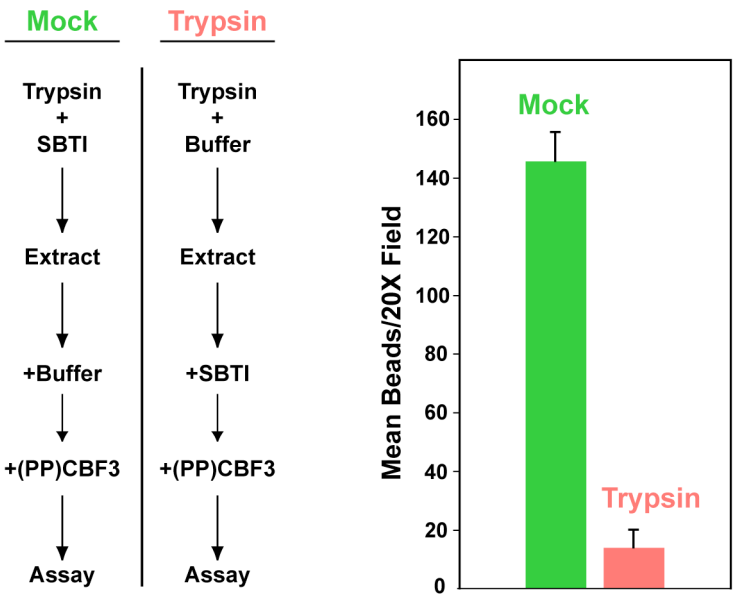


Figure S2.1 The CBF3 complementing activity is sensitive to protease treatment.

Mock reactions, where trypsin was pre-inhibited by incubation with Soybean Trypsin Inhibitor (SBTI) before addition to extract, and trypsin reactions, where extract was incubated first with trypsin and SBTI subsequently added, were analyzed for their ability to complement partially purified CBF3 in the bead assay. Trypsin treatment dramatically reduced complementing activity, indicating that the responsible factor is a protein(s). Inhibition of trypsin after SBTI addition was confirmed by doping control assays performed using untreated extract with the trypsin reaction after SBTI addition. No negative effect was observed indicating that the reduction of binding cannot be explained by the action of residual active trypsin on (PP)CBF3. Error bars=SD

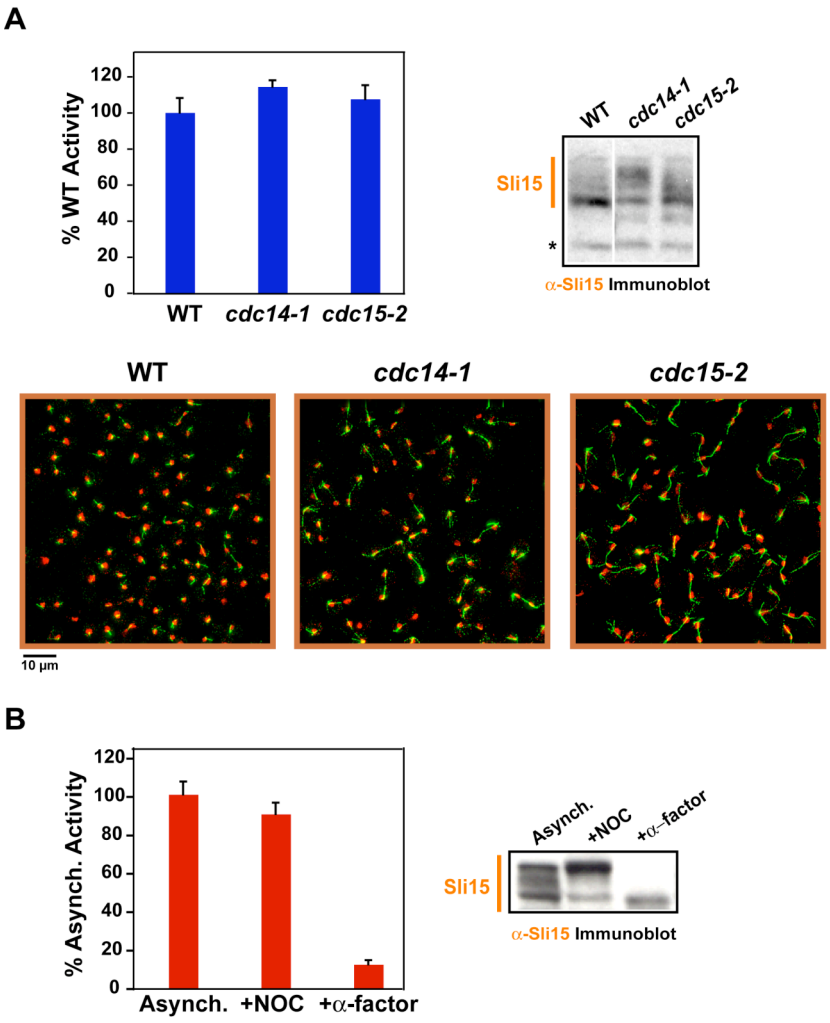


Figure S2.2 The Bir1-Sli15 mediated in vitro linkage between CEN DNA and spindle microtubules does not specifically reflect activity of anaphase dephosphorylated Sli15.

(A) Comparison of CEN DNA-microtubule linkage activity in extracts prepared from wildtype, *cdc14-1*, and *cdc15-2* cell following incubation at 35°C for 2 hours. No significant differences were detected in 5 experiments on 3 independently prepared extracts. Immunoblots indicate the persistence of phosphorylated Sli15 forms despite the late anaphase arrest in the mutants. Image panels show that mutants exhibited the elongated spindle arrest phenotype at the time when cells were harvested for extract preparation. Scale bar is 10 μm. Error bars=SD

(B) Comparison of CEN DNA-microtubule linkage activity and Sli15 migration on immunoblots in asynchronous, nocodazole-treated and alpha-factor treated cells. Sli15 accumulates in a hyperphoshorylated state in nocodazole-arrested mitotic cells and is almost fully dephosphorylated in alpha-factor arrested G1 cells. CEN DNA-microtubule linkage activity is high in the former but very low in the latter, which is converse to the proportion of dephosphorylated Sli15 present in the assayed extracts. Error bars=SD

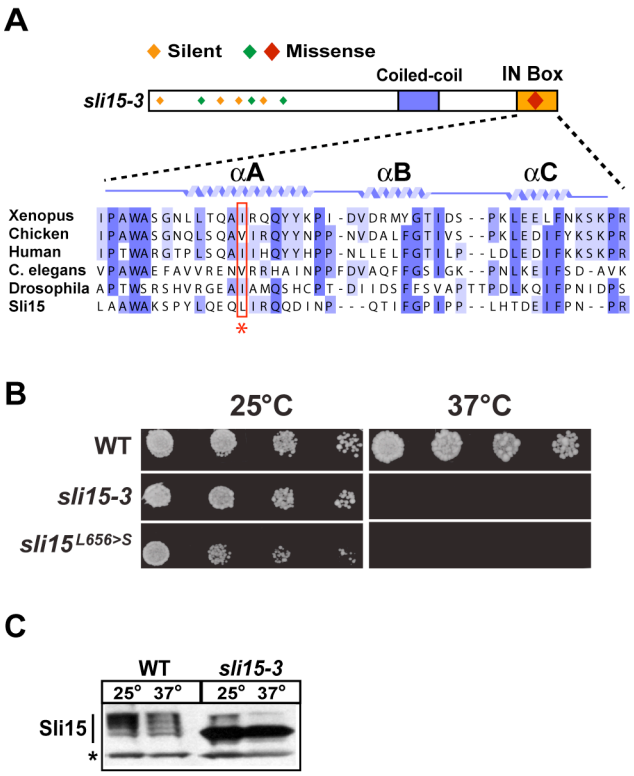


Figure S2.3 *sli15-3* encodes a mutant protein specifically defective in Ipl1 activation.

(A) The *sli15-3* mutant harbors an amino acid change indicating a specific defect in Ipl1 activation. The 7 nucleotide changes include 4 silent mutations (orange diamonds), 3 missense mutations outside the IN box (green diamonds), and 1 missense mutation within the IN box (large red diamond). Alignment of IN boxes from the indicated organisms indicates that leucine 656 (*red asterisk*), the residue mutated to serine in *sli15-3*, represents a conserved hydrophobic residue in the amphipathic £\-A helix (Sessa et al., 2005). Genomic DNA from *sli15-3* was isolated and the *SLI15* locus amplified in four independent PCR reactions. The resulting PCR product was sequenced using 6 primers spanning the locus and each mutation was verified by its presence in both the forward and reverse directions in at least 3 of the 4 independent PCR reactions.

(B) The Leucine 656-to-serine mutation is sufficient to confer the temperature sensitive growth phenotype observed in *sli15-3* cells. Five-fold dilutions of wildtype (WT), *sli15-3,* or $SLI15_{L656>S}$ (ODY182) were plated onto YPD and grown at 25° or 37° for 3 days.

(C) In *sli15-3* extracts, mutant Sli15 protein is present but with altered phosphorylation. Mid-log phase wildtype (WT) or *sli15-3* cultures were kept at 25°C or shifted to 37°C for 3 hours. Immunoblot analysis revealed that slower migrating phosphoisoforms of Sli15 are absent in *sli15-3* extracts. The asterisk denotes a background band, which serves as a loading control.

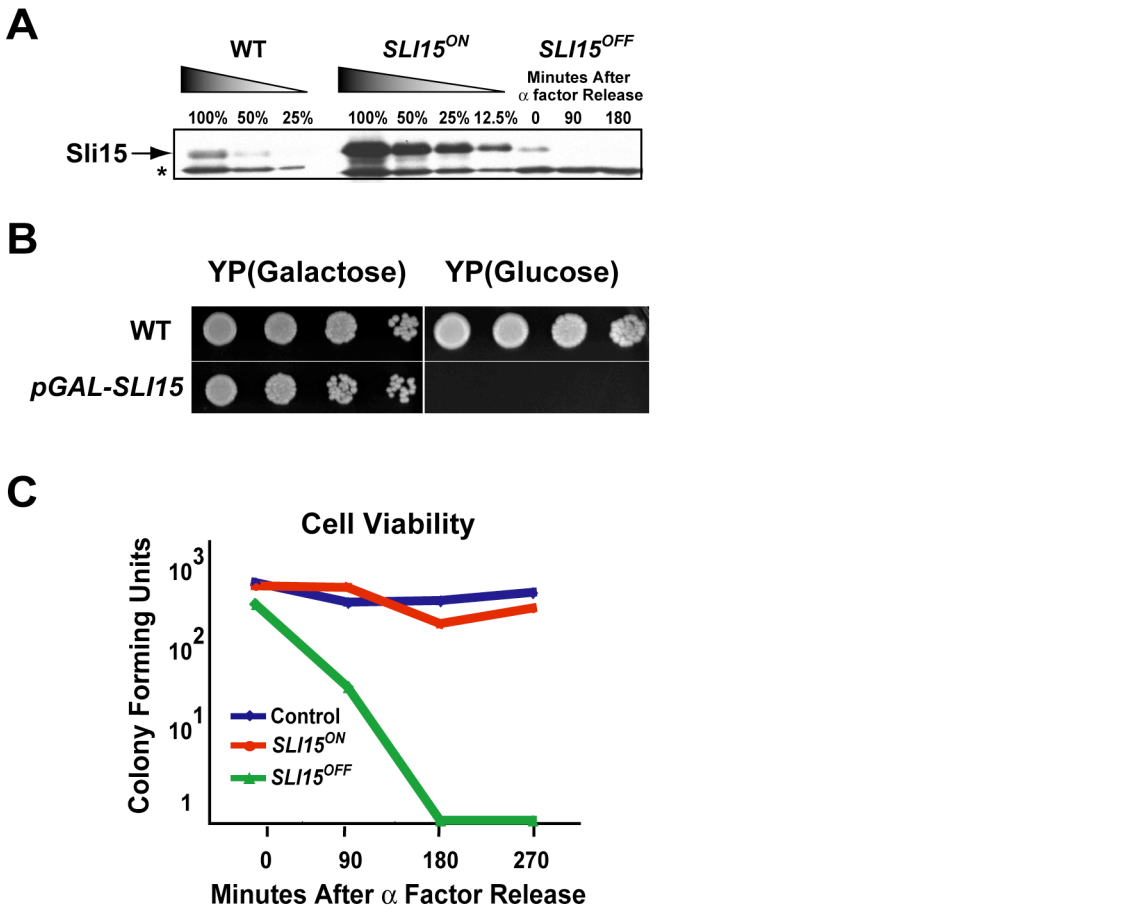


Figure S2.4 Repressing Sli15 expression causes rapid loss of cell viability.

(A) A promoter-shutoff strategy effectively eliminates Sli15 protein in vivo. Samples of WT (SBY214) and *pGAL-SLI15* (ODY155) cells arrested using alpha factor in the presence of galactose were used for the "WT" and "$SLI15^{ON}$" standard curves. Cultures were transferred into glucose ($SLI15^{OFF}$) or galactose ($SLI15^{ON}$) medium containing alpha factor and released from the arrest after 1 hour into fresh medium. Lysates were immunoblotted using the anti-Sli15 polyclonal antibody. Asterisk denotes the background band that serves as a loading control.

(B) *pGAL-SLI15* cells fail to grow on glucose-containing medium. Five-fold dilutions of either wildtype (WT) or *pGAL-SLI15* (ODY170) were plated onto YP that contained either 2% glucose or 1% each of raffinose and galactose and grown at 30°C for 3 days.

(C) Shutting off Sli15 expression causes rapid loss of cell viability. Cells were synchronized using alpha factor in medium containing galactose. At the indicated time points after releasing from the alpha factor arrest and shifting the medium to glucose ($SLI15^{OFF}$) or galactose ($SLI15^{ON}$), cultures were serially diluted and plated onto galactose-containing agar plates. Colonies formed after 3 days at 25°C were counted.

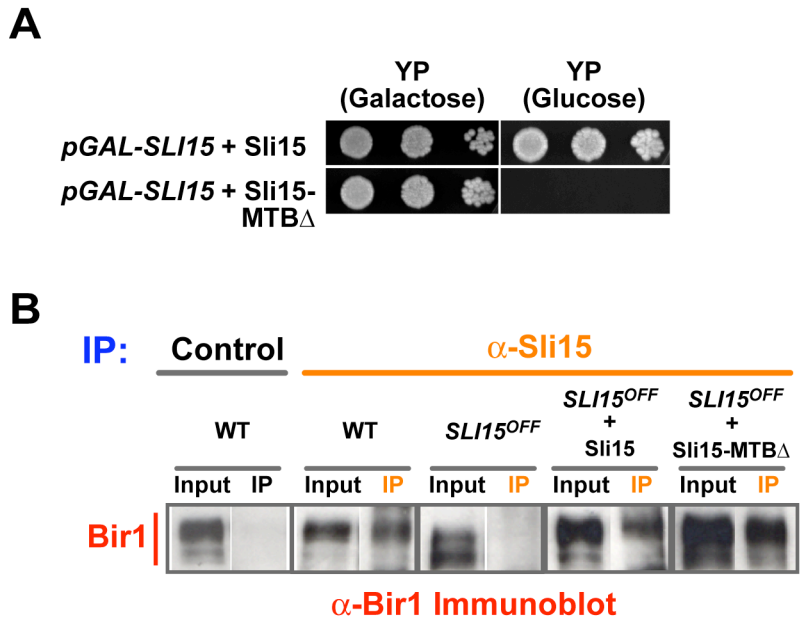


Figure S2.5 The Sli15-MTBΔ mutant fails to support cell viability but retains the ability to interact with Bir1.

(A) *pGAL-SLI15* cells expressing either full length Sli15 or Sli15-MTBΔ (ODY192 and ODY193, respectively) were plated as described in Suppl. Figure 4B. The Sli15-MTBΔ mutant failed to support cell viability when *pGALSLI15* expression was silenced.

(B) The Sli15-MTBΔ mutant retains the ability to interact with Bir1. The indicated extracts were used as the inputs for either random rabbit IgG (Control) or anti-Sli15 immunoprecipitations. The input extract and the immunoprecipitates were blotted with the affinity-purified anti-Bir1 antibody. All extracts in which *pGAL-SLI15* expression had been shut off were prepared from cells arrested with nocodazole to maintain cell viability. The dramatic change in Bir1 migration in cells lacking any Sli15 (*SLI15*^{OFF}) suggests that in the absence of its binding partner, Bir1 modification status is significantly altered; proteolysis may also contribute to the mobility shift. The comparable migration profile of Bir1 in the wild-type, *SLI15*^{OFF}+Sli15, and *SLI15*^{OFF}+Sli15-MTBΔ extracts supports the conclusion from the immunoprecipitations that the Sli15-MTBΔ mutant retains the ability to interact with Bir1.

Table 2.1 Candidates Tested in the In Vitro CEN DNA-Microtubule Interaction Assay Using Mutants / Immunodepletions

Candidate	Mutants / Immunodepletions Tested[1]	Binding in Bead Assay[2]
CBF3 Complex	*ndc10-1, ctf13-30, cep3-2*	***Eliminated***
Ctf19 Complex	*ctf19*Δ*, mcm21*Δ*, okp1-5*	Normal
	CTF19:6HA, MCM21:6HA OKP1:6HA	Normal
Mis12 Complex	*mtw1-1*	Normal
	MTW1:6HA	
Ndc80 Complex	*ndc80-1, nuf2-61, spc24-1, spc25-1*	Normal
	NDC80:6HA, NUF2:3HA, SPC24:3HA, SPC25:3HA	Normal
Dam1 Complex	*dam1-11, duo1^{TD}, ask1-1*	Normal
	DAM1:6HA	
Mitotic Checkpoint Pathway	*mad1*Δ*, mad2*Δ*, mad3*Δ*, bub1*Δ*, bub2*Δ*, bub3*Δ	Normal
Centromeric Chromatin	*cse4, mif2-3*	Normal
	MIF2:6HA	
Microtubule-Associated Proteins	*stu2 (Cu^{++}-shutoff); bim1*Δ*, bik1*Δ*, ase1*Δ	Normal
	STU1:6HA, ASE1:6HA	
Motor Proteins	*cin8*Δ*, kip1*Δ*, kip2*Δ*, kip3*Δ*, kar3*Δ	Normal
Other	*slk19*Δ, cohesin (*scc1*), *sgo1-100, sgo1*Δ	Normal

[1]Isogenic wildtype cells were processed in parallel with all mutants tested

[2]Except for CBF3 mutants, serial extract dilutions in the presence of constant (PP)CBF3 were performed to quantitatively assess complementing activity in mutant/immunodepleted extracts; for mutants, extracts were also tested without (PP)CBF3 addition

Table 2.2 Composition of MonoS Pool

Locus	% Coverage	MW	PI	Other Names
RNA Processing				
YBL092W	73.1	11284	9.8	RPL32
YEL026W	58.7	13569	7.9	Snu13
YPL011C	56.7	40296	4.8	Taf3/Taf47
YPL129W	56.1	27440	5.3	Taf14/SWP29, TAF30, TFG3, ANC1
YDR190C	53.6	50453	5.9	Rvb1
YNL182C	51.5	61773	5.7	Ipi3
YPL235W	49.9	51612	5.3	Rvb2
YNL113W	49.3	16151	4.4	Rpc19
YLR182W	48.7	90559	4.58	Swi6/ PSL8/ SDS11/
YHR197W	45.9	86667	5.7	Rix1
YMR044W	44.8	55427	5.3	Ioc4
YKL014C	44.8	203286	7.3	Urb1
YNL178W	43.1	26372	9.4	Rps3
YLR221C	42.7	24656	4.9	Rsa3
YMR236W	42.7	17315	6.3	Taf9/Taf17
GR271W	42.6	224828	6.5	SLH1
YKR026C	42.6	34025	5.3	GCN3
YLR197W	41.7	56864	8.9	SIK1/NOP56
YHL034C	40.1	32990	5.7	SBP1
YGL112C	38.6	57902	5.4	Taf6/Taf60
YDL014W	38.5	34465	10.2	Nop1
YPL007C	38.3	67684	6.2	Tfc8
YML015C	38.2	40624	5.7	Taf11/Taf40
YBR103W	37.8	59145	5	SIF2/EMB1
YOR210W	37.1	8278	7.8	RPB10
YGR145W	36.9	81748	6.6	ENP2
YLR175W	36	54705	8.9	CBF5
YOR310C	35.8	56956	8.9	NOP5/NOP58
YDR045C	35.5	12513	5	Rpc11
YJR041C	35.4	27112	9.9	Urb2
YDR167W	35	23019	4.6	Taf10/Taf23/Taf25
YBR245C	34.5	131102	6.6	Isw1/Sgn2
YLR291C	33.6	42570	7.9	Gcd7
YPR043W	33	9960	10.4	Rpl43A
YLL036C	32.6	56570	5.2	Prp19/Pso4
YIL018W	32	27277	11.1	Rpl2B/Rpl5A/Lot2
YFR037C	32	63168	5.4	Rsc8
YBR191W	31.9	18242	10.4	Rpl21A/Urp1
YOL144W	31.2	56966	6	Nop8
YBR198C	31.2	88968	7.4	Taf5
YDL056W	31.1	93908	9.3	Mbp1
YGR274C	31.1	120696	7.5	Taf1/Taf130/Taf145
YLR106C	30.5	559316	5	Mdn1/Rea1
YER127W	30.3	40794	6.9	LCP5/
YLR384C	30	152990	5.1	IKI3/ELP1/TOT1
YPR034W	29.4	54832	5.5	ARP7/SWP61
YML063W	29.1	28612	10	RPS1B/PLC2/RP10B
YAL035W	29	112268	5.8	FUN12/YIF2
YCR031C	28.5	14537	10.7	RPS14A
YLR095C	28.4	93446	5.8	Ioc2
YLR321C	27.9	48777	5.2	SFH1
YIL126W	27.6	156742	6.7	STH1/NPS1
YML127W	27.4	65218	7.8	Rsc9
YPL220W	26.7	24486	9.7	RPL1A/SSM1
YCR052W	25.9	54165	4.9	Rsc6
YKL180W	25.5	14473	10.3	RPL17A
YHR165C	25.4	279502	7.3	PRP8/DBF3/RNA8
YML093W	25.3	103023	5.1	Utp14
YIL148W	25.1	27994	10	RPL40A/UBL1
YPL139C	24.8	51022	5.3	UME1
YDR211W	24.7	81161	4.8	GCD6
YMR005W	24.5	42336	9.7	TAF4/MPT1
YML063W	24	28812	10.8	RPS1B/PLC2/RP10B
YGL194C	22.1	51455	5.2	HOS2
YLR033W	21.9	57795	8.2	Rsc58
YMR033W	21.4	53810	5.5	ARP9
YNR009W	21.3	27564	10	Nrm1
YPR101W	21.1	20709	8.5	SNT309
YDR485C	21	92248	5.2	Vps72/Swc2
YBR123C	20.5	73554	5.4	Tfc1
YOR063W	20.2	43626	10.3	Rpl3/Mak8/Tcm1/Yor29-14
YKL156W/YHR021C	19.5	8879	9.1	Rps27A/B
YDL150W	19.4	46667	8.6	Rpc53/Rpc4
YNL330C	18.9	48904	5.5	Rpd3/Rec3/SDI2/SDS6/Mof6
YKL173W	18.7	114041	5.9	Snu114/Gin10
YBL074C	18.6	41688	5.1	Aar2
YML114C	18.6	57986	5	Taf8

Locus	% Coverage	MW	PI	Other Names
Heat Shock Proteins				
YDL229W	55.6	66470	5.4	SSB1
YAL005C	54.9	69526	5.1	SSA1
YNL209W	53.4	66463	5.5	SSB2
YLL024C	53.1	69339	5.1	SSA2
YBR072W	48.4	23748	5.5	HSP26
YNL064C	46.7	44671	6.3	Ydj1/Hsp40
YLR259C	34.4	60752	5.3	Hsp60
YHR064C	27.8	62186	5.2	SSZ1/PDR13
YBL075C	15.9	70546	4.89	SSA3/YG106
YDR171W	12.8	42817	5.1	Hsp42
YER103W	12.8	69520	5.1	SSA4
YJR045C	11.2	70628	5.6	SSC1
Mitochondrial Proteins				
YKR027W	38.6	88044	5.7	FMP50
YGR086C	35.1	38349	4.6	PIL1
YJL005W	16.4	227832	7.3	Cyr1/CDC35/HSR1
YKR010C	11	86366	8	Tof2
YPL004C	10.3	38071	4.7	Lsp1
Metabolic Enzymes				
YJL130C	47	245123	5.9	URA2
YLR330W	45.5	73639	4.6	CHS5
YHR174W	22.5	46783	6	ENO2
YLK152C	19.5	27477	8.8	GPM1
YGR254W	18.8	46783	6	ENO1
YGR240C	14.7	107970	6.4	PFK1
YLR180W	14.4	41818	5.2	SAM1
YMR246W	14.1	77267	6.6	FAA4
YNR016C	12	250351	6.3	ACC1
YAL038W	11.6	54545	7.7	CDC19
YGR192C	11.2	35615	7	TDH3
Nuclear Import/Export				
YLR347C	44.9	94776	4.6	Kap95/RSL1
YNL189W	31	60441	4.9	Srp1/Kap60/SCM1
YLR335W	21.7	77880	7.3	NUP2
YJL041W	16.3	86516	6.3	NSP1
YAR002W	16	59039	9.3	Nup60
YMR091C	10.8	49651	5	NPL6
Proteasome				
YHR027C	50.2	109492	4.6	RPN1
YDR394W	40.7	47970	5.5	RPT3
YBL068W	38	48828	6	PRS4
YER148W	29	48256	5.1	SPT15
YKL145W	28.3	51983	5.5	RPT1
YLR421C	28.2	17902	4.5	Rpn13
YOR259C	25.6	49408	5.7	RPT4
YIL075C	24.7	104232	6.2	RPN2/SEN3
YGL048C	15.6	45272	9	RPT6
Cytoskeletal & Membrane Trafficking				
YMR237W	56.5	82049	5.4	Bch1
YPL032C	44.5	92144	8.7	Svl3
YIL076W	41.9	33829	4.6	SEC28
YBR109C	38.8	16135	4.3	CMD1
YCR002C	38.5	37025	5.7	CDC10
YNL138W	37.5	57522	5.6	Srv2
YGL137W	36.7	99445	4.7	SEC27
YCR030C	35.9	96137	8.6	Syp1
YDR299W	35.6	61203	4.8	Bfr2
YLR208W	35.4	33043	5.7	Sec13
YFL039C	32	41690	5.7	ACT1/END7/ABY1
YHR158C	30.8	131094	5.4	Kel1
YBR127C	30.2	57749	5.1	VMA2/VAT2
YDR238C	29.5	109019	5.6	SEC26
YOR299W	29.5	84830	5.2	Bud7
YJL008C	29.4	58814	6.1	CCT8
YMR231W	27.1	117477	5.8	Pep5
YGL008C	25.7	99619	5.1	Pma1
YML085C	24.4	49800	5.1	Tub1
YPL218W	24.2	21451	5.4	Sar1
YBR102C	23.2	85538	7.9	Exo84
YNL287W	23	104831	5.1	SEC21
YGL233W	22	105064	4.9	Sec15
YPL045W	20.4	92741	7.1	VPS16
YFL037W	19.3	50923	4.7	Tub2/Arm10/She8
YPR055W	19.1	122224	6.8	SEC8
YLR166C	18.6	100342	6.3	Sec10
YIL068C	18.5	93428	5.1	SEC6
YDR080W	18.1	113412	4.9	VPS41

Table 2.2 (Continued) Composition of MonoS Pool

Locus	% Coverage	MW	PI	Other Names
RNA Processing (Contd.)				
YHR085W	18.3	37867	9.5	IPI1
YLR075W	18.1	25361	10	RPL10/GRC5/QSR1
YKR099W	17.9	89604	8.2	BAS1
YGL147C	17.8	21569	9.7	RPL9A
YGR047C	17.8	120229	5.3	TFC4
YGR178C	17.7	78782	6.9	PBP1
YNL075W	17.6	33482	9	IMP4
YML026C	17.4	17618	10.8	RPS18B
YOR207C	17.4	129456	8.2	RET1/PDS2/RPC2/RPC128
YBR154C	17.2	25079	9.1	RPB5
YHR121W	17.1	21314	9.4	Lsm12
YMR227C	17.1	67556	4.6	Taf7
YPL131W	16.8	33743	6.8	RPL5/LPI14/RPL1
YKR025W	16.7	32142	4.5	RPC37
YOR110W	16.6	49146	4.9	Tfc7
YNL096C	16.2	21634	10.7	RPS7B
YOR001W	15.8	84039	7.1	Rrp6
YHL004W	15.7	44152	8.8	MRP4
YMR309C	15.6	93204	5	NIP1
YGR083C	15.4	70852	9.4	GCD2/GCD12
TOL004W	15.3	174838	5.6	SIN3/UME4
YOR260W	14.7	65700	5	GCD1
YPR144C	14.7	63637	6.1	NOC4
YNL167C	14.4	70192	9.3	SKO1
YDR145W	14.3	61073	9.6	Taf12/Taf61/Taf68
YJL033W	14.2	87193	7.4	HCA4/DBP4/ECM24
*YGL031C:YGR148C	14.2	7614:175	11.9:1	RPL24A:RPL24B
YDL076C	13.9	33812	6.5	Rxt3
YLR357W	13.7	102300	8.9	RSC2
YOR116C	13.6	162301	8.2	RPO31
YCR042C	13.6	161470	5.7	TAF2
YKR0008	13.6	72276	5.2	RSC4
YJL081C	12.9	54832	5.5	ARP4/ACT3
*YIL133C:YNL069C	12.8	2201:222	3:11	RPL16A/RPL16B
YKL054C	12.5	83973	5	Def1
YPL151C	11.8	50700	7.2	PRP46
YDR334W	11.8	174530	6.2	Swr1
YOL139C	11.7	24254	5.5	CDC33
YDL152C	11.6	70260	4.7	SAS10/UTP3
YER111C	11.3	123806	8.8	SWI4/ART1
YKL143W	11.2	53390	4.7	LTV1
YMR019W	11.2	109825	7.3	STB4
YCR093W	10.5	240332	6.5	CDC39
DNA Replication/Repair				
YNL261W	50.3	55290	5.9	ORC5
YPR162C	43.9	60706	6.8	ORC4
YLL004W	43.5	72077	5.5	ORC3
YBR060C	39.5	71238	9.4	RRR1/SIR5
YML065W	37.1	104400	5.7	ORC1
YLR150W	21.6	29995	9.7	STM1/MPT4
YHR118C	17.7	50296	7.9	ORC6
YOL094C	13	36149	9.1	RFC4

*Almost identical proteins; peptides from mass spec were overlapping

Locus	% Coverage	MW	PI	Other Names
Cytoskeletal & Membrane Trafficking (Contd.)				
YAR014C	18.1	78334	4.6	Bud14
YDL077C	17.3	122881	7.1	VAM6
YPL036W	17.1	102171	4.75	Pma2
YDL145C	17.1	135607	6	COP1/RET1/SEC33
YDR166C	17	112121	5.8	SEC5
YJL123C	16.7	53477	4.6	/
YJL085W	16.7	71294	7.5	Exo70
YJR076C	16.1	47649	5	CDC11
YOR127W	15.3	112831	6.4	Rga1/Dbm1/The1
YLR314C	15.2	60039	5.5	CDC3
YLR396C	14.9	79271	5.3	VPS33
YER008C	14.7	154694	5.4	SEC3
YDR379W	14.5	113291	7.9	Rga2
YDL126C	12.5	91996	4.9	CDC48
YFR051C	12.5	60497	5.2	Ret2
YPL085W	12.4	241694	5.4	Sec16
YDL2266C	11.9	39396	5.9	Gcs1
YML124C	11.9	49694	4.9	Tub3
YLR148W	10.9	107398	7	Pep3
YJR064W	10.9	60677	5.5	CCT5/TCP5
Kinases & Phosphatases				
YBR059C	39.8	123989	7.7	AKL1
YNR031C	12.3	180527	5.9	SSK2
YJL095W	11.4	164195	9.5	BCK1
YLR006C	8.3	78529	7.2	Ssk1
YHR082C	3.4	117082	6.6	KSP1
YAL016W	33.1	70951	4.7	TPD3
YFR028C	30.7	61907	8	CDC14
YER133W	14.1	43047	4.8	GLC7
YDL188C	10.6	35907	5.5	PPH22
Centromere/Kinetochore Proteins				
YJR089W	18.7	108667	6.5	BIR1
Function unknown & Cellular Compartment Unknown				
YGR039W	20.4	198520	8.2	
YLR036C	17.8	198460	8.5	
Function unknown/Localize to Cytoplasm				
YIL041W	51.8	36670	5	GVP36
YGL110C	26.6	72043	7	Cue3
YMR031C	17.2	93345	6.3	
YOR042W	16.1	46870	4.8	Cue5
YIL161W	14.9	27112	10.7	ORF
YPR148C	14.7	49279	4.8	
YCL028W	12.8	42580	6.6	Rnq1
YBR172C	11.9	87098	8.8	Smy2
YPL070W	10.8	69539	8.5	Muk1
Function unknown/Localizes to Nucleus				
YMR075W	5.7	78836	8.8	Rco1
Function unknown/Localizes to Vacuoles				
YDR262W	5	146557	8.2	

Table 2.3 Composition of (PP)CBF3

NAME	LOCUS	% Coverage	MW	NAME	LOCUS	% Coverage	MW	NAME	LOCUS	% Coverage	MW	NAME	LOCUS	% Coverage	MW
SPT4	YGR063C	78.40%	11158	RPN8	YOR261C	31.80%	38181	NMA2	YGR010W	20.50%	44909	CCT2	YIL142W	13.50%	57203
EF1B	YAL003W	75.60%	22689	KAR2	YJL034W	31.70%	74468	DIP2	YLR129W	20.40%	106342	TEF1	YPR080W	13.50%	50033
TEF4	YKL081W	72.80%	46520	NUP2	YLR335W	31.50%	77881	CDC73	YLR418C	20.40%	44456	VPS41	YDR080W	13.40%	113412
RET3	YPL010W	72.50%	21688	RPB8	YOR224C	31.50%	16511	CBF5	YLR175W	20.30%	54705	EDC3	YEL015W	13.40%	61340
SEC21	YNL287W	68.40%	104831	TFA1	YKL028W	31.30%	54742	BMH1	YER177W	20.30%	29960		YHR122W	13.40%	25675
PUP2	YGR253C	68.10%	28617	CCT4	YDL143W	31.20%	57604	SHP1	YBL058W	20.10%	46987	RMP1	YLR145W	13.40%	23619
CDC48	YDL126C	67.40%	91996		YOL098C	30.80%	118392	LAA1	YJL207C	19.80%	229898	SSA4	YER103W	13.30%	69520
RPB4	YJL140W	65.60%	25414	NAP1	YKR048C	30.70%	47885	HPR1	YDR138W	19.80%	87829	IMP2'	YIL154C	13.30%	39071
PRE9	YJL140W	65.10%	28714	RXT3	YDL076C	30.60%	33812	SPT8	YLR055C	19.40%	66190	GGC1	YDL198C	13.30%	33215
SCL1	YGL011C	64.70%	28001	CCT8	YJL008C	30.50%	61662	HSP33	YOR391C	19.40%	25926	PAN1	YIR006C	13.20%	160266
GRX3	YGL011C	64.60%	32481	UTP15	YMR093W	30.40%	57686	SGF29	YCL010C	19.30%	29381	SAP155	YFR040W	13.20%	114880
CAM1	YPL048W	63.90%	47088	ARG82	YDR173C	30.40%	40353	FUN12	YAL035W	19.20%	112268	DRS1	YLL008W	13.20%	84843
SUI2	YJR007W	63.20%	34718	RIM1	YCR028C-A	30.40%	15386	BRE2	YLR015W	19.20%	58348	NPA3	YJR072C	13.20%	43195
PRE1	YJR007W	63.10%	22517	SPT5	YML010W	30.30%	115650	SEC13	YLR208W	19.20%	33043	YIP5	YGL161C	13.20%	34843
SUP45	YBR143C	62.70%	48991	ARP8	YOR141C	30.30%	100209	RPC37	YKR025W	19.10%	32142	PRS2	YER099C	13.20%	34765
RPN1	YHR027C	62.10%	109361	RPC34	YNR003C	30.30%	36135	HBS1	YKR084C	19.00%	68730	SIR3	YLR442C	13.10%	111360
SEC27	YGL137W	61.60%	99445	PUP1	YOR157C	30.30%	28268	TEX1	YNL253W	19.00%	47167	SIF2	YBR103W	13.10%	59145
RPB10	YOR210W	61.40%	8278	TOA2	YKL058W	30.30%	13458		YIL091C	18.90%	83991	VBA3	YCL069W	13.10%	50225
RPB7	YDR404C	58.50%	19058	UTP5	YDR398W	30.20%	72002	TSR2	YLR435W	18.90%	29003	PRY1	YJL079C	13.00%	30634
PRE4	YFR050C	58.30%	29443		YDR063W	30.20%	17130	TPS2	YDR074W	18.80%	102976	RPS1A	YLR441C	13.00%	28612
PRE5	YMR314W	57.70%	25604		YGR237C	30.10%	89241	THP2	YHR167W	18.80%	30299	RPS1B	YML063W	13.00%	28681
SSZ1	YHR064C	57.00%	62186	SRP68	YPL243W	30.10%	69006	OCA2	YNL056W	18.80%	22472	SIN3	YOL004W	12.90%	174838
PRE6	YOL038W	56.70%	28439	CTR9	YOL145C	29.90%	124751	UBP8	YMR223W	18.70%	53623	LCP5	YER127W	12.90%	40794
RNA1	YMR235C	56.50%	45816		YGL242C	29.80%	20074	ACT1	YFL039C	18.70%	41690	GRC3	YLL035W	12.80%	72258
RPC31	YNL151C	55.80%	27724	RPT1	YKL145W	29.60%	51983	RRP1	YDR087C	18.70%	33203	SDS3	YIL084C	12.80%	37625
RPB3	YIL021W	55.70%	35298	NIP7	YPL211W	29.30%	20381	YRB30	YGL164C	18.60%	50296	PCT1	YGR202C	12.70%	49406
COP1	YDL145C	54.90%	135607		YGR017W	29.00%	34679	TCP1	YDR212W	18.40%	60481	VTA1	YLR181C	12.70%	37316
PUP3	YER094C	54.10%	22605	CET1	YPL228W	28.80%	61822	HSM3	YBR272C	18.30%	55543	TDH3	YGR192C	12.70%	35615
RAD6	YGL058W	53.50%	19706	RPT4	YOR259C	28.80%	49408	RPN11	YFR004W	18.30%	34398		YHL026C	12.70%	30667
PRE7	YBL041W	53.10%	26871	IES3	YLR052W	28.80%	28243	LAG2	YOL025W	18.20%	77541	MCM1	YMR043W	12.60%	32802
RPC19	YNL113W	52.80%	16151	LTV1	YKL143W	28.50%	53390	PSY2	YNL201C	18.10%	98053	SWI6	YLR182W	12.50%	90560
PRE2	YPR103W	52.60%	31637	FCP1	YMR277W	28.40%	83441	SIW14	SIW14	18.10%	32755	TAF2	YCR042C	12.40%	161470
SEC28	YIL076W	52.00%	33829	VPS75	YNL246W	28.40%	30615	TFA2	YKR062W	18.00%	37054	SNU114	YKL173W	12.40%	114041
IK13	YLR384C	51.80%	152990	FAP7	YDL166C	28.40%	22723	CDC34	YDR054C	18.00%	34065	NPL6	YMR091C	12.40%	49651
PRE8	YML092C	51.60%	27162	SWH1	YAR042W	28.10%	135070	MET13	YGL125W	17.90%	68472	PRP4	YPR178W	12.30%	52442
ABP1	YCR088W	51.40%	65576		YGR001C	28.00%	22153	SAP30	YMR263W	17.90%	23026	SIP2	YGL208W	12.30%	46273
SNF4	YGL115W	51.20%	36401	ELP2	YGR200C	27.90%	89410		YOL087C	17.80%	125382	ATG3	YNR007C	12.30%	35887
PRE3	YJL001W	50.20%	23548	DPB4	YDR121W	27.60%	21997	NHP10	YDL002C	17.70%	23857		YAL027W	12.30%	29770
SEC26	YDR238C	49.80%	109019	PAH1	YMR165C	27.50%	95031	HFI1	YPL254W	17.60%	54466	OSH2	YDL019C	12.20%	145796
BCP1	YDR361C	47.70%	32661	TIF11	YMR260C	27.50%	17435	RTN1	YDR233C	17.60%	32916	NAN1	YPL126W	12.20%	101237
TAF14	YPL129W	47.50%	27440	DRE2	YKR071C	27.30%	38543	SPT20	YOL148C	17.50%	67797	AAR2	YBL074C	12.10%	41688
CIA1	YDR267C	47.30%	37275	MCM2	YBL023C	27.20%	98779		YMR258C	17.50%	64405	PRP8	YHR165C	12.00%	279502
POL30	YBR088C	47.30%	28916		YPL260W	27.10%	32759	NSP1	YJL041W	17.40%	86516	TRM11	YOL124C	12.00%	50073
RPB2	YOR151C	46.30%	138751	TOP2	YNL088W	27.00%	164214	IES1	YFL013C	17.30%	78753	RPA135	YPR010C	11.80%	135742
	YBR094W	45.80%	86439	RPT6	YGL048C	26.90%	45272	BUD21	YOR078W	17.30%	24385	CKA1	YIL035C	11.80%	44668
PIL1	YGR086C	45.70%	38349	CTF4	YPR135W	26.50%	104293	SEC16	YPL085W	17.10%	241694	ENO1	YGR254W	11.70%	46671
	YPR148C	45.50%	49279	AKL1	YBR059C	26.40%	123989	SKY1	YMR216C	17.10%	83238	ENO2	YHR174W	11.70%	46783
RPT5	YOR117W	45.40%	48256	GRX1	YCL035C	26.40%	12380	SIK1	YLR197W	17.10%	56864	ETR1	YBR026C	11.60%	40898
LSP1	YPL004C	45.20%	38071	RLR1	YNL139C	26.30%	183930	NBP1	YLR457C	16.90%	37354	SIT4	YDL047W	11.60%	35538
RRP5	YMR229C	45.10%	193133	UBP12	YJL197W	26.30%	143192	HSH155	YMR288W	16.70%	110028	RPS0A	YGR214W	11.60%	27893
DCP1	YOL149W	43.30%	26266	NUP60	YAR002W	26.30%	59039	GYS2	YLR258W	16.70%	80379	CDC27	YBL084C	11.50%	85437
GVP36	YIL041W	42.90%	36670	TPS1	YBR126C	26.10%	56148	RTG2	YGL252C	16.70%	65572	RUP1	YOR138C	11.50%	75361
SUI3	YPL237W	42.50%	31574	SRP54	YPR088C	25.70%	59624	SLG1	YOR008C	16.70%	39270	COG8	YML071C	11.50%	69829
RPB11	YOL005C	42.50%	13616	MDN1	YLR106C	25.40%	559316	LEU3	YLR451W	16.60%	100153	GAL83	YER027C	11.50%	46648
RPB5	YBR154C	42.30%	25079		YPL260W	25.40%	62780	VPS33	YLR396C	16.60%	79271	RPA190	YOR341W	11.40%	186431
KAP95	YLR347C	42.00%	94776	BBC1	YJL020C	25.00%	128296	PPH3	YDR075W	16.60%	35264	REB1	YBR049C	11.40%	91874
ZUO1	YGR285C	41.80%	49020	RPC53	YDL150W	24.60%	46667	SAP190	YKR028W	16.50%	117098	YMC1	YPR058W	11.40%	33376
RPC82	YPR190C	41.60%	74017	RPL5	YPL131W	24.60%	33743	POP1	YNL221C	16.50%	100395	VPS16	YPL045W	11.30%	92741
MET12	YPL023C	41.60%	73942	RPD3	YNL330C	24.50%	48904	SDS23	YGL056C	16.50%	58112	ARK1	YNL020C	11.30%	71373
PRE10	YOR362C	41.50%	31405	PEA2	YER149C	24.50%	48165	PRS1	YKL181W	16.40%	47048	**NDC10**	**YGR140W**	**11.10%**	**111917**
SNU13	YEL026W	41.30%	13569	RPC25	YKL144C	24.50%	24326	NRG2	YBR066C	16.40%	25009	HOS2	YGL194C	11.10%	51455
RPN13	YLR421C	41.00%	17902	NUP159	YIL115C	24.40%	158907	PEP5	YMR231W	16.30%	117477	MND2	YIR025W	11.10%	42826
	YJL123C	40.40%	53477	USO1	YDL058W	24.40%	147463	TFC7	YOR110W	16.30%	49146	HSP7F.	YPL106C	11.00%	77235
HCR1	YLR192C	40.40%	29564	NOP2	YNL061W	24.40%	69812	END3	YNL084C	16.30%	40297	IPI3	YNL182C	11.00%	61773
GCD11	YER025W	40.20%	57866		YBR030W	24.30%	62594	SSB2	YNL209W	16.00%	66463		YLR049C	11.00%	49493
SSA1	YAL005C	40.10%	69526	RPN5	YDL147W	24.30%	51769	SSB1	YDL229W	16.00%	66470	RTF1	YGL244W	10.90%	65869
SSA2	YLL024C	40.10%	69339	UME1	YPL139C	24.30%	51022	RPA43	YOR340C	16.00%	36224	ZPR1	YGR211W	10.90%	55072
GLC7	YER133W	40.10%	35907	NBP2	YDR162C	24.20%	26571	UBP2	YOR124C	15.80%	146354	GDH3	YAL062W	10.90%	49627
RPT2	YDL007W	39.80%	48828	SRP21	YKL122C	24.10%	18294	LSB1	YGR136W	15.80%	26139	IRR1	YIL026C	10.80%	133009
	YBR137W	39.70%	20454	CKA2	YOR061W	24.00%	39272	UTP10	YJL109C	15.70%	200080	EGT2	YNL327W	10.80%	108495
RPO26	YPR187W	39.40%	17910	RCK2	YLR248W	23.90%	68041	EDE1	YBL047C	15.70%	150783	DPS1	YLL018C	10.80%	63384
RPT3	YDR394W	39.00%	47970	RRP9	YPR137W	23.90%	65054	UTP21	YLR409C	15.70%	104791	MFB1	YDR219C	10.80%	53168
NMA1	YLR328W	38.90%	45859	LEO1	YOR123C	23.90%	53920	MAK5	YBR142W	15.70%	87048	RPN10	YHR200W	10.80%	29747
SKP1	**YDR328C**	**38.90%**	**22199**	CHD1	YER164W	23.60%	168240	RTT103	YDR289C	15.60%	46488	TBS1	YBR150C	10.70%	126903
CHZ1	YER030W	38.80%	18306	SPA2	YLL021W	23.20%	163142	TPM1	YNL079C	15.60%	23541	NAM9	YNL137C	10.70%	56356
CMD1	YBR109C	38.80%	16135	UFD4	YKL010C	23.10%	167842	SPT7	YBR081C	15.50%	152617	CUS1	YMR240C	10.60%	50253
CEG1	YGL130W	38.60%	52764	RPN6	YDL097C	23.00%	49774	TBS1	YBR150C	15.50%	41583		YLR057W	10.50%	96997
RPO21	YDL140C	38.50%	191610	RPN2	YIL075C	22.90%	104101	ESP2	YNR054C	15.50%	36408	UFO1	YML088W	10.50%	76860
RPO31	YOR116C	38.40%	162301	TAF6	YGL112C	22.90%	57902	DOC1	YGL240W	15.50%	32822	TFC8	YPL007C	10.50%	67684
CKB2	YOR039W	38.40%	29842	MET18	YIL128W	22.80%	117882	APL4	YPR029C	15.30%	93624	BFR2	YDR299W	10.50%	61203
DPH5	YLR172C	38.00%	33847	UBX5	YDR330W	22.80%	56737	RCY1	YJL204C	15.30%	75856	VPS5	YOR069W	10.40%	76484
SRP14	YDL092W	37.70%	16430		YLR287C	22.80%	40928		YOR051C	15.30%	47352	VMA2	YBR127C	10.40%	57749
HGH1	YGR187C	37.30%	44952	YKE2	YLR200W	22.80%	13284	CUE5	YOR042W	15.10%	46870	POP5	YAL033W	10.40%	19574
DCP2	YNL118C	36.90%	108667	PLP2	YOR281C	22.70%	32793	CCT6	YDR188W	15.00%	59924		YKR105C	10.30%	63361
RPC11	YDR045C	36.40%	12513	MAM33	YIL070C	22.60%	30132	PIR1	YKL164C	15.00%	34622	PWP2	YCR057C	10.30%	103983
SPT6	YGR116W	36.30%	168291	RPC17	YJL011C	22.40%	18610	PEX18	YHR160C	14.80%	32037	SFL1	YOR140W	10.30%	83317
SDS22	YKL193C	36.10%	38887	RLF2	YPR018W	22.30%	70210	ARP4	YJL081C	14.70%	54832	ATG7	YHR171W	10.30%	71428
RPC40	YPR110C	36.10%	37687	MSI1	YBR195C	22.30%	47365	BMH2	YDR099W	14.70%	30930	RAD18	YCR066W	10.30%	55230
RVB1	YDR190C	35.90%	50453	PAF1	YBR279W	22.00%	51801		YLR243W	14.70%	30653		YDL233W	10.30%	51320
POP3	YNL282W	35.90%	22612	MFT1	YML062C	21.90%	44996	PAA1	YDR071C	14.70%	21947	RPL4B	YDR012W	10.20%	38931
ENP1	YBR247C	35.80%	55137	TOA1	YOR194C	21.70%	32201	RPN12	YFR052W	14.60%	31919	RPL4A	YBR031W	10.20%	38961
RVB2	YPL235W	35.50%	51612	TAF5	YBR198C	21.60%	88968	POP6	YGR030C	14.60%	18210	ZTA1	YBR046C	10.20%	37019
UBP1	YDL122W	35.40%	92753	TAF8	YML114C	21.60%	57986	ADA2	YDR448W	14.50%	50569	VID27	YNL212W	10.10%	88846
SDC1	YDR469W	35.40%	19446	RPN9	YDR427W	21.60%	45783	SPP1	YPL138C	14.40%	41468	CIT6	YPL181W	10.10%	57053
MSH2	YOL090W	35.20%	108884	SRP72	YPL210C	21.50%	74273		YBL010C	14.30%	32639	MRS6	YOR370C	10.00%	67374
RET2	YFR051C	34.90%	60497	DMA1	YHR115C	21.40%	46098	FMS1	YMR020W	14.20%	57806	RME1	YGR044C	10.00%	33904
CCT7	YJL111W	34.20%	59736		YOR006C	21.40%	35686	CAC2	YML102W	14.10%	51252	GSP2	YOR185C	10.00%	24991
	YHR009C	34.20%	57034	RPS3	YNL178W	21.30%	26372	BUG1	YDL099W	14.10%	38295	GSP1	YLR293C	10.00%	24810
LSB5	YCL034W	34.20%	39872	FUN30	YAL019W	21.20%	128507	CDC45	YLR103C	14.00%	74249		YDR131C	9.90%	65243
ABP140	YOR239W	34.00%	71355	GSY2	YLR258W	21.20%	79948	RPA49	YNL248C	14.00%	46651	MKT1	YNL085W	9.80%	94494
OCA1	YNL099C	34.00%	27205	MSH6	YDR097C	20.90%	140080	INO80	YGL150C	13.90%	171454		YGR130C	9.80%	92698
RET1	YOR207C	33.60%	129456	CRP1	YHR146W	20.90%	51116	PNT1	YOR266W	13.90%	48934	SSN3	YPL042C	9.80%	61193
PDI1	YCL043C	33.10%	58227	CKB1	YGL019W	20.90%	32265	STE4	YOR212W	13.90%	46581	MNI2	YPR045C	9.80%	53719
PTC1	YDL006W	33.10%	31550	SSN2	YDR443C	20.80%	160000	SPT3	YDR392W	13.90%	38800	RPN7	YPR108W	9.80%	48959
RPB9	YGL070C	32.80%	14288	ENP2	YGR145W	20.80%	81748	TRA1	YHR099W	13.70%	433182	CDC12	YHR107C	9.80%	46668
ELP3	YPL086C	32.70%	63657	CDC123	YLR215C	20.80%	41852	RSE1	YML049C	13.70%	153784	SCW10	YMR305C	9.80%	40469
TIF5	YPR041W	32.60%	45261	RPN3	YER021W	20.70%	60423	SWD2	YKL018W	13.70%	37122	PHO85	YPL031C	9.80%	34906
SNF1	YDR477W	32.40%	72045		YOR352W	20.70%	39275	FIT1	YDR534C	13.60%	52491	RIX1	YHR197W	9.70%	86667
UTP8	YGR128C	32.30%	80191	COG2	YQR100C	20.70%	31800		YJL213W	13.60%	35905	**CEP3**	**YMR168C**	**9.70%**	**71358**
UTP9	YHR196W	32.20%	65272	UTP13	YLR222C	20.60%	91032		YFL034W	13.50%	119496	HEM15	YOR176W	9.70%	44596
SRP1	YNL189W	31.90%	60441	PSY4	YBL046W	20.60%	50655	NGG1	YDR176W	13.50%	79282		YJR119C	9.60%	84984

179 additional polypeptides > 5% sequence coverage

Table 2.4 Yeast Strains Used in This Study

Name	Genotype	Source
ODY34	*MAT**a**, ade2-1, trp1-1, can1-100, leu2-3,112, his3-11,15, ura3-1, CTF19-HA6:TRP*	1#
ODY35	*MAT**a**, ade2-1, trp1-1, can1-100, leu2-3,112, his3-11,15, ura3-1, MCM21-HA6:TRP*	1#
ODY36	*MAT**a**, ade2-1, trp1-1, can1-100, leu2-3,112, his3-11,15, ura3-1, OKP1-HA6:TRP*	1#
ODY37	*MAT**a**, ade2-1, trp1-1, can1-100, leu2-3,112, his3-11,15, ura3-1, MTW1-HA6:TRP*	1#
ODY38	*MAT**a**, ade2-1, trp1-1, can1-100, leu2-3,112, his3-11,15, ura3-1, NDC80-HA6:TRP*	1#
ODY39	*MAT**a**, ade2-1, trp1-1, can1-100, leu2-3,112, his3-11,15, ura3-1, DAM1-HA6:TRP*	1#
ODY40	*MAT**a**, ade2-1, trp1-1, can1-100, leu2-3,112, his3-11,15, ura3-1, MIF2-HA6:TRP*	1#
ODY41	*MAT**a**, ade2-1, trp1-1, can1-100, leu2-3,112, his3-11,15, ura3-1, STU1-HA6:TRP*	1#
ODY42	*MAT**a**, ade2-1, trp1-1, can1-100, leu2-3,112, his3-11,15, ura3-1, ASE1-HA6:TRP*	1#
ODY49	*MAT**a**, trp1Δ63, ura3-52, his3Δ200*	1*
ODY54	*MATα, trp1Δ63, ura3-52, his3Δ200, SLI15-HA6::TRP1*	1*
ODY55	*MATα, trp1Δ63, ura3-52, his3Δ200, IPL1-HA6::TRP1*	1*
ODY62	*MAT**a**/MATα, trp1Δ63/trp1Δ63, ura3-52/ura3-52, his3Δ200/ his3Δ200, Δbir1::TRP1/BIR1*	1*
ODY65	*MAT**a**, trp1Δ63, ura3-52, his3Δ200, Δbir1::TRP1*	1*
ODY97	*MAT**a**, trp1Δ63, ura3-52, his3Δ200, BIR1-HA6::TRP1, SLI15-MYC13::HIS3MX6*	1*
ODY101	*MAT**a**, trp1Δ63, ura3-52, his3Δ200, BIR1-STag-TEV-ZZ::KanMX*	1*
ODY114	*MAT**a**, trp1Δ63, ura3-52, his3Δ200, Δbir1::TRP, (pSS024, BIR1, HIS3, CEN)*	1*
ODY155	*MAT**a**, ura3-1, leu2,3-112, his3-11::pCUP1-GFP12-lacI12::HIS3, trp1-1::256lacO::TRP1, lys2Δ, ade2-1, can1-100, bar1Δ, pGAL-HA3-SLI15::KAN, (pSS070, ADE2, CEN)*	1#
ODY164	*MAT**a**/MATα, ura3-1/ura3-1, leu2,3-112/LEU2, his3-11::pCUP1-GFP12-lacI12::HIS3/his3-11::pCUP1-GFP12-lacI12::HIS3, trp1-1::256lacO::TRP1/trp1-1::256lacO::TRP1, lys2Δ, ade2-1, can1-100, bar1Δ, (pSS070, ADE2, CEN)*	1#
ODY170	*MAT**a**/MATα, ura3-1/ura3-1, leu2,3-112/LEU2, his3-11::pCUP1-GFP12-lacI12::HIS3/his3-11::pCUP1-GFP12-lacI12::HIS3, trp1-1::256lacO::TRP1/trp1-1::256lacO::TRP1, lys2Δ, ade2-1, can1-100, bar1Δ, (pSS070, ADE2, CEN), pGAL-HA3-SLI15::KAN*	1#
ODY181	*MAT**a**, ura3-1, leu2,3-112::, his3-11::pCUP1-GFP12-lacI12::HIS3, trp1-1::256lacO::TRP1, lys2Δ, ade2-1, can1-100, bar1Δ, pGAL-HA3-SLI15::KAN, (pSS070, ADE2, CEN), PDS1-MYC18::LEU2*	1#

Table 2.4 (Continued) Yeast Strains Used in This Study

Name	Genotype	Source
ODY170	*MAT**a**/MATα, ura3-1/ura3-1, leu2,3-112/LEU2, his3-11::pCUP1-GFP12-lacI12::HIS3/his3-11::pCUP1-GFP12-lacI12::HIS3, trp1-1::256lacO::TRP1/trp1-1::256lacO::TRP1, lys2Δ, ade2-1, can1-100, bar1Δ, (pSS070, ADE2, CEN), pGAL-HA3-SLI15::KAN*	1[#]
ODY181	*MAT**a**, ura3-1, leu2,3-112::, his3-11::pCUP1-GFP12-lacI12::HIS3, trp1-1::256lacO::TRP1, lys2Δ, ade2-1, can1-100, bar1Δ, pGAL-HA3-SLI15::KAN, (pSS070, ADE2, CEN), PDS1-MYC18::LEU2*	1[#]
ODY182	*MAT**a**, trp1Δ63, ura3-52, his3Δ200, sli15(L656S)::TRP1*	1*
ODY190	*MAT**a**/MATα, ura3-1/ura3-1::SLI15::URA3**, leu2,3-112/LEU2, his3-11::pCUP1-GFP12-lacI12::HIS3/his3-11::pCUP1-GFP12-lacI12::HIS3, trp1-1::256lacO::TRP1/trp1-1::256lacO::TRP1, lys2Δ, ade2-1, can1-100, bar1Δ, (pSS070, ADE2, CEN), pGAL-HA3-SLI15::KAN*	1[#]
ODY191	*MAT**a**/MATα, ura3-1/ura3-1::SLI15ΔMTB::URA3**, leu2,3-112/LEU2, his3-11::pCUP1-GFP12-lacI12::HIS3/his3-11::pCUP1-GFP12-lacI12::HIS3, trp1-1::256lacO::TRP1/trp1-1::256lacO::TRP1, lys2Δ, ade2-1, can1-100, bar1Δ, (pSS070, ADE2, CEN), pGAL-HA3-SLI15::KAN*	1[#]
ODY192[&]	*MAT**a**, ura3-1::SLI15::URA3, leu2,3-112, his3-11::pCUP1-GFP12-lacI12::HIS3, trp1-1::256lacO::TRP1, lys2Δ, ade2-1, can1-100, bar1Δ, pGAL-HA3-SLI15::KAN, (pSS070, ADE2, CEN)*	1[#]
ODY193[&]	*MAT**a**, ura3-1::SLI15-MTBΔ::URA3, leu2,3-112, his3-11::pCUP1-GFP12-lacI12::HIS3, trp1-1::256lacO::TRP1, lys2Δ, ade2-1, can1-100, bar1Δ, pGAL-HA3-SLI15::KAN, (pSS070, ADE2, CEN)*	1[#]
DDY2473	*MAT**a**, leu2, ura3-52, trp1, prb1-1122, pep4-3, pre1-451, SLI15-Stag-TEV-ZZ::KanMX*	2
CCY1124-4B	*MAT**a**, his3Δ200, leu2-3,112, ura3-52, ade2, sli15-3*	2
SBY213	*MATα, ura3-1, leu2,3-112, his3-11::pCUP1-GFP12-lacI12::HIS3, trp1-1::256lacO::TRP1, lys2Δ, ade2-1, can1-100, bar1Δ*	3
SBY214	*MAT**a**, ura3-1, leu2,3-112, his3-11::pCUP1-GFP12-lacI12::HIS3, trp1-1::256lacO::TRP1, lys2Δ, ade2-1, can1-100, bar1Δ*	3
SBY818	*MAT**a**, ura3-1, leu2,3-112, his3-11::pCUP1-GFP12-lacI12::HIS3, trp1-1::256lacO::TRP1, lys2Δ, ade2-1, can1-100, bar1Δ, PDS1-MYC18::LEU2*	3
SBY611	*MAT**a**, ura3-1, leu2-3,112, his3-11, trp1-1, can1-100, ade2-1, bar1-1, cdc14-1*	3
SBY203	*MAT**a**, ura3-1, leu2-3,112, his3-11, trp1-1, can1-100, ade2-1, bar1-1, cdc15-2, LYS2*	3
PS886	*Mat **a**/α, leu2/leu2, trp1/trp1, ura3-52/ura3-52, prb1-1122/prb1-1122, pep4-3/pep4-3, prc1-407/prc1-407, GAL*	1[#]

Table 2.4 (Continued) Yeast Strains Used in This Study

[&]Sli15 and Sli15-MTBΔ coding regions were placed under control of the endogenous *SLI15* promoter (1 kb upstream of start codon) and cloned into pRS306, linearized with Stu1 and integrated at the URA3 locus.

Sources:

1. This study. Strains were derived from S288C (*) or W303 (#) backgrounds.
2. D. Drubin/G. Barnes, University of California, Berkeley, Berkeley, CA
3. S. Biggins, Fred Hutchinson Cancer Research Center, Seattle, WA

Chapter 3: Molecular characterization of the Bir1-Sli15 connection between CEN-DNA and microtubules

3.1 Introduction

In order for chromosome segregation to occur without error each and every cell cycle, cells must utilize savvy mechanisms. One such mechanism exists to discriminate between kinetochores that are attached, albeit incorrectly, versus kinetochores attached correctly to microtubules. While the phenomenon of this particular cellular surveillance function has been appreciated for many decades, the molecular components and mechanisms responsible for this behavior have only begun to be understood in the last few years. Identification of the link between CEN-DNA, CBF3, Bir1/Survivin-Sli15/INCENP, and microtubules described in Chapter 2 revealed a potential mechanism for how cells sense and correct microtubule attachments in vivo in the local vicinity of individual chromosome kinetochore interactions. While this is an intriguing model and provides a testable hypothesis for how cells sense incorrect attachments, the molecular details of how this function might be carried out remain unanswered. I have sought to shed light on the molecular mechanism of the Bir1/Sli15 mediated CEN-DNA microtubule connection by taking two different approaches. First, I have carried out detailed analysis of the Sli15 microtubule-binding domain and second, I have utilized biophysical

approaches to understand how the Bir1/Sli15 mediated connection both regulates and is regulated by Aurora B/Ipl1.

When chromosome alignment is occurring, the chromosomal passenger proteins localize to the inner centromere region between sister chromatids (Ruchaud et al., 2007). While this has not been determined for budding yeast, it provokes the question of how the Bir1/Survivin-Sli15/INCENP link between CEN-DNA and microtubules is spatially arranged and how exactly it is interacting with the microtubule. In Chapter 2, I presented results demonstrating that a large domain of the middle part of Sli15 was important in vivo for both activating Ipl1 and bridging CEN-DNA to microtubules. To further understand how Sli15 interacts with microtubules I have attempted to precisely map the microtubule-binding domain such that it might be examined in structural detail. Although protein purification difficulties have limited any structural studies, I have determined that approximately 290 amino acids of the middle portion of Sli15 can bind microtubules and that the entire region is required for cell viability. Unexpectedly, a 40 amino acid stretch that was originally predicted to contain a coiled-coil (Kang et al., 2001) does not bind microtubules but is still required for cell viability.

Ipl1/Aurora B is clearly regulating proteins responsible for making the “core attachments” between microtubules and centromeric DNA, which include the KMN network (KNL-1, Mis12, Ndc80) (Cheeseman et al., 2006; Ciferri et al., 2008; DeLuca et al., 2006) and the Dam1 complex in budding yeast

(Cheeseman et al., 2002; Wang et al., 2007). Previous studies have also implicated Ipl1/Aurora B as regulating the Bir1-Sli15 mediated attachment between CEN-DNA and microtubules (Biggins et al., 1999; Sandall et al., 2006). Both the Ndc10 subunit of the CBF3 complex as well as Sli15 are phosphorylated by Ipl1 in vitro and are the most likely candidates for how Ipl1 exerts its effects on the attachment (Biggins et al., 1999; Cheeseman et al., 2002). Additionally, the Bir1-Sli15 connection appears to be regulating the catalytic activity of Ipl1 since eliminating the Sli15 portion that connects to microtubules also affects Ipl1 kinase activity (Sandall et al., 2006). Because the Bir1-Sli15 mediated connection between CEN-DNA and microtubules can be assembled in vitro, it is directly amenable to biophysical analysis, which provides the opportunity to test how Ipl1 regulates the linkage. Furthermore, the availability of kinase inactive *ipl1* mutants as well as a *sli15* mutant that is unable to activate Ipl1 but still maintains the Bir1-Sli15 mediated linkage, provides a tool to probe how Ipl1 activity is regulated by the attachment.

Optical trap microscopy has provided researchers with a valuable tool to apply and measure small forces as well as track movements of individual molecules. By focusing a laser beam to a single spot in the focal plane, which can trap particles in its center due to the laws of reflection and refraction, an optical trap holds a particle in its' center due to scattering and gradient forces. When the particle is displaced from the center of the beam, it is pulled back to the center due to the restoring force of the optical trap, which can then be

measured. By exploiting this principle, optical traps can be utilized to quantify the strength of molecular interactions as well as apply tension to them (Kuo, 2001). I have utilized the power of optical trap microscopy to examine how Ipl1 is exerting its effects on the Bir1-Sli15 mediated attachment between CEN-DNA and microtubules. This approach has led to the discovery that Ipl1 causes weakening of the CEN-DNA Bir1/Sli15 mediated interaction once bound to microtubules, and prevents the formation prior to binding microtubules.

3.2 Results

3.2.1 A region of 290 amino acids contributes to the microtubule binding activity of Sli15

Beyond the well-conserved C-terminal IN box, sequence conservation between Sli15 and other INCENP homologues is relatively weak (Adams et al., 2001b). To determine if there might be an obvious microtubule-binding domain, Sli15 protein sequences from six other *Saccharomyces* species were aligned using ClustalW (Figure S3.1). While there appeared to be clumps of conservation within the original microtubule-binding domain defined in Chapter 2 (amino acids 227-559) the most obvious conserved region was the region with unusual charge distribution, once predicted to be a putative coiled coil (amino acids 517-559 highlighted in pink in Figure S3.1). Using this alignment as a rough guide, several different fragments were cloned and expressed as

GST fusion proteins (Figure 3.1A, S3.1, and Table 3.2). A preliminary screen of microtubule binding affinity was conducted by testing the ability of each fragment to cosediment with polymerized microtubules at various protein concentrations (Figure 3.1B-G). This initial survey revealed that with the exception of the C-terminal 42 amino acids, 517-559 (Figure 3.1D), almost the entirety of the original microtubule binding domain (Kang et al., 2001), amino acids 227-516, could bind microtubules with a varying degree of affinity (Figure 3.1 B-C, E-G). While the binding was quantified using only the correct size fragment, considering the unequal presence of breakdown products in several of the protein preparations of the Sli15 fragments, there was some uncertainty if the variation in microtubule binding was real or rather a consequence of these smaller fragments (Figure 3.1B-F).

3.2.1.1 Microtubule binding and bundling activity of Sli15 fragments

In an attempt to more accurately quantify the relative binding affinities of the various Sli15 fragments, I further analyzed the four microtubule binding fragments from Figure 3.1 by cleaving the GST tag and using gel filtration to eliminate some of the smaller breakdown fragments. The largest of the four fragments, $Sli15^{227-449}$, was the most stable of all the fragments, however eluted as two discernable peaks after gel filtration (Fig S3.2). The larger of the two peaks was stable when dialyzed into buffer optimal for microtubule binding assays (BRB80). The smaller of the two peaks, however, precipitated out of

solution when dialyzed. The larger peak was assessed for its ability to bind GMPCCP stabilized microtubules in the cosedimentation assay and was found to bind microtubules with a Kd of 1.4 μM (Figure 3.2A). The second largest fragment, Sli15$^{397-559}$, still contained break down products which were not separated by gel filtration, nevertheless this protein not only bound GMPCCP microtubules with a Kd of 60 nM, the protein also seemed to be stabilizing microtubules as evidenced by the increasing amount of tubulin in the supernatant fractions as less Sli15$^{397-559}$ was added to the reaction (Figure 3.2B). To further assess the microtubule stabilization property, the cosedimentation assay was repeated using taxol-stabilized microtubules. Consistent with the results using GMPCPP microtubules, the taxol microtubules were indeed stabilized with increasing amounts of Sli15$^{397-559}$. The Kd in this particular experiment was an order of magnitude higher at 500 nM, which could be due to the different microtubules, but most likely reflects experimental variability and needs to be repeated (Figure 3.2C). Unfortunately, the small size of Sli15$^{397-516}$ and Sli15$^{450-516}$, as well as the relative low abundance of the proteins following gel filtration made it difficult to assess microtubule binding using the methods employed in Figure 3.1. Even with gradient gels and silver staining, I was not able to detect the proteins with enough confidence to make accurate quantifications of their microtubule binding affinity.

To address microtubule binding in a different way, I looked at the ability of each fragment to bundle GMPCCP microtubules (Figure 3.2D). Similar to the cosedimentation assay, both Sli15$^{227-449}$ and Sli15$^{397-559}$ bundled microtubules. Sli15$^{227-449}$ bundled microtubules at concentrations as low as 0.85 μM whereas Sli15$^{397-559}$ clearly bundled microtubules at 2.5 μM but not as readily at 1.25 μM. Of the two smaller fragments, Sli15$^{450-516}$ bundled microtubules at 10 μM, but at even half this concentration did not show bundling activity. Sli15$^{397-516}$ was too dilute to test at concentrations above 5 μM and at this concentration did not bundle microtubules.

Although the Sli15$^{227-449}$ fragment bound and bundled microtubules well and could be purified to a single band, the behavior over gel filtration precluded further analysis of the microtubule binding. This result led us to analyze all the fragments by gel filtration to see if they had similar behavior to Sli15$^{227-449}$. While none of the other fragments had two peaks like Sli15$^{227-449}$, all the fragments, including Sli15$^{517-559}$, displayed an elution profile that correlated with much larger proteins than the predicted molecular weight (Figure S3.2), suggesting either an elongated shape or possible aggregation or self-assembly.

3.2.1.2 Localization of Sli15 microtubule binding domain to centromeres and the mitotic spindle

In the instance that the Sli15 fragments were binding microtubules in vitro because of artificial aggregation, I decided to also test the in vivo localization of each fragment when expressed as a GFP fusion protein in WT yeast, reasoning that localization to the spindle would be another indication of each fragments' ability to bind microtubules. The results obtained correlated with the in vitro binding experiments- all fragments except Sli15$^{517-559}$ were able to localize to the mitotic spindle. However, the degree to which each fragment localized to the spindle as well as the centromere during early cell cycle stages varied somewhat (Figure 3.3). For Sli15$^{227-449}$ the localization was predominantly centromeric and even appeared to localize to nuclear microtubules in G1 (Figure 3.3A). While this fragment also localized to the spindle during anaphase, the majority of protein seemed to remain centromere associated, unlike endogenous full-length Sli15, which localizes primarily on the spindle during anaphase (Kang et al., 2001). Sli15$^{397-559}$ showed a similar pattern as Sli15$^{227-449}$ except that there was a much higher level of background signal during G1 and metaphase (Figure 3.3B). Sli15$^{397-516}$ did not appear to localize to centromeres, but did show spindle staining in both metaphase and anaphase. However, the background levels of Sli15$^{397-516}$ remained quite high, suggesting that most of the protein is not able to localize (Figure 3.3C). Sli15$^{450-516}$ also showed high levels of background signal, but localized

opposite to Sli15$^{397-516}$. The centromere localization was very clear, while the anaphase spindle localization, particularly in anaphase was weak. While the metaphase localization appeared predominately centromeric, there was also some protein on the spindle, confirming that this fragment can indeed bind microtubules in vivo (Figure 3.3D). Sli15$^{517-559}$ did not localize to either the centromere or the spindle and in fact was not even in the nucleus, which was surprising considering a putative nuclear localization signal exists within the 517-559 region (Figure 3.3E and (Kang et al., 2001)).

3.2.2 Eliminating any portion of Sli15 from amino acids 227-559 results in cell death

Since the entire Sli15 microtubule-binding domain is essential for viability in budding yeast (Sandall et al., 2006), I decided to determine if all the Sli15 fragments analyzed for microtubule binding were also essential. To test this, I integrated *SLI15* plus 1 Kb upstream of the Sli15 start codon at the *ura3-52* locus into a diploid yeast strain that was heterozygous for Sli15. I then repeated this with several versions of Sli15 that lacked the amino acid sequences of the Sli15 microtubule-binding domain fragments characterized in Figures 3.1-3 (Tables 3.1 and 3.2). The diploid yeast strains were then sporulated and the resulting meiotic products analyzed by tetrad dissection and genotyping. Full-length *SLI15* was used as a positive control and *SLI15*$^{\Delta 227-559}$ was used as a negative control. All deletions tested, including

SLI15$^{\Delta 517\text{-}559}$, which did not bind microtubules, resulted in cell lethality (Table 3.1). One fragment however, *SLI15*$^{\Delta 450\text{-}516}$ resulted in one tetratype tetrad out of 17 analyzed that produced a viable *Δsli15:SLI15*$^{\Delta 450\text{-}516}$ spore. When this strain was analyzed by PCR, it did appear that there was also a full-length copy of *SLI15* present, however this has not been confirmed by Southern blot (data not shown). Similarly peculiar incidents happened with *SLI15*$^{\Delta 227\text{-}449}$ and *SLI15*$^{\Delta 227\text{-}397}$. One viable *Δsli15:SLI15*$^{\Delta 227\text{-}449}$ spore was also isolated, however rather than originating from a tetratype, this spore belonged to a tetrad that contained two viable spores: one was *Δsli15:SLI15*$^{\Delta 227\text{-}449}$ and the other was wild-type. Two other similar tetrads produced two viable *Δsli15:SLI15*$^{\Delta 227\text{-}397}$ spores. Since this genotype is not expected for either a parental or non-parental ditype, these tetrads were not counted in the analysis. Furthermore, when these strains were analyzed by PCR they also showed the presence of full-length *SLI15* (data not shown). Due to the fact that the tetrads in which these strains were derived were unusual, as well as the likely presence of wild-type *SLI15*, none of these strains were further characterized.

3.2.3 Ipl1 prevents the Bir1-Sli15 mediated link between CEN-DNA and microtubules from forming, but has less effect on the linkage after initial formation

While it is clear from previous studies that Ipl1 kinase is responsible for regulating the Bir1-Sli15 mediated CEN-DNA microtubule attachments, what

has remained unclear is what it is targeting that leads to no attachments (Biggins et al., 1999; Sandall et al., 2006). In addition to the target being unknown, the mechanism of regulation is also unclear. When Ipl1 is added to the CEN-DNA bead extract mix, the CEN-DNA is unable to bind microtubules (Figure 2.4B). To determine if Ipl1 could also regulate the Bir1-Sli15 mediated CEN-DNA attachments after binding to microtubules, I modified the CEN-DNA bead assays as outlined in Figure 3.4A. In the modified experiment, attachments are first made using WT extract and quantified. Next, various combinations of either ATP, Ipl1, or extract are added to the flow chamber, allowed to incubate, and then chambers are washed and the number of beads bound re-quantified. I tested several permutations of initial reaction conditions, components added after initial bead counting, and time of incubation. Interestingly, none of the conditions I tested resulted in a change in the number of beads bound (Figure 3.4A-B).

Original conditions of the CEN-DNA bead assay utilized beads that were 0.2 μm in diameter and had ~1000 molecules of CEN-DNA/bead (Sorger et al., 1994). For the experiments described in Figure 3.4, beads with a diameter of 0.44 μm were used and a range of 33-1000 CEN-DNA molecules/bead tested. While the data represented in Figure 3.4A and B utilizes 333 molecules CEN-DNA/bead, both 1000 and 111 molecules/bead were also tested with similar results (data not shown). When the number of CEN-DNA molecules/bead was decreased below 111, the beads did not bind

well enough to achieve reproducible numbers. Based on the surface area of a bead 0.44 μm in diameter and assuming the CEN-DNA molecules are randomly distributed across the surface, a conservative estimate reveals that only 4% of the CEN-DNA surface could be in contact with a microtubule at any given time. Based on this number, one could assume that beads with 333 molecules of CEN-DNA/bead have approximately 13 CEN-DNA molecules attached to a single microtubule.

3.2.4 Ipl1 weakens the interaction between CEN-DNA, CBF3 complex, Bir1-Sli15, and microtubules

Since the Bir1-Sli15 mediated CEN-DNA binding appeared to be resistant to Ipl1 modification after binding to microtubules, I next sought to temporally assess how Ipl1 prevented attachments. The CEN-DNA beads were initially mixed with either WT or *sli15*^{L656S} extract (Sandall et al., 2006) and ATP was added at various time points during the 45-minute incubation, prior to flowing the reaction over microtubules. If ATP was added for as little as 1 minute the CEN-DNA beads that had been incubated with WT extract had an 80% reduction in the number of beads bound to microtubules whereas the *sli15*^{L656} extract was insensitive to the ATP addition (data not shown). ATP addition longer than 1 minute completely abolished CEN-DNA binding with WT

extract as did increasing the ATP concentration by as little as 2-fold (data not shown).

3.2.4.1 ATP addition makes Bir1-Sli15 mediated CEN-DNA microtubule attachments weaker

ATP addition appeared to have no effect on attachments after binding, at least based on what could be detected using the classic CEN-DNA bead assay. However, it was clear that ATP addition made a significant impact on attachment formation prior to binding microtubules, even when only exposed to ATP for 1 min. Therefore, I wanted to determine if there was a subtle difference in the attachments when ATP was present that could be measured independently of counting the number of CEN-DNA beads bound. To do this, I employed the use of an optical trap microscope to test the strength of attachments in both the presence and absence of ATP (Asbury et al., 2003; Asbury et al., 2006; Block et al., 2003; Lang et al., 2002). The CEN-DNA bead assay was performed as described (Sandall et al., 2006) and then beads that were attached to microtubules were held continuously in the optical trap while its position was monitored by back focal plane interferometry (Lang et al., 2002). Software was then modified to deliver a “force ramp” where tension is increased linearly by using a feedback-controlled piezoelectric stage to maintain a fixed offset between the bead and the trap center. Rates of both 0.1 pN/sec and 1.0 pN/sec resulted in beads disassociating from the

microtubule at forces between ~2-5 pN, a measurement referred to as a rupture force (Figure 3.4C). A higher rupture force was observed for the faster rate, which is expected since applying load more quickly generally increases the force at which attachments will break. However, the sensitivity to loading rate was fairly mild as mean rupture forces increased only two-fold over a ten-fold increase in rate. Nevertheless, the slower force ramp was chosen for further experiments to maximize any differences that may be observed between different experimental conditions.

For reasons that are still unclear, delivery of any buffer into the flow cells used for the optical trap studies, after CEN-DNA beads had been added to the microtubules, seemed to disrupt the beads from the microtubules. Therefore, in order to test rupture forces +/-ATP, the bead assay was set up and ATP spiked into the reaction 1 min. prior to binding. While there were less attachments overall with ATP present, there were enough present to measure the rupture forces. Interestingly, there was an approximate two-fold decrease in the mean rupture force when ATP was present (Figure 3.4D). Attachments that were ruptured and then subsequently re-attached using the optical trap showed the same trend as initial attachments only (data not shown).

3.2.4.2 Mutant extracts of Sli15 and Ipl1 that lack Ipl1 activity have similar rupture forces with and without ATP

To confirm that the ATP dependent weakening was indeed due to the activity of Ipl1, the rupture force measurements were repeated using two different mutant extracts that are defective for ipl1 kinase activity, *ipl1-321,* and *sli15*^{L656S} (Sandall et al., 2006). These mutant extracts did not have a significant difference in rupture forces when ATP was present or absent. However, unexpectedly, rather than maintaining the same rupture force as the WT extract without ATP, the rupture forces were more in par with WT extracts with ATP, suggesting the attachments, while insensitive to ATP, were weaker overall (Figure 3.4D).

3.3 Discussion

3.3.1 Over one-third of Sli15 can bind microtubules and is essential for viability

While it had been previously demonstrated that the middle portion of Sli15 (amino acids 227-559) could bind microtubules, it was unknown if the whole region was actually required or just a minimal domain within the region. It has been widely assumed that the coiled-coil domain of INCENP is functioning to bind microtubules, which is based on in vitro microtubule binding experiments using both chicken INCENP (Wheatley, 2001) and Sli15 (Kang et al., 2001). The coiled-coil domain is well over 200 amino acids in Chicken and

the fragment shown to bind microtubules fell solely within this domain. Furthermore, simple domain analysis of the Sli15 microtubule binding domain predicts a coiled-coil within the region, from amino acids 517-559, that when analyzed in more detail appears to be a region of unusual charge distribution rather than a real coil (data not shown). Therefore, it was quite surprising when microtubule binding assays of smaller Sli15 microtubule binding fragments showed that the only region not required for binding was the original predicted coiled-coil (Figures 3.1-3). While there were subtle differences in both microtubule-binding and localization assays, protein behavior and some inconsistencies preclude any strong predictions about whether there are real differences in the region.

All fragments tested were strongly positively charged, with predicted isoelectric points well above 10 (Figure 3.1A). Therefore, it can be assumed that the interaction between Sli15 and microtubules is mediated by charge, a common mechanism by which microtubule associated proteins interact with microtubules. Another interesting observation resulting from this study is the behavior of these fragments when analyzed by gel filtration. Each fragment eluted in fractions much higher than would be expected based on the predicted molecular weight, suggesting that they are either highly elongated or oligimerizing in some fashion. I have tested whether full-length Sli15 can dimerize in vivo by performing a HA-immunoprecipitation in a diploid yeast strain that expresses only one copy of HA-tagged Sli15. Western blot analysis

using the Sli15 antibody revealed that the HA-tagged copy was not interacting with untagged Sli15 (data not shown). Since this experiment was done in the context of the full-length protein, it may suggest that if any oligimerization is occurring in the microtubule-binding domain other regions of Sli15 might inhibit it. Furthermore, there are several Ipl1 consensus sites within the microtubule-binding domain, which may be important, especially considering Ipl1 was shown to phosphorylate this region in vitro. It would be interesting to test whether the microtubule binding domain can oligimerize and how Ipl1 activity influences this as well as its ability to bind microtubules.

Tetrad dissection of yeast strains expressing Sli15$^{\Delta 227\text{-}449}$, Sli15$^{\Delta 397\text{-}559}$, Sli15$^{\Delta 397\text{-}516}$, and Sli15$^{\Delta 450\text{-}516}$, which represent the four fragments able to bind microtubules in vitro and in vivo revealed that they are all essential for cell viability. While this could reflect the importance of the microtubule binding function of Sli15, it could also suggest that the entire region is structural unstable when disrupted and renders the protein non-functional, especially considering there should theoretically still be microtubule binding activity remaining in each deletion. However, since deleting 227-559 resulted in an expressed protein that was capable of binding to Bir1 in vivo (Figure S2.5B), it seems unlikely. Furthermore, each diploid yeast strain was examined by Western Blot analysis and proteins were detected in the correct size range for all of the Sli15 deletion proteins (data not shown), confirming they were expressed. The results could suggest that partial microtubule binding activity

is not sufficient for in vivo function, or that the region is participating in a function beyond microtubule binding that is essential for cell viability.

3.3.2 A 42 amino acid fragment that links the microtubule binding region to the conserved IN box is essential for Sli15 function

Although not required for microtubule binding or proper localization, cells expressing Sli15$^{\Delta 517\text{-}559}$ as the only copy of Sli15 did not survive. It would be interesting to examine this allele in the background of the Sli15 galactose inducible strain such that the phenotype causing cell death could be determined. Several possibilities exist for why this region is important; however, it is clearly not because of microtubule binding or phosphorylation by Ipl1 or Cdk, as there are no predicted consensus sites of either kinase in this domain. The two most likely possibilities are that the region is contributing either to the structural integrity of Sli15 itself, or mediating an important interaction with another protein, the best candidate being Dam1 considering it was shown to interact with Sli15 in both the microtubule binding domain and to some extent in the C-terminus (Kang et al., 2001). It has not been determined in what capacity the Sli15/Dam1 interaction is functionally relevant. Since Dam1 is an important target of Ipl1 (Cheeseman et al., 2002) and Sli15 a bona fide Ipl1 activator (Kang et al., 2001), it could be an indirect interaction relating to Ipl1 kinase regulation, or there could be an additional direct role of Sli15 regulating Dam1 function. It was recently demonstrated in human studies that

removing the coiled coil in INCENP caused a spindle checkpoint defect that was independent of Aurora B localization or activity (Vader et al., 2007). The coiled-coil was also demonstrated to lack any ability to bind other chromosomal passenger proteins (Klein et al., 2006). This lends the possibility that this region, which is highly conserved across *Saccharomyces* species and has unusual charge distribution, is playing a critical, yet undescribed role in the function of Sli15.

3.3.3 Ipl1 controls the Bir1-Sli15 mediated connection between CEN-DNA and microtubules at multiple levels

Well before the proteins linking CBF3 bound CEN-DNA to microtubules were identified, it was appreciated that Ipl1 was regulating the binding activity (Biggins et al., 1999). However, even now that the molecular components are known, it has remains unclear how exactly Ipl1 is exerting its effects. Experiments presented here make it clear that the regulation is most likely complex and contrary to previous assumptions may primarily function to prevent attachments from forming. When Ipl1 is added to the CEN-DNA reaction, prior to microtubule binding, the connection between CEN-DNA, CBF3, and Bir1-Sli15 is modified such that attachments to microtubules do not form (Figure 2.4B). Whether Ipl1 exerts its' effect by breaking the connection between CEN-DNA and CBF3, CBF3 and Bir1, or Bir1 and Sli15 prior to addition to microtubules is not understood. While it cannot be ruled out that

Ipl1 is directly affecting Sli15 at the microtubule interface, because the attachment seems less sensitive to Ipl1 regulation after binding microtubules (Figure 3.4A,B) this seems less likely, unless the microtubule attachment masks or changes the interface to a degree that Ipl1 has limited access to Sli15. It could also be that Ipl1 regulates the attachment at multiple connection points and the difference between activity before and after addition to microtubules is the result of a change in the stability of the attachment.

Ipl1 is known to modulate attachments in a tension dependent manner (Dewar et al., 2004). The model proposed in Chapter 2 puts forth the hypothesis that the Bir1-Sli15 mediated attachment between CEN-DNA and microtubules is acting as a tension sensor in order to regulate Ipl1 activity. This predicts that the Bir1-Sli15 interaction, when under tension, can no longer activate Ipl1. While I initially made the assumption that the CEN-DNA bead interaction with microtubules is not under tension, it is possible that this is not the case and that the amount of force produced when flowing the CEN-DNA beads over the microtubules is enough to re-capitulate “tension”, and turn off Ipl1 activity. However, in the experiments summarized in Figure 3.4A & B, there would be ample time between the flowing steps such that if flow is creating force, it should be eliminated during no flow situations and cause Ipl1 to become active. Nevertheless, since Ipl1 can cause almost a complete abolition of attachments in 1 minute when added prior to microtubule binding (Figure 3.4C), it is also possible that Ipl1 activity is finely tuned to respond to

tension such that even if inactive when no flow occurs, the activity is quickly turned off once flow resumes, CEN-DNA re-binds to the microtubule surface, and attachments are stabilized. Since the experiment is done in a manner that only quantifies number of beads before and after several flow steps, it is possible that the assay wouldn't detect subtle detachment and reattachment events. Considering that attachments are weaker in the presence of ATP, which is dependent on Ipl1 since mutant extracts defective for Ipl1 kinase activity do not demonstrate the same ATP weakening (Figure 3.4D), it does suggest Ipl1 is active in no flow situations when ATP is present.

3.3.4 Using the optical trap and flow to test how tension affects Ipl1 activity

Experiments that took advantage of the optical trap demonstrated that in the presence of active Ipl1, the attachment between CEN-DNA and microtubules is weakened, evidenced by the decreased rupture forces when ATP is present. Mutant extracts that could not activate Ipl1, *ipl1-321* and *sli15*^{L656S} are resistant to the ATP weakening (Figure 3.4D). Interestingly, these same mutant extracts were weaker overall, with or without ATP. Since the data presented is representative of only one extract preparation, it is important to repeat as this result could simply reflect extract variability. Alternatively, if the trend is repeatable, it could suggest that Ipl1 kinase activity is somehow important for the overall integrity of the interaction, a finding that is

contradicted by earlier results that show no difference in CEN-DNA bead binding in both mutant extracts (Figure 2.4B & 2.5A).

Current efforts are underway to incorporate flow into the optical trap experiments as a way to generate tension. Coupling a peristaltic pump to the optical trap would allow one to add flow while trapping a bead to test if increased tension stabilizes attachments and results in an increased rupture force. The peristaltic pump can generate flow rates as low as 5 μl/min, which is equivalent to forces ranging from 0.2-2 pN, depending on the position in the flow chamber. Depending on the outcome of this type of experiment, the availability of various *ipl1* and *sli15* mutants would allow us to directly test the tension model put forth in Chapter 2.

3.4 Methods

3.4.1 Strains, plasmids & protein purification

Genomic DNA from *Saccharomyces cerevisiae* was amplified using appropriate oligos and cloned into pGEX6P.1 (GE Healthcare) and the C-terminal GFP expression construct under the control of the ADH1 promoter, pBP73a (generous gift of Dr. William Parrish). Constructs used to generate yeast strains were cloned into pRS306 (generous gift from Dr. Huilin Zhou) after amplifying the regions distal and proximal to each appropriate deletion. One kilobase upstream of the Sli15 start codon was included for each of these constructs to ensure expression from the Sli15 promoter. Before

transformation into yeast, the constructs were digested with Stu1 to promote homologous recombination into the *ura3-52* locus. Yeast strains were constructed using standard transformation and sporulation protocols.

Protein expression in BL21-CodonPlus (Stratagene) E. coli was induced when cells were in log phase growth with 0.1 mM IPTG for 3–4 hr at 28ºC. Cells were resuspended in Lysis Buffer (1X PBS, 10mM EDTA [pH 8.0], 10mM EGTA [pH 8.0], 250 mM NaCl, 0.1% Tween- 20, 1mM PMSF, and 2mM Benzamidine-HCl) and incubated on ice for 15 minutes after the addition of 1mg/ml Lysozyme. 5mM dithiothreitol [DTT] was added prior to 1.5 minute sonification (15 sec. on followed by 30 sec. rest on ice) and lysates were clarified at 30,000 RPM for 30 min at 4ºC. Supernatant was added to glutathione-agarose slurry for 1 hour at 4ºC followed by 3 washes with Wash Buffer (1X PBS, 250 mM NaCl, 0.1% Tween- 20, and 1mM DTT) and an additional wash with the same Wash Buffer minus the Tween-20. Proteins were then either eluted with Elution Buffer (50mM Tris [pH 8.0], 10mM reduced glutathione, and 150mM KCl [pH was adjusted to slightly higher than 8.0]) or equilibrated into Cleavage Buffer (50mM Hepes [pH 7.0], 150mM NaCl, 1mM EDTA [pH 8.0], 1mM DTT, and 0.01% Tween-20). Approximately 40 ng/μl of GST tagged PreScission Protease was added to the samples being cleaved and they were rotated overnight at 4ºC. Cleaved proteins were eluted in Cleavage Buffer and in some cases additional NaCl was added (up to 0.5M) to aid in elution. Gel filtration of cleaved proteins was conducted in

Cleavage Buffer on a Superose 6 column. Protein concentrations were determined with a combination of Bradford protein assays and densitometry of Coomassie-stained gels relative to a BSA standard. For proteins that had breakdown products, the reported concentrations are for the highest molecular weight species, corresponding to the predicted molecular weight of the respective Sli15 fragment.

3.4.2 Microtubule co-sedimentation assays

Microtubule assembly and measurement of polymeric tubulin concentration were performed as described (Desai et al., 1999). For microtubule-binding reactions, purified proteins were dialyzed into BRB80 (80 mM PIPES, 1 mM $MgCl_2$, and 1 mM EGTA [pH 6.8]) plus 1 mM DTT and pre-cleared at 70,000 rpm for 10 min in a TLA100 rotor. Proteins were serially diluted before adding a constant amount to microtubules such that the final microtubule concentration was 2.5 μM (microtubules were resuspended in BRB80 with 1 mM taxol) and the final volume was 35 μl. Protein concentration varied for each Sli15 fragment and is indicated in each figure. Reactions were incubated at room temperature for 20 min and pelleted for 10 min at 70,000 rpm in a TLA100 rotor at 25ºC. For the supernatant sample, 30 μl was removed from the top of the tube. For the pellet sample, the remaining supernatant was removed and 30 μl BRB80 + 5 mM $CaCl_2$ and 50 mM KCl was added to the pellet for 10 min on ice. Equivalent amounts of supernatant

(S) and pellet (P) fractions were separated by SDS-PAGE and stained with Coomassie. Microtubule bundling assays were performed in the same manner as the cosedimentation assays except instead of spinning the reaction 5μl was squashed onto a coverslip and pictures were taken using a 60X, 1.4 NA objective.

3.4.3 Microscopy and CEN-DNA Optical Trap Assays

For confocal imaging, yeast strains expressing Sli15-GFP constructs were grown to log phase in minimal media. Imaging was done on a spinning disk confocal (McBain Instruments) mounted live in minimal media on an inverted microscope (TE2000e; Nikon). Images were acquired using a 100X 1.4 NA Plan Apo objective lens with 1.5X auxiliary magnification (150X magnification total) and a charge-coupled device camera (Orca ER; Hamamatsu) with 2 X 2 binning. Acquisition parameters, shutters, and focus were controlled by MetaMorph software (Universal Imaging). All fluorescence images were acquired using the same settings, including laser intensity. Each fluorescence image presented is a maximum intensity projection of a z-series stack through the entire yeast cell (5–8 μm), whereas a single differential interference contrast image was acquired at the midpoint of the z stack. All imaging was conducted at room temperature (~23ºC).

CEN-DNA bead assays were performed as described in Chapter 2, exceptions and additions to the protocol are noted in the legend of Figure 3.4.

With regards to reagents, the only notable change was the size and source of beads, which were 0.44μm (Sperotech SVP-05-10 for optical trap assays and SVFP-0552-5 for traditional CEN-DNA bead assays). Labeling of CEN-DNA to the beads was performed as described (Severin et al., 1999). Flow slides for optical trap assays were cleaned with KOH rather than ethanol and anti-digoxigenin was used at 20 μg/ml. Additionally, the wash step after binding CEN-DNA beads to microtubules was eliminated. Optical trap microscopy was performed as described (Asbury et al., 2006).

3.5 Acknowledgements

I am grateful to members of Charles Asbury lab at the University of Washington for their expertise and help with the optical trap microscopy as well as many stimulating conversations that resulted in new hypothesis and experiments. In particular, the experiments shown in Figure 3.4C & D were performed in equal collaboration with Andrew Powers from the Asbury lab. This work was supported by a training grant from the National Cancer Institute (to S.S.), by grants from the Human Frontier Science Program and the NIH to Arshad Desai, and salary and additional support from the Ludwig Institute for Cancer Research.

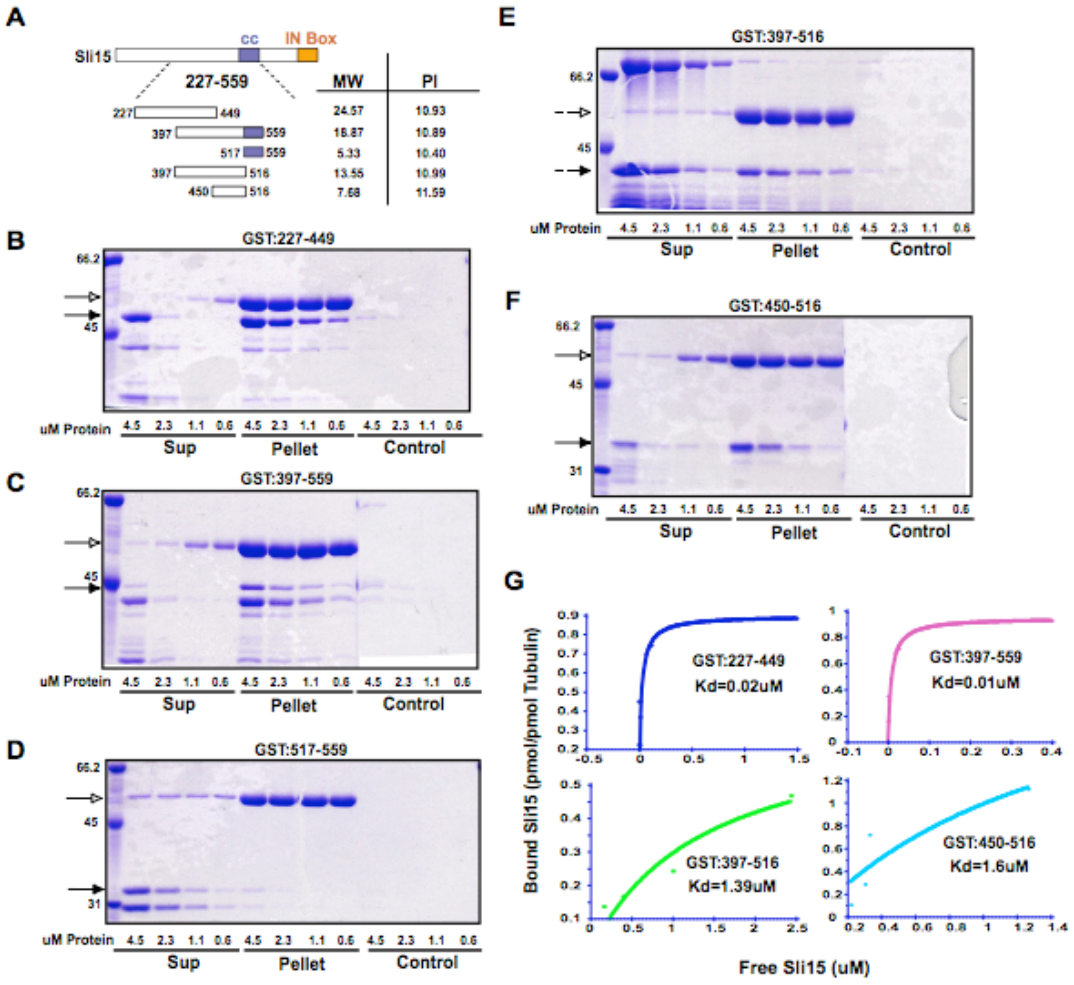


Figure 3.1 All Sli15-MTB GST fragments, except the conserved region from amino acids 517-559, bind microtubules with varying affinity.

A) Schematic of the Sli15 microtubule-binding domain. Fragments that were tested for microtubule binding affinity are depicted.

B-F) Co-sedimentation analysis of GST-Sli15 fragments and microtubules. Amount of pre-spun protein added to 2.5 μM GMPCPP stabilized microtubules or 1X BRB80 (control) is indicated below each gel. Proteins were incubated 20 minutes at room temperature, and then spun at 70,000 RPM for 10 min. The supernatant was collected and the pellet resuspended in BRB80 + 50 mM KCl and 50 mM $CaCl_2$ and incubated on ice for 10 minutes. Samples were separated by SDS-PAGE and stained with coomassie.

G) The amount of the GST-Sli15 fragments bound to microtubules (normalized as moles protein per mole of tubulin heterodimer) was plotted against the amount of free protein. The dissociation constants were calculated and indicated for each GST-Sli15 fragment.

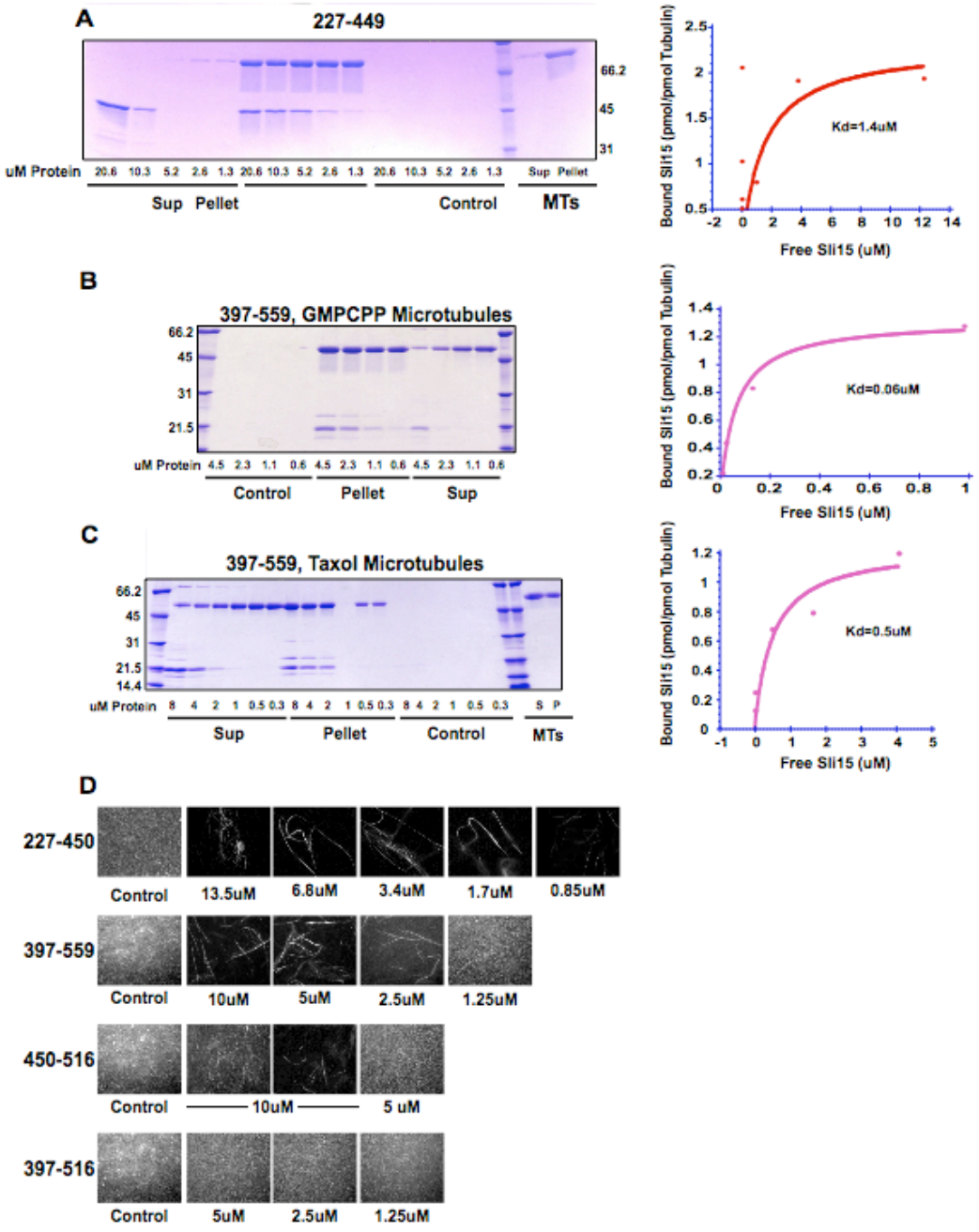


Figure 3.2 (A-C) Analysis of microtubule binding and bundling affinity of Sli15-MTB proteins.

A) Microtubule binding activity of Sli15 fragment 227-449. Experiment was done as described in Figure 3.1 except the GST tag was cleaved from the protein before co-sedimentation analysis.

B-C) Co-sedimentation analysis of the GST cleaved 397-559 fragment with either 2 μM GMPCPP stabilized microtubules (B) or 2 μM taxol stabilized microtubules (C).

D) Sli15 fragments bundle microtubules. The indicated amount of each fragment was mixed with CY3 labeled GMPCPP stabilized microtubules or BRB80 (Control) and imaged.

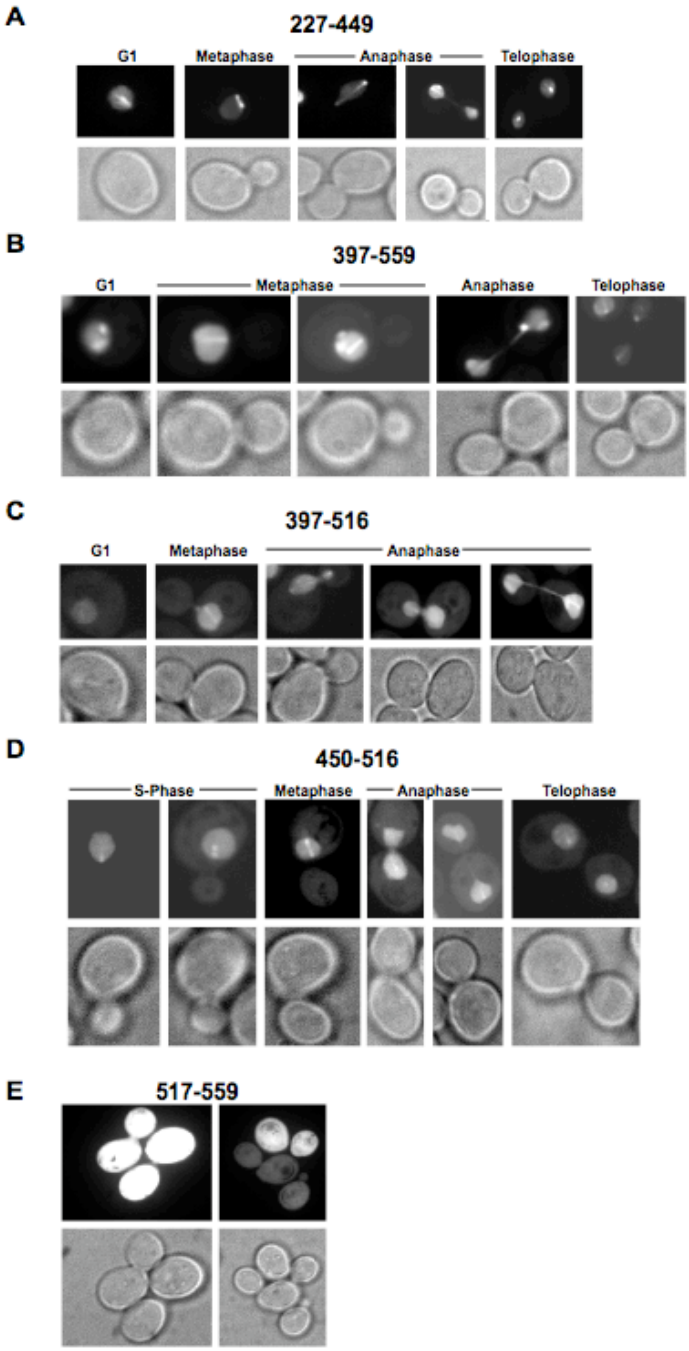
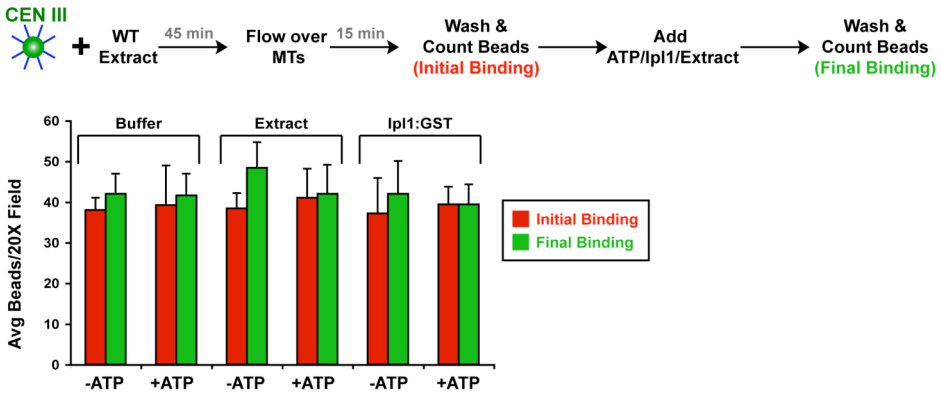


Figure 3.3 In vivo localization of Sli15-MTB:GFP fragments.
A-E) Various Sli15 fragments were expressed as C-terminally tagged GFP proteins in WT budding yeast under the control of the ADH1 promoter (see Table 3.1 for details). Log phase cultures were examined for GFP expression using a confocal spinning disk microscope. DIC images are shown below as a method to determine cell cycle stage. Representative images of various cell cycles are depicted. All fragments except for Sli15$^{517-559}$ localize to kinetochores during G1 through metaphase and then subsequently localize to the mitotic spindle during anaphase.

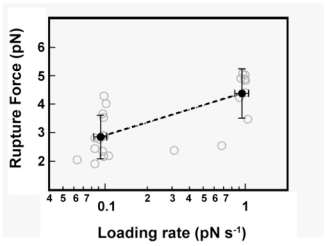
A



B

Initial Reaction	Reagent Added	Incubation Time	Change in Binding
WT (-)ATP	WT Extract	15 min	No
WT (-)ATP	Ipl1:GST	15 min	No
WT (-)ATP	Ipl1:GST + Sli15-CT :GST	15 min	No
ipl1-321 (+)ATP	*ipl1-321* Extract	15 min	No
ipl1-321 (+)ATP	*ipl1-321* Extract + Ipl1:GST	15 min	No
WT (-)ATP	Ipl1:GST	45 min	No
WT (-)ATP	Ipl1:GST + microcystin	45 min	No

C



D

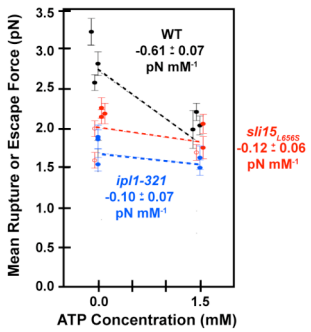


Figure 3.4 Bir1-Sli15 mediated binding of CEN-DNA and microtubules is insensitive to Ipl1/ATP regulation after initial binding, but attachments made in the presence of ATP are weaker.

A) CEN-DNA binding experiment was performed as described in Chapter 2 with 0.44 μm beads. After initial binding and counting, various combinations of ATP, GST-Ipl1, and extract were added to the flow chambers, allowed to incubate for 15-45 min., and then washed and re-counted. 333 molecules of CEN-DNA/bead were used and counts were plotted as the average bead number in a 20X field.

B) Summary of conditions tested for their ability to detach CEN-DNA beads from microtubules.

C) Rupture forces in piconewtons for WT CEN-DNA beads at two different loading rates.

D) WT extracts form CEN-DNA microtubule attachments that display an ATP dependent weakening whereas *sli15*^{L656S} and *ipl1-321* extracts are insensitive to ATP. Each circle represents one experiment with ~50 rupture events. The dashed lines between pooled –ATP and +ATP samples represent the slope, or change in rupture force for each extract condition.

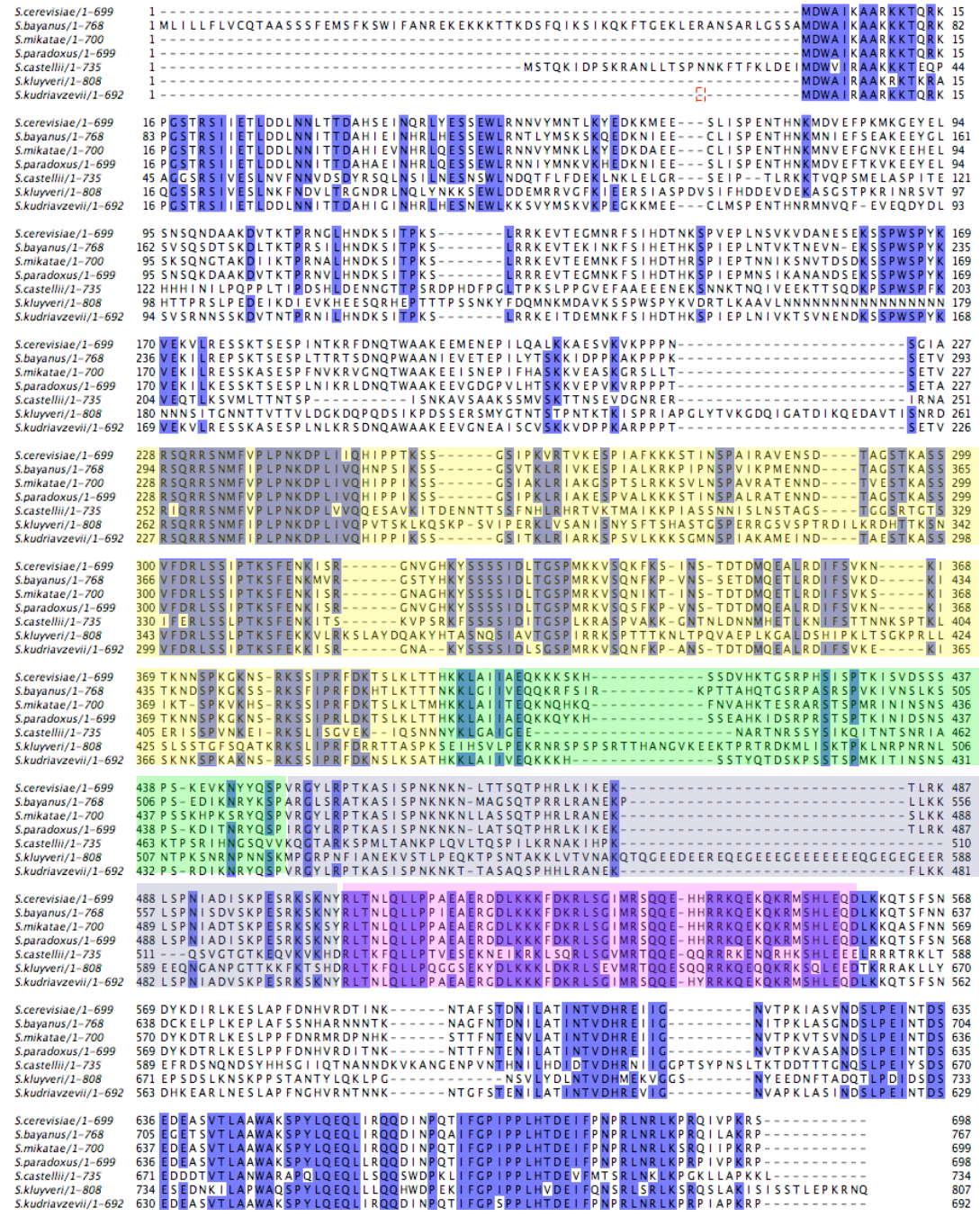


Figure S3.1 Sli15 conservation among *Saccharomyces* species.
Protein sequences of *Saccharomyces cerevisiae, bayanus, mikatae, paradoxus, castellii, kluyveri, kudriavzevii* Sli15 were aligned using ClustalW. Residues above a 75% identity threshold are colored in blue. Regions of the microtubule-binding domain are shaded to represent various fragments. Yellow:227-396, Green:397-449, Grey:450-516, Pink:517-559.

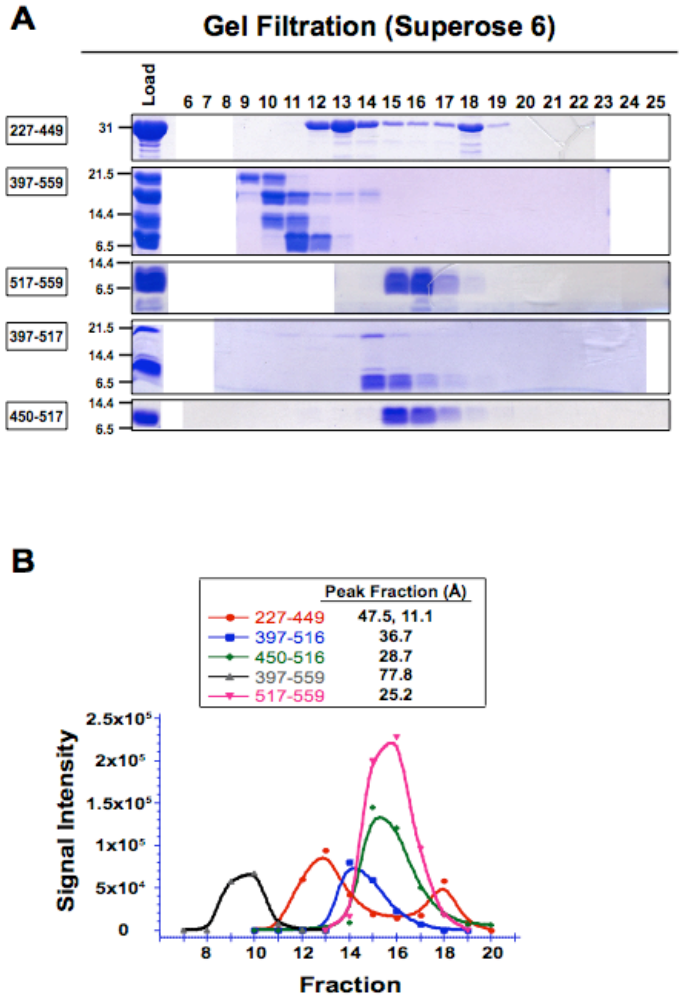


Figure S3.2 Gel Filtration analysis of Sli15 microtubule fragments

A) Sli15 fragments were fractionated using a Superose 6 column. Fractions were analyzed by SDS-PAGE and stained with Coomassie. All fragments except for 227-449 showed a single peak of protein.

B) Stokes radius of Sli15 fragments are larger than expected based on predicted molecular weight. Coomassie signal intensity from each gel in (A) was quantified in photoshop by determining the average pixel intensity for each band and plotted as "signal intensity". After calibrating the superose 6 column, approximate stokes radii for each fragment was calculated based on the peak fraction of each protein. For $Sli15^{227-449}$ the size of both peak fractions was calculated.

Table 3.1 Disrupting Any Portion of the Sli15 Microtubule Binding Domain Results in Cell Lethality

Sli15 Fragment Assessed	Number of Tetrads Analyzed	Number of viable *Δsli15 +SLI15* spores / Number of expected *Δsli15 +SLI15* spores [#]
Sli15	11	10/10
Sli15$^{\Delta 227\text{-}559}$	13	0/14
Sli15$^{\Delta 227\text{-}449}$	14	0/15[&]
Sli15$^{\Delta 397\text{-}559}$	11	0/11
Sli15$^{\Delta 397\text{-}516}$	17	0/15
Sli15$^{\Delta 450\text{-}516}$	17	1/19
Sli15$^{\Delta 517\text{-}559}$	14	0/12
Sli15$^{\Delta 227\text{-}397}$	11	0/22*

[#]This analysis was done based on the genotype of each tetrad analyzed. In each case, except for the full-length Sli15 and one tetrad of Sli15$^{\Delta 450\text{-}516}$, all tetrads resulted in 2 spores alive and 2 spores dead, suggesting the inability of the fragments to rescue the *Δsli15* strain. Based on the genotypes of the two viable spores, it was possible to predict which of the dead spores should have been *Δsli15 +SLI15* and is indicated. Since variable numbers of parental and non-parental ditypes as well as tetratypes were observed for each Sli15 fragment tested, the number of expected *Δsli15 +SLI15* spores varies.

[&]One tetrad resulted in two viable spores that genotyping revealed as *Δsli15 +SLI15*$^{\Delta 227\text{-}449}$ and *Sli15 +SLI15*$^{\Delta 227\text{-}449}$. Since this is not an expected genotype of a ditype tetrad it could have been a tetratype in which the wild-type spore did not survive. PCR analysis of the one viable *Δsli15 +SLI15*$^{\Delta 227\text{-}449}$ spore amplified both full-length Sli15 as well as Sli15$^{\Delta 227\text{-}449}$ so this strain was not analyzed further, nor was it counted in the tetrad analysis shown above since it was questionable as to the validity of it being a real tetrad.

***** All tetrads isolated for this strain were non-parental ditypes in which the two viable spores were wild-type. Additionally, two apparent tetrads resulted in two viable spores in which one spore was wild-type and one spore was *Δsli15 +SLI15*$^{\Delta 227\text{-}397}$. Like the situation described for the *Δsli15 +SLI15*$^{\Delta 227\text{-}449}$ strain, these two spores also amplified both a full-length Sli15 and Sli15$^{\Delta 227\text{-}397}$. Therefore, these two spores were not analyzed further and not counted in the tetrad analysis.

Table 3.2 Plasmids and Yeast Strains Used in This Study

Name	Relevant Features	Source
pSS109	*lacI^{q}, GST-Sli15$^{558-698}$* under *tac* promoter control with PreScission protease site in between *GST* and *Sli15$^{558-698}$* (in pGEX-6P-1)	This study
pSS141	*lacI^{q}, GST-Ipl1* under *tac* promoter control with PreScission protease site in between *GST* and *Ipl1* (in pGEX-6P-1)	This study
pSS89	*lacI^{q}, GST-Sli15$^{397-559}$* under *tac* promoter control with PreScission protease site in between *GST* and *Sli15$^{397-559}$* (in pGEX-6P-1)	This study
pSS102	*lacI^{q}, GST-Sli15$^{517-559}$* under *tac* promoter control with PreScission protease site in between *GST* and *Sli15$^{517-559}$* (in pGEX-6P-1)	This study
pSS104	*lacI^{q}, GST-Sli15$^{397-516}$* under *tac* promoter control with PreScission protease site in between *GST* and *Sli15$^{397-516}$* (in pGEX-6P-1)	This study
pSS105	*lacI^{q}, GST-Sli15$^{450-516}$* under *tac* promoter control with PreScission protease site in between *GST* and *Sli15$^{450-516}$* (in pGEX-6P-1)	This study
pSS106	*lacI^{q}, GST-Sli15$^{227-449}$* under *tac* promoter control with PreScission protease site in between *GST* and *Sli15$^{227-449}$* (in pGEX-6P-1)	This study
pSS118	*URA3,* CEN, *Sli15$^{397-559}$-GFP* under *ADH1* promoter (in pBP73a)	This study
pSS119	*URA3,* CEN, *Sli15$^{517-559}$-GFP* under *ADH1* promoter (in pBP73a)	This study
pSS120	*URA3,* CEN, *Sli15$^{397-516}$-GFP* under *ADH1* promoter (in pBP73a)	This study
pSS121	*URA3,* CEN, *Sli15$^{450-516}$-GFP* under *ADH1* promoter (in pBP73a)	This study
pSS122	*URA3,* CEN, *Sli15$^{227-449}$-GFP* under *ADH1* promoter (in pBP73a)	This study
pBP73a	*URA3, GFP* under *ADH1* promoter	Scott Emr
pRS306	*URA3*	Sikorski and Hieter, 1989
pOD594	*URA3, Sli15*+1Kb upstream of Sli15 start (in pRS306)	This study
pOD595	*URA3, Sli15$^{\Delta 227-559}$*+1Kb upstream of Sli15 start (in pRS306)	This study
pSS143	*URA3, Sli15$^{\Delta 227-449}$*+1Kb upstream of Sli15 start (in pRS306)	This study
pSS144	*URA3, Sli15$^{\Delta 397-559}$*+1Kb upstream of Sli15 start (in pRS306)	This study
pSS145	*URA3, Sli15$^{\Delta 397-516}$*+1Kb upstream of Sli15 start (in pRS306)	This study
pSS146	*URA3, Sli15$^{\Delta 450-516}$*+1Kb upstream of Sli15 start (in pRS306)	This study
pSS147	*URA3, Sli15$^{\Delta 517-559}$*+1Kb upstream of Sli15 start (in pRS306)	This study
pSS148	*URA3, Sli15$^{\Delta 227-397}$*+1Kb upstream of Sli15 start (in pRS306)	This study
ODY49	*MAT**a**, trp1Δ63, ura3-52, his3Δ200* (S288C)	This study
SBY203	*MAT**a**, ura3-1, leu2-3,112, his3-11, trp1-1, can1-100, ade2-1, bar1-1, cdc15-2, LYS2* (W303)	Sue Biggins
ODY182	*MAT**a**, trp1Δ63, ura3-52, his3Δ200, sli15(L656S)::TRP1* (S288C)	This study
SBY630	*MAT**a** ura3-1 leu2-3,112 his3-11 trp1-1 LSY2 BAR1 can1-100 ade2-1 ipl1-321* (W303)	Sue Biggins
SSY16	*MAT**a**/MATα, trp1Δ63/trp1Δ63, ura3-52/ura3-52, his3Δ200/ his3Δ200, Δsli15::TRP1/SLI15*	This Study*
SSY236	*MAT**a**/MATα, trp1Δ63/trp1Δ63, ura3-52::SLI15::URA3, his3Δ200/ his3Δ200, Δsli15::TRP1/SLI15*	This Study*
SSY237	*MAT**a**/MATα, trp1Δ63/trp1Δ63, ura3-52::SLI15$^{\Delta 227-559}$::URA3, his3Δ200/ his3Δ200, Δsli15::TRP1/SLI15*	This Study*
SSY238	*MAT**a**/MATα, trp1Δ63/trp1Δ63, ura3-52::SLI15$^{\Delta 227-449}$::URA3, his3Δ200/ his3Δ200, Δsli15::TRP1/SLI15*	This Study*

Table 3.2 (Continued) Plasmids and Yeast Strains Used in This Study

Name	Relevant Features	Source
SSY239	*MAT**a**/MATα, trp1Δ63/trp1Δ63, ura3-52::SLI15$^{\Delta 397\text{-}559}$::URA3, his3Δ200/ his3Δ200, Δsli15::TRP1/SLI15*	This Study*
SSY240	*MAT**a**/MATα, trp1Δ63/trp1Δ63, ura3-52::SLI15$^{\Delta 397\text{-}516}$::URA3, his3Δ200/ his3Δ200, Δsli15::TRP1/SLI15*	This Study*
SSY241	*MAT**a**/MATα, trp1Δ63/trp1Δ63, ura3-52::SLI15$^{\Delta 450\text{-}516}$::URA3, his3Δ200/ his3Δ200, Δsli15::TRP1/SLI15*	This Study*
SSY242	*MAT**a**/MATα, trp1Δ63/trp1Δ63, ura3-52::SLI15$^{\Delta 517\text{-}559}$::URA3, his3Δ200/ his3Δ200, Δsli15::TRP1/SLI15*	This Study*
SSY243	*MAT**a**/MATα, trp1Δ63/trp1Δ63, ura3-52::SLI15$^{\Delta 227\text{-}397}$::URA3, his3Δ200/ his3Δ200, Δsli15::TRP1/SLI15*	This Study*

*Strains SSY236-SSY243 were created by digesting plasmids pOD594, pOD595, and pSS143-148 with Stu1 and transforming into SSY16, which allowed for integration of each Sli15 fragment under the control of the endogenous Sli15 promoter at the *URA* locus.

Chapter 4: Conclusions and Future Directions

4.1 Conclusions

The importance of the kinetochore and its essential role in chromosome segregation has been appreciated for centuries. Work in the last decade has advanced our knowledge about the molecular sub-complexes that make up the kinetochore and how they are working together to couple microtubule dynamics into productive forces that push and pull chromosomes (Cheeseman and Desai, 2008). At the beginning of these dissertation studies, many molecular kinetochore proteins had been identified, but our understanding of how they assemble and what distinct roles they were playing, were unclear (De Wulf, 2003). The work described in this dissertation is based on an in vitro assay utilized to determine which kinetochore proteins connect centromeric DNA to microtubules (Sorger et al., 1994). This approach led to the unexpected discovery that two kinetochore proteins, Bir1/Survivin and Sli15/INCENP were connecting CEN-DNA to microtubules in a manner utilized to detect and ultimately correct incorrect centromere microtubule attachments (Sandall et al., 2006).

The initial assumption when initiating these studies was that the in vitro assay would identify proteins making “core” kinetochore attachments, ones that serve to couple chromosome movements to dynamic microtubules. The results indicate otherwise, as eliminating the CEN-DNA microtubule interaction

in vivo led to an inability of cells to correct syntelic attachments. If the in vitro Bir1/Survivin-Sli15/INCENP mediated connection were required for core attachments, the expected phenotype would be a complete lack of attachments instead of incorrect attachments. Because Bir1/Survivin and Sli15/INCENP form a complex with Ipl1/Aurora B kinase, which is one of the few molecules known to regulate incorrect attachments such as syntelic attachments (Ruchaud et al., 2007), and Sli15 activates Ipl1/Aurora B (Kang et al., 2001; Sessa et al., 2005), this led me to propose that the Bir1/Sli15 mediated interaction between CEN-DNA and microtubules is acting to regulate Ipl1 when attachments are incorrect (Sandall et al., 2006).

Understanding the mechanism for how Ipl1 discerns correct and incorrect attachments has been an area of intense research. The common consensus from experiments in both yeast and other eukaryotes is that Ipl1 senses incorrect attachments through tension (Dewar et al., 2004; Lampson et al., 2004). Correctly attached chromosomes (amphitelic) are pulled in opposite directions by spindle microtubules and this force is opposed by the cohesion that connects sister chromatids until anaphase onset. The result of such an arrangement is a high amount of tension felt across the sister centromeres. When sister chromatids are attached to microtubules emanating from the same spindle pole, this tension is decreased immensely. Therefore an appealing model is that the Bir1/Sli15 mediated attachment between CEN-DNA and microtubules is acting as a tension sensor to regulate Ipl1.

Considering the importance of the Ipl1 regulatory function, there have been major efforts to understand how it relays a mechanical state such as tension into a chemical signal. My work is the first concrete hypothesis to describe a plausible mechanism for how this function is achieved.

Chromosome segregation errors are either deadly to cells, or result in aneuploidy, a condition known to cause birth defects and cancer. The first chemotherapy agents discovered and put to use actually target mitotically dividing cells by inhibiting microtubule dynamics (Desai and Mitchison, 1997). Considering microtubules have a wide variety of other cellular functions in the human body, these types of chemotherapies have unpleasant side effects. For this reason, the kinetochore has increasingly become a hot target for new cancer therapies. Specific kinetochore therapies are attractive not just because they would ultimately halt cell division, but because several kinetochore proteins are over-expressed or mis-regulated in cancer cells. This provides an ideal target as it potentially meets the criteria of both specificity and potency. The chromosomal passenger proteins, particularly Ipl1/Aurora B and Bir1/Survivin fit these criteria and in fact Survivin is often used as a prognostic marker for cancer cells (Altieri, 2008). While finding specific drugs that target Survivin have been more difficult due to the non-enzymatic nature of the protein, several Aurora B inhibitors are in clinical trials with some even making it into Phase II (Meraldi et al., 2004; Mountzios et al., 2008).

Understanding the detailed mechanisms of Ipl1/Aurora B function is essential for its future as a potent and specific cancer therapy target.

4.2 Future Directions

This dissertation has laid the foundation to understand a how kinetochores monitor and correct their own attachments, a fundamental function to ensure genetic fidelity. Studies described in Chapter 3 have begun to answer some fundamental questions about how the Bir1/Sli15 mediated connection between CEN-DNA and microtubules is sensing tension to regulate Ipl1, including how Sli15 interacts with microtubules and how the attachment regulates and is regulated by Ipl1. Nevertheless, there are still many important questions to be answered.

The region of Sli15 that binds microtubules has been identified, but has proven difficult to study on the structural level. Nevertheless, the work presented in Chapter 3 should provide a framework for continuing to attempt purification of a stable microtubule-binding fragment that can be examined on microtubules and/or crystallized. Determining whether Sli15 interacts with microtubules laterally or end-on would provide information to distinguish how the “tension sensing” attachment is spatially arranged in vivo. Considering the inner centromere localization of the CPC in higher eukaryotes (Ruchaud et al., 2007), this is a major outstanding question that my work described in Chapter 2 provokes.

An end-on attachment would almost certainly predict that the proteins are linking the CEN-DNA and microtubules in the outer region of the centromere. Since the CPC proteins have extremely fast turnover rates at the centromere (Ahonen et al., 2008; Beardmore et al., 2004; Murata-Hori and Wang, 2002), this might suggest a mechanism whereby sequestering the majority of the protein pool into the inner centromere region is how the tension sensor is “turned-off” of regulated. On the other hand, a lateral interaction would leave open the possibility that the linkage was indeed occurring in the inner centromere and that only when microtubules enter this zone is the tension sensor utilized. One could imagine that an attachment under tension may prevent microtubules as well as relevant Ipl1 substrates from entering the “active” inner centromere, effectively turning off the tension sensor as well as restricting substrate accessibility. However, a less tense attachment may allow microtubule access to Bir1/Sli15 effectively turning on the tension sensor, activating Ipl1, and leading to a release of the microtubule such that a new attempt can be made. This sort of spatial regulation would also explain how the tension sensor might be activated when attachments are merotelic, a situation in which both sister kinetochores are attached to opposite spindle poles but an additional attachment is also made between one of the kinetochores and microtubules emanating from the incorrect spindle pole. While these types of attachments are most likely not encountered at the single microtubule attachment site of budding yeast, it is a commonly observed

problem in higher eukaryotes. By keeping the tension sensor located between sister kinetochores, microtubules that cross this region and attach incorrectly to a kinetochore would encounter the sensor that would ultimately activate Aurora B/Ipl1 and facilitate correction, possibly by regulating the microtubule depolymerase MCAK. Understanding the interaction of Sli15 and microtubules would greatly enhance the mechanistic insight into the in vivo relevance and organization of the tension sensor.

If structural studies of the Sli15 microtubule-binding region prove to be unfeasible, an alternate approach would be a genetic screen in yeast to search for point mutants that abolish microtubule binding and/or affect Sli15 function in some new, undescribed way. I have already laid the groundwork for this type of genetic screen by devising a strategy to use error prone PCR specifically in the microtubule-binding domain of Sli15 such that it can be recombined into a diploid strain heterozygous for *Sli15*. This strain contains a haploid specific marker that will allow for selection of haploid mutants that are *MAT**a*** and contain *sli15Δ* along with the *sli15* mutant (Huang et al., 2008). By screening for both temperature sensitivity and benomyl sensitivity, I hope to isolate new alleles of *sli15* that will further our understanding of the Sli15 microtubule-binding domain.

The optical trap studies have provided an exciting new tool to truly test how tension influences the Bir1/Sli15 mediated CEN-DNA microtubule interaction. Technical challenges have prevented experiments that would

directly test this, but has allowed for studies that suggest Ipl1 weakens the interaction (Figure 3.4D). By coupling flow into the optical trap studies I am confident that we will be able to directly test how tension influences the Bir1-Sli15 mediated interaction. If tension stabilizes the attachment and prevents Ipl1 activity, then that would suggest the model proposed in Chapter 2 (Figure 2.6) is correct. On the other hand, if tension does not have an effect on the attachment and Ipl1 activity, it would provide evidence that Ipl1 activity is not regulated, but rather is controlled primarily by substrate accessibility. Either way, these studies are essential for understanding tension, Ip1l regulation, and how Bir1/Sli15 is relates to both.

References

Adams, R.R., Eckley, D.M., Vagnarelli, P., Wheatley, S., Gerloff, D.L., Mackay, A.M., Svingen, P.A., Kaufmann, S.H., and Earnshaw, W. (2001a). Human INCENP colocalizes with the Aurora-B/AIRK2 kinase on chromosomes and is overexpressed in tumour cells. Chromosoma *110*, 65-74.

Adams, R.R., Maiato, H., Earnshaw, W., and Carmena, M. (2001b). Essential roles of Drosophila inner centromere protein (INCENP) and aurora B in histone H3 phosphorylation, metaphase chromosome alignment, kinetochore disjunction, and chromosome segregation. J Cell Biol *153*, 865-880.

Adams, R.R., Wheatley, S.P., Gouldsworthy, A.M., Kandels-Lewis, S.E., Carmena, M., Smythe, C., Gerloff, D.L., and Earnshaw, W.C. (2000). INCENP binds the Aurora-related kinase AIRK2 and is required to target it to chromosomes, the central spindle and cleavage furrow. Curr Biol *10*, 1075-1078.

Ahonen, L., Kukkonen, A.M., Pouwels, J., Bolton, M., Jingle, C.D., Stukenberg, P., and Kallio, M. (2008). Perturbation of Incenp function impedes anaphase chromatid movements and chromosomal passenger protein flux at centromeres. Chromosoma.

Al-Bassam, J., van Breugel, M., Harrison, S., and Hyman, A. (2006). Stu2p binds tubulin and undergoes an open-to-closed conformational change. The Journal of Cell Biology *172*, 1009-1022.

Altieri, D.C. (2006). The case for survivin as a regulator of microtubule dynamics and cell-death decisions. Current Opinion in Cell Biology *18*, 609-615.

Altieri, D.C. (2008). Survivin, cancer networks and pathway-directed drug discovery. Nat Rev Cancer *8*, 61-

Amor, D.J., and Choo, K.H. (2002). Neocentromeres: role in human disease, evolution, and centromere study. Am J Hum Genet *71*, 695-714.

Andersen, S.S., Ashford, A.J., Tournebize, R., Gavet, O., Sobel, A., Hyman, A.A., and Karsenti, E. (1997). Mitotic chromatin regulates phosphorylation of Stathmin/Op18. Nature *389*, 640-643.

Andrews, P.D., Knatko, E., Moore, W.J., and Swedlow, J.R. (2003). Mitotic mechanics: the auroras come into view. Curr Opin Cell Biol *15*, 672-683.

Andrews, P.D., Ovechkina, Y., Morrice, N., Wagenbach, M., Duncan, K., Wordeman, L., and Swedlow, J.R. (2004). Aurora B regulates MCAK at the mitotic centromere. Developmental Cell *6*, 253-268.

Asbury, C.L., Fehr, A.N., and Block, S.M. (2003). Kinesin moves by an asymmetric hand-over-hand mechanism. Science *302*, 2130-2134.

Asbury, C.L., Gestaut, D.R., Powers, A.F., Franck, A.D., and Davis, T. (2006). The Dam1 kinetochore complex harnesses microtubule dynamics to produce force and movement. Proc Natl Acad Sci USA *103*, 9873-9878.

Ault, J.G., and Rieder, C.L. (1992). Chromosome mal-orientation and reorientation during mitosis. Cell Motil Cytoskeleton *22*, 155-159.

Baker, R.E., Fitzgerald-Hayes, M., and O'Brien, T.C. (1989). Purification of the yeast centromere binding protein CP1 and a mutational analysis of its binding site. J Biol Chem *264*, 10843-10850.

Bansal, P.K., Abdulle, R., and Kitagawa, K. (2004). Sgt1 associates with Hsp90: an initial step of assembly of the core kinetochore complex. Mol Cell Biol *24*, 8069-8079.

Baumann, C., Korner, R., Hofmann, K., and Nigg, E. (2007). PICH, a Centromere-Associated SNF2 Family ATPase, Is Regulated by Plk1 and Required for the Spindle Checkpoint. Cell *128*, 101-114.

Beardmore, V.A., Ahonen, L., Gorbsky, G., and Kallio, M. (2004). Survivin dynamics increases at centromeres during G2/M phase transition and is regulated by microtubule-attachment and Aurora B kinase activity. J Cell Sci *Pt*.

Biggins, S. (2001). The budding yeast protein kinase Ipl1/Aurora allows the absence of tension to activate the spindle checkpoint. Genes & Development *15*, 3118-3129.

Biggins, S. (2003). Captivating Capture: How Microtubules Attach to Kinetochores. Current Biology *13*, R449-R460.

Biggins, S., Severin, F.F., Bhalla, N., Sassoon, I., Hyman, A.A., and Murray, A.W. (1999). The conserved protein kinase Ipl1 regulates microtubule binding to kinetochores in budding yeast. Genes & Development *13*, 532-544.

Bishop, J.D., and Schumacher, J.M. (2002). Phosphorylation of the carboxyl terminus of inner centromere protein (INCENP) by the Aurora B Kinase stimulates Aurora B kinase activity. J Biol Chem *277*, 27577-27580.

Block, S.M., Asbury, C.L., Shaevitz, J.W., and Lang, M.J. (2003). Probing the kinesin reaction cycle with a 2D optical force clamp. Proc Natl Acad Sci USA *100*, 2351-2356.

Blower, M.D., Sullivan, B.A., and Karpen, G.H. (2002). Conserved organization of centromeric chromatin in flies and humans. Developmental Cell *2*, 319-330.

Bolton, M.A., Lan, W., Powers, S.E., McCleland, M.L., Kuang, J., and Stukenberg, P.T. (2002). Aurora B kinase exists in a complex with survivin and INCENP and its kinase activity is stimulated by survivin binding and phosphorylation. Mol Biol Cell *13*, 3064-3077.

Bouck, D., and Bloom, K. (2005). The kinetochore protein Ndc10p is required for spindle stability and cytokinesis in yeast. Proc Natl Acad Sci USA *102*, 5408-5413.

Brinkley, B.R., and Stubblefield, E. (1966). The fine structure of the kinetochore of a mammalian cell in vitro. Chromosoma *19*, 28-43.

Burke, D.J., and Stukenberg, P.T. (2008). Linking kinetochore-microtubule binding to the spindle checkpoint. Developmental Cell *14*, 474-479.

Buvelot, S., Tatsutani, S.Y., Vermaak, D., and Biggins, S. (2003). The budding yeast Ipl1/Aurora protein kinase regulates mitotic spindle disassembly. J Cell Biol *160*, 329-339.

Cai, M., and Davis, R.W. (1990). Yeast centromere binding protein CBF1, of the helix-loop-helix protein family, is required for chromosome stability and methionine prototrophy. Cell *61*, 437-446.

Camahort, R., Li, B., Florens, L., Swanson, S., Washburn, M., and Gerton, J. (2007). Scm3 Is Essential to Recruit the Histone H3 Variant Cse4 to Centromeres and to Maintain a Functional Kinetochore. Molecular Cell *26*, 853-865.

Carmena, M., and Earnshaw, W. (2003). The cellular geography of aurora kinases. Nat Rev Mol Cell Biol *4*, 842-854.

Carvalho, A., Carmena, M., Sambade, C., Earnshaw, W., and Wheatley, S.P. (2003). Survivin is required for stable checkpoint activation in taxol-treated HeLa cells. Journal of Cell Science *116*, 2987-2998.

Cesario, J.M., Jang, J.K., Redding, B., Shah, N., Rahman, T., and McKim, K.S. (2006). Kinesin 6 family member Subito participates in mitotic spindle assembly and interacts with mitotic regulators. Journal of Cell Science *119*, 4770-4780.

Chan, C., and Botstein, D. (1993). Isolation and characterization of chromosome-gain and increase-in-ploidy mutants in yeast. Genetics *135*, 677-691.

Cheeseman, I. (2004). A conserved protein network controls assembly of the outer kinetochore and its ability to sustain tension. Genes & Development *18*, 2255-2268.

Cheeseman, I., Anderson, S., Jwa, M., Green, E.M., Kang, J., Yates, J., Chan, C.S., Drubin, D., and Barnes, G. (2002). Phospho-regulation of kinetochore-microtubule attachments by the Aurora kinase Ipl1p. Cell *111*, 163-172.

Cheeseman, I., Chappie, J., Wilsonkubalek, E., and Desai, A. (2006). The Conserved KMN Network Constitutes the Core Microtubule-Binding Site of the Kinetochore. Cell *127*, 983-997.

Cheeseman, I., and Desai, A. (2008). Molecular architecture of the kinetochore–microtubule interface. Nat Rev Mol Cell Biol *9*, 33-46.

Chen, J., Jin, S., Tahir, S.K., Zhang, H., Liu, X., Sarthy, A.V., McGonigal, T.P., Liu, Z., Rosenberg, S.H., and Ng, S.C. (2003). Survivin enhances Aurora-B kinase activity and localizes Aurora-B in human cells. J Biol Chem *278*, 486-490.

Ciferri, C., Musacchio, A., and Petrovic, A. (2007). The Ndc80 complex: hub of kinetochore activity. FEBS Lett *581*, 2862-2869.

Ciferri, C., Pasqualato, S., Screpanti, E., Varetti, G., Santaguida, S., Dos Reis, G., Maiolica, A., Polka, J., De Luca, J.G., De Wulf, P*., et al.* (2008). Implications for kinetochore-microtubule attachment from the structure of an engineered Ndc80 complex. Cell *133*, 427-439.

Clarke, L. (1998). Centromeres: proteins, protein complexes, and repeated domains at centromeres of simple eukaryotes. Curr Opin Genet Dev *8*, 212-218.

Cleveland, D.W., Mao, Y., and Sullivan, K.F. (2003). Centromeres and kinetochores: from epigenetics to mitotic checkpoint signaling. Cell *112*, 407-421.

Collins, K.A., Castillo, A.R., Tatsutani, S.Y., and Biggins, S. (2005). De novo kinetochore assembly requires the centromeric histone H3 variant. Mol Biol Cell *16*, 5649-5660.

Cooke, C.A., Heck, M.M., and Earnshaw, W.C. (1987). The inner centromere protein (INCENP) antigens: movement from inner centromere to midbody during mitosis. The Journal of Cell Biology *105*, 2053-2067.

Cottarel, G., Shero, J.H., Hieter, P., and Hegemann, J.H. (1989). A 125-base-pair CEN6 DNA fragment is sufficient for complete meiotic and mitotic centromere functions in Saccharomyces cerevisiae. Mol Cell Biol *9*, 3342-3349.

Crosio, C., Fimia, G.M., Loury, R., Kimura, M., Okano, Y., Zhou, H., Sen, S., Allis, C.D., and Sassone-Corsi, P. (2002). Mitotic phosphorylation of histone H3: spatio-temporal regulation by mammalian Aurora kinases. Mol Cell Biol *22*, 874-885.

De Wulf, P. (2003). Hierarchical assembly of the budding yeast kinetochore from multiple subcomplexes. Genes & Development *17*, 2902-2921.

DeLuca, J.G., Gall, W.E., Ciferri, C., Cimini, D., Musacchio, A., and Salmon, E.D. (2006). Kinetochore microtubule dynamics and attachment stability are regulated by Hec1. Cell *127*, 969-982.

Desai, A., and Mitchison, T.J. (1997). Microtubule polymerization dynamics. Annu Rev Cell Dev Biol *13*, 83-117.

Desai, A., Verma, S., Mitchison, T.J., and Walczak, C.E. (1999). Kin I kinesins are microtubule-destabilizing enzymes. Cell *96*, 69-78.

Dewar, H., Tanaka, K., Nasmyth, K., and Tanaka, T. (2004). Tension between two kinetochores suffices for their bi-orientation on the mitotic spindle. Nature *428*, 93-97.

Ditchfield, C., Johnson, V.L., Tighe, A., Ellston, R., Haworth, C., Johnson, T., Mortlock, A., Keen, N., and Taylor, S.S. (2003). Aurora B couples chromosome alignment with anaphase by targeting BubR1, Mad2, and Cenp-E to kinetochores. J Cell Biol *161*, 267-280.

Dong, Y., Vanden Beldt, K.J., Meng, X., Khodjakov, A., and McEwen, B.F. (2007). The outer plate in vertebrate kinetochores is a flexible network with multiple microtubule interactions. Nat Cell Biol *9*, 516-522.

Enquist-Newman, M., Cheeseman, I., Van Goor, D., Drubin, D., Meluh, P.B., and Barnes, G. (2001). Dad1p, third component of the Duo1p/Dam1p complex involved in kinetochore function and mitotic spindle integrity. Mol Biol Cell *12*, 2601-2613.

Espelin, C.W., Kaplan, K.B., and Sorger, P.K. (1997). Probing the architecture of a simple kinetochore using DNA-protein crosslinking. The Journal of Cell Biology *139*, 1383-1396.

Espelin, C.W., Simons, K.T., Harrison, S., and Sorger, P. (2003). Binding of the essential Saccharomyces cerevisiae kinetochore protein Ndc10p to CDEII. Mol Biol Cell *14*, 4557-4568.

Fitzgerald-Hayes, M., Clarke, L., and Carbon, J. (1982). Nucleotide sequence comparisons and functional analysis of yeast centromere DNAs. Cell *29*, 235-244.

Flemming, W. *Zellsubstanz, Kern und Zelltheilung (Cell Substance, Nucleus and Cell Division)*, F.C.W.Vogel, Leipzig, 1882.

Foltz, D.R., Jansen, L.E., Black, B.E., Bailey, A.O., Yates, J., and Cleveland, D.W. (2006). The human CENP-A centromeric nucleosome-associated complex. Nat Cell Biol *8*, 458-469.

Franck, A.D., Powers, A.F., Gestaut, D.R., Gonen, T., Davis, T.N., and Asbury, C.L. (2007). Tension applied through the Dam1 complex promotes microtubule elongation providing a direct mechanism for length control in mitosis. Nat Cell Biol *9*, 832-837.

Fujita, Y., Hayashi, T., Kiyomitsu, T., Toyoda, Y., Kokubu, A., Obuse, C., and Yanagida, M. (2007). Priming of centromere for CENP-A recruitment by human hMis18alpha, hMis18beta, and M18BP1. Developmental Cell *12*, 17-30.

Furuyama, T., Dalal, Y., and Henikoff, S. (2006). Chaperone-mediated assembly of centromeric chromatin in vitro. Proc Natl Acad Sci USA *103*, 6172-6177.

Gadea, B.B., and Ruderman, J.V. (2006). Aurora B is required for mitotic chromatin-induced phosphorylation of Op18/Stathmin. Proc Natl Acad Sci USA *103*, 4493-4498.

Gassmann, R., Carvalho, A., Henzing, A.J., Ruchaud, S., Hudson, D.F., Honda, R., Nigg, E., Gerloff, D.L., and Earnshaw, W. (2004). Borealin: a novel chromosomal passenger required for stability of the bipolar mitotic spindle. J Cell Biol *166*, 179-191.

Gaudet, A., and Fitzgerald-Hayes, M. (1987). Alterations in the adenine-plus-thymine-rich region of CEN3 affect centromere function in Saccharomyces cerevisiae. Mol Cell Biol *7*, 68-75.

Giet, R., and Glover, D.M. (2001). Drosophila aurora B kinase is required for histone H3 phosphorylation and condensin recruitment during chromosome condensation and to organize the central spindle during cytokinesis. The Journal of Cell Biology *152*, 669-682.

Gillis, A. (2005). A novel role for the CBF3 kinetochore-scaffold complex in regulating septin dynamics and cytokinesis. The Journal of Cell Biology *171*, 773-784.

Goh, P.Y., and Kilmartin, J.V. (1993). NDC10: a gene involved in chromosome segregation in Saccharomyces cerevisiae. J Cell Biol *121*, 503-512.

Goshima, G., Wollman, R., Goodwin, S.S., Zhang, N., Scholey, J.M., Vale, R.D., and Stuurman, N. (2007). Genes required for mitotic spindle assembly in Drosophila S2 cells. Science *316*, 417-421.

Goto, H., Kiyono, T., Tomono, Y., Kawajiri, A., Urano, T., Furukawa, K., Nigg, E., and Inagaki, M. (2006). Complex formation of Plk1 and INCENP required for metaphase–anaphase transition. Nat Cell Biol *8*, 180-187.

Greaves, I.K., Rangasamy, D., Ridgway, P., and Tremethick, D.J. (2007). H2A.Z contributes to the unique 3D structure of the centromere. Proc Natl Acad Sci USA *104*, 525-530.

Gruneberg, U., Neef, R., Honda, R., Nigg, E., and Barr, F.A. (2004). Relocation of Aurora B from centromeres to the central spindle at the metaphase to anaphase transition requires MKlp2. The Journal of Cell Biology *166*, 167-172.

Guse, A., Mishima, M., and Glotzer, M. (2005). Phosphorylation of ZEN-4/MKLP1 by aurora B regulates completion of cytokinesis. Curr Biol *15*, 778-786.

Hagstrom, K.A., Holmes, V.F., Cozzarelli, N.R., and Meyer, B.J. (2002). C. elegans condensin promotes mitotic chromosome architecture, centromere organization, and sister chromatid segregation during mitosis and meiosis. Genes & Development *16*, 729-742.

Hardwick, K., Weiss, E., Luca, F.C., Winey, M., and Murray, A. (1996). Activation of the budding yeast spindle assembly checkpoint without mitotic spindle disruption. Science *273*, 953-956.

Hauf, S., Cole, R.W., LaTerra, S., Zimmer, C., Schnapp, G., Walter, R., Heckel, A., van Meel, J., Rieder, C.L., and Peters, J.M. (2003). The small molecule Hesperadin reveals a role for Aurora B in correcting kinetochore-microtubule attachment and in maintaining the spindle assembly checkpoint. J Cell Biol *161*, 281-294.

Hayashi, T. (2004). Mis16 and Mis18 Are Required for CENP-A Loading and Histone Deacetylation at Centromeres. Cell *118*, 715-729.

Hill, T.L. (1985). Theoretical problems related to the attachment of microtubules to kinetochores. Proc Natl Acad Sci USA *82*, 4404-4408.

Hofmann, C., Cheeseman, I., Goode, B.L., McDonald, K.L., Barnes, G., and Drubin, D. (1998). Saccharomyces cerevisiae Duo1p and Dam1p, novel proteins involved in mitotic spindle function. J Cell Biol *143*, 1029-1040.

Honda, R., Körner, R., and Nigg, E. (2003). Exploring the functional interactions between Aurora B, INCENP, and survivin in mitosis. Mol Biol Cell *14*, 3325-3341.

Howman, E.V., Fowler, K.J., Newson, A.J., Redward, S., MacDonald, A.C., Kalitsis, P., and Choo, K.H. (2000). Early disruption of centromeric chromatin organization in centromere protein A (Cenpa) null mice. Proc Natl Acad Sci USA *97*, 1148-1153.

Hoyt, M.A., Totis, L., and Roberts, B.T. (1991). S. cerevisiae genes required for cell cycle arrest in response to loss of microtubule function. Cell *66*, 507-517.

Hsu, J.Y., Sun, Z.W., Li, X., Reuben, M., Tatchell, K., Bishop, D.K., Grushcow, J.M., Brame, C.J., Caldwell, J.A., Hunt, D.F.*, et al.* (2000). Mitotic phosphorylation of histone H3 is governed by Ipl1/aurora kinase and Glc7/PP1 phosphatase in budding yeast and nematodes. Cell *102*, 279-291.

Huang, Z., Sucgang, R., Lin, Y., Shi, X., Boeke, J., and Pan, X. (2008). Plasmid-chromosome shuffling for non-deletion alleles in yeast. Nat Meth *5*, 167-169.

Hyman, A.A., Middleton, K., Centola, M., Mitchison, T.J., and Carbon, J. (1992). Microtubule-motor activity of a yeast centromere-binding protein complex. Nature *359*, 533-536.

Indjeian, V.B., and Murray, A.W. (2007). Budding yeast mitotic chromosomes have an intrinsic bias to biorient on the spindle. Curr Biol *17*, 1837-1846.

Indjeian, V.B., Stern, B.M., and Murray, A.W. (2005). The centromeric protein Sgo1 is required to sense lack of tension on mitotic chromosomes. Science *307*, 130-133.

Inoué, S., and Salmon, E.D. (1995). Force generation by microtubule assembly/disassembly in mitosis and related movements. Mol Biol Cell *6*, 1619-1640.

Janke, C., Ortiz, J., Tanaka, T., Lechner, J., and Schiebel, E. (2002). Four new subunits of the Dam1-Duo1 complex reveal novel functions in sister kinetochore biorientation. EMBO J *21*, 181-193.

Jansen, L.E., Black, B.E., Foltz, D.R., and Cleveland, D.W. (2007). Propagation of centromeric chromatin requires exit from mitosis. The Journal of Cell Biology *176*, 795-805.

Jeyaprakash, A., Klein, U., Lindner, D., Ebert, J., Nigg, E., and Conti, E. (2007). Structure of a Survivin–Borealin–INCENP Core Complex Reveals How Chromosomal Passengers Travel Together. Cell *131*, 271-285.

Joglekar, A., Bouck, D., Finley, K., Liu, X., Wan, Y., Berman, J., He, X., Salmon, E.D., and Bloom, K. (2008). Molecular architecture of the kinetochore-microtubule attachment site is conserved between point and regional centromeres. The Journal of Cell Biology *181*, 587-594.

Joglekar, A., Bouck, D., Molk, J., Bloom, K., and Salmon, E. (2006). Molecular architecture of a kinetochore–microtubule attachment site. Nat Cell Biol *8*, 581-585.

Johnson, V.L., Scott, M.I., Holt, S.V., Hussein, D., and Taylor, S.S. (2004). Bub1 is required for kinetochore localization of BubR1, Cenp-E, Cenp-F and Mad2, and chromosome congression. Journal of Cell Science *117*, 1577-1589.

Jones, M., He, X., Giddings, T.H., and Winey, M. (2001). Yeast Dam1p has a role at the kinetochore in assembly of the mitotic spindle. Proc Natl Acad Sci U S A *98*, 13675-13680.

Jones, M., Huneycutt, B., Pearson, C., Zhang, C., Morgan, G., Shokat, K., Bloom, K., and Winey, M. (2005). Chemical Genetics Reveals a Role for Mps1 Kinase in Kinetochore Attachment during Mitosis. Current Biology *15*, 160-165.

Kalitsis, P., MacDonald, A.C., Newson, A.J., Hudson, D.F., and Choo, K.H. (1998). Gene structure and sequence analysis of mouse centromere proteins A and C. Genomics *47*, 108-114.

Kallio, M., McCleland, M.L., Stukenberg, P., and Gorbsky, G. (2002). Inhibition of aurora B kinase blocks chromosome segregation, overrides the spindle checkpoint, and perturbs microtubule dynamics in mitosis. Curr Biol *12*, 900-905.

Kang, J., Cheeseman, I., Kallstrom, G., Velmurugan, S., Barnes, G., and Chan, C. (2001). Functional cooperation of Dam1, Ipl1, and the inner centromere protein (INCENP)-related protein Sli15 during chromosome segregation. J Cell Biol *155*, 763-774.

Kapoor, T., Lampson, M., Hergert, P., Cameron, L., Cimini, D., Salmon, E.D., McEwen, B.F., and Khodjakov, A. (2006). Chromosomes can congress to the metaphase plate before biorientation. Science *311*, 388-391.

Karpen, G.H., and Allshire, R.C. (1997). The case for epigenetic effects on centromere identity and function. Trends Genet *13*, 489-496.

Kawashima, S., Tsukahara, T., Langegger, M., Hauf, S., Kitajima, T., and Watanabe, Y. (2007). Shugoshin enables tension-generating attachment of kinetochores by loading Aurora to centromeres. Genes & Development *21*, 420-435.

Keith, K.C., and Fitzgerald-Hayes, M. (2000). CSE4 genetically interacts with the Saccharomyces cerevisiae centromere DNA elements CDE I and CDE II but not CDE III. Implications for the path of the centromere dna around a cse4p variant nucleosome. Genetics *156*, 973-981.

Kelly, A., Sampath, S., Maniar, T., Woo, E., Chait, B., and Funabiki, H. (2007). Chromosomal Enrichment and Activation of the Aurora B Pathway Are Coupled to Spatially Regulate Spindle Assembly. Developmental Cell *12*, 31-43.

Kim, J.H., Kang, J.S., and Chan, C.S. (1999). Sli15 associates with the ipl1 protein kinase to promote proper chromosome segregation in Saccharomyces cerevisiae. The Journal of Cell Biology *145*, 1381-1394.

Kimura, M., Matsuda, Y., Yoshioka, T., and Okano, Y. (1999). Cell cycle-dependent expression and centrosome localization of a third human aurora/Ipl1-related protein kinase, AIK3. J Biol Chem *274*, 7334-7340.

King, S.M., Hyams, J.S., and Luba, A. (1982a). Absence of microtubule sliding and an analysis of spindle formation and elongation in isolated mitotic spindles from the yeast Saccharomyces cerevisiae. The Journal of Cell Biology *94*, 341-349.

King, S.M., Hyams, J.S., and Luba, A. (1982b). Ultrastructure of mitotic spindles isolated from a cell division cycle mutant of the yeast, Saccharomyces cerevisiae. Eur J Cell Biol *28*, 98-102.

Kingsbury, J., and Koshland, D. (1991). Centromere-dependent binding of yeast minichromosomes to microtubules in vitro. Cell *66*, 483-495.

Kitagawa, K., Skowyra, D., Elledge, S.J., Harper, J.W., and Hieter, P. (1999). SGT1 encodes an essential component of the yeast kinetochore assembly pathway and a novel subunit of the SCF ubiquitin ligase complex. Molecular Cell *4*, 21-33.

Kitajima, T., Sakuno, T., Ishiguro, K., Iemura, S., Natsume, T., Kawashima, S., and Watanabe, Y. (2006). Shugoshin collaborates with protein phosphatase 2A to protect cohesin. Nature *441*, 46-52.

Kitamura, E., Tanaka, K., Kitamura, Y., and Tanaka, T. (2007). Kinetochore microtubule interaction during S phase in Saccharomyces cerevisiae. Genes & Development *21*, 3319-3330.

Klein, U.R., Nigg, E., and Gruneberg, U. (2006). Centromere targeting of the chromosomal passenger complex requires a ternary subcomplex of Borealin, Survivin, and the N-terminal domain of INCENP. Mol Biol Cell *17*, 2547-2558.

Kline-Smith, S., Sandall, S., and Desai, A. (2005). Kinetochore spindle microtubule interactions during mitosis. Current Opinion in Cell Biology *17*, 35-46.

Koshland, D.E., Mitchison, T.J., and Kirschner, M.W. (1988). Polewards chromosome movement driven by microtubule depolymerization in vitro. Nature *331*, 499-504.

Kotwaliwale, C.V., Frei, S.B., Stern, B.M., and Biggins, S. (2007). A pathway containing the Ipl1/aurora protein kinase and the spindle midzone protein Ase1 regulates yeast spindle assembly. Developmental Cell *13*, 433-445.

Kufer, T.A., Sillje, H.H., Korner, R., Gruss, O.J., Meraldi, P., and Nigg, E. (2002). Human TPX2 is required for targeting Aurora-A kinase to the spindle. J Cell Biol *158*, 617-623.

Kunitoku, N., Sasayama, T., Marumoto, T., Zhang, D., Honda, S., Kobayashi, O., Hatakeyama, K., Ushio, Y., Saya, H., and Hirota, T. (2003). CENP-A phosphorylation by Aurora-A in prophase is required for enrichment of Aurora-B at inner centromeres and for kinetochore function. Developmental Cell *5*, 853-864.

Kuo, S.C. (2001). Using optics to measure biological forces and mechanics. Traffic *2*, 757-763.

Lampson, M., and Kapoor, T. (2005). The human mitotic checkpoint protein BubR1 regulates chromosome-spindle attachments. Nat Cell Biol *7*, 93-98.

Lampson, M., Renduchitala, K., Khodjakov, A., and Kapoor, T. (2004). Correcting improper chromosome–spindle attachments during cell division. Nat Cell Biol *6*, 6-237.

Lan, W., Zhang, X., Klinesmith, S., Rosasco, S., Barrettwilt, G., Shabanowitz, J., Hunt, D., Walczak, C., and Stukenberg, P. (2004). Aurora B Phosphorylates Centromeric MCAK and Regulates Its Localization and Microtubule Depolymerization Activity. Current Biology *14*, 273-286.

Lang, M.J., Asbury, C.L., Shaevitz, J.W., and Block, S.M. (2002). An automated two-dimensional optical force clamp for single molecule studies. Biophys J *83*, 491-501.

Lechner, J., and Carbon, J. (1991). A 240 kd multisubunit protein complex, CBF3, is a major component of the budding yeast centromere. Cell *64*, 717-725.

Lee, Y.T., Jacob, J., Michowski, W., Nowotny, M., Kuznicki, J., and Chazin, W.J. (2004). Human Sgt1 binds HSP90 through the CHORD-Sgt1 domain and not the tetratricopeptide repeat domain. J Biol Chem *279*, 16511-16517.

Lens, S., Vader, G., and Medema, R. (2006). The case for Survivin as mitotic regulator. Current Opinion in Cell Biology *18*, 616-622.

Lens, S.M., and Medema, R.H. (2003). The survivin/Aurora B complex: its role in coordinating tension and attachment. Cell Cycle *2*, 507-510.

Li, F., Flanary, P.L., Altieri, D.C., and Dohlman, H.G. (2000). Cell division regulation by BIR1, a member of the inhibitor of apoptosis family in yeast. J Biol Chem *275*, 6707-6711.

Li, R., and Murray, A.W. (1991). Feedback control of mitosis in budding yeast. Cell *66*, 519-531.

Li, X., and Nicklas, R.B. (1995). Mitotic forces control a cell-cycle checkpoint. Nature *373*, 630-632.

Lingelbach, L.B., and Kaplan, K.B. (2004). The interaction between Sgt1p and Skp1p is regulated by HSP90 chaperones and is required for proper CBF3 assembly. Mol Cell Biol *24*, 8938-8950.

Lipp, J., Hirota, T., Poser, I., and Peters, J. (2007). Aurora B controls the association of condensin I but not condensin II with mitotic chromosomes. Journal of Cell Science *120*, 1245-1255.

MacCallum, D.E., Losada, A., Kobayashi, R., and Hirano, T. (2002). ISWI remodeling complexes in Xenopus egg extracts: identification as major chromosomal components that are regulated by INCENP-aurora B. Mol Biol Cell *13*, 25-39.

Mackay, A.M., Ainsztein, A.M., Eckley, D.M., and Earnshaw, W.C. (1998). A dominant mutant of inner centromere protein (INCENP), a chromosomal protein, disrupts prometaphase congression and cytokinesis. The Journal of Cell Biology *140*, 991-1002.

Maddox, P.S., Hyndman, F., Monen, J., Oegema, K., and Desai, A. (2007). Functional genomics identifies a Myb domain-containing protein family required for assembly of CENP-A chromatin. The Journal of Cell Biology *176*, 757-763.

Maddox, P.S., Oegema, K., Desai, A., and Cheeseman, I. (2004). "Holo"er than thou: chromosome segregation and kinetochore function in C. elegans. Chromosome Res *12*, 641-653.

Maiato, H., DeLuca, J., Salmon, E.D., and Earnshaw, W. (2004). The dynamic kinetochore-microtubule interface. Journal of Cell Science *117*, 5461-5477.

Maure, J. (2007). Mps1 Kinase Promotes Sister-Kinetochore Bi-orientation by a Tension-Dependent Mechanism. Current Biology *17*, 2175-2182.

Mcainsh, A., Tytell, J., and Sorger, P. (2003). STRUCTURE, FUNCTION, AND REGULATION OF BUDDING YEAST KINETOCHORES. Annu Rev Cell Dev Biol *19*, 519-539.

McEwen, B.F., Dong, Y., and VandenBeldt, K.J. (2007). Using electron microscopy to understand functional mechanisms of chromosome alignment on the mitotic spindle. Methods Cell Biol *79*, 259-293.

McGrew, J., Diehl, B., and Fitzgerald-Hayes, M. (1986). Single base-pair mutations in centromere element III cause aberrant chromosome segregation in Saccharomyces cerevisiae. Mol Cell Biol *6*, 530-538.

Measday, V., Hailey, D.W., Pot, I., Givan, S.A., Hyland, K.M., Cagney, G., Fields, S., Davis, T.N., and Hieter, P. (2002). Ctf3p, the Mis6 budding yeast homolog, interacts with Mcm22p and Mcm16p at the yeast outer kinetochore. Genes Dev *16*, 101-113.

Mellor, J., Jiang, W., Funk, M., Rathjen, J., Barnes, C.A., Hinz, T., Hegemann, J.H., and Philippsen, P. (1990). CPF1, a yeast protein which functions in centromeres and promoters. EMBO J *9*, 4017-4026.

Meluh, P.B., Yang, P., Glowczewski, L., Koshland, D., and Smith, M.M. (1998). Cse4p is a component of the core centromere of Saccharomyces cerevisiae. Cell *94*, 607-613.

Meraldi, P., Honda, R., and Nigg, E. (2004). Aurora kinases link chromosome segregation and cell division to cancer susceptibility. Curr Opin Genet Dev *14*, 29-36.

Meraldi, P., Mcainsh, A., Rheinbay, E., and Sorger, P. (2006). SorgerPhylogentic. Genome Biol *7*, R23.

Meraldi, P., and Sorger, P. (2005). A dual role for Bub1 in the spindle checkpoint and chromosome congression. EMBO J *24*, 1621-1633.

Minoshima, Y., Kawashima, T., Hirose, K., Tonozuka, Y., Kawajiri, A., Bao, Y.C., Deng, X., Tatsuka, M., Narumiya, S., May, W.S.*, et al.* (2003). Phosphorylation by aurora B converts MgcRacGAP to a RhoGAP during cytokinesis. Developmental Cell *4*, 549-560.

Miranda, J.J., King, D.S., and Harrison, S.C. (2007). Protein arms in the kinetochore-microtubule interface of the yeast DASH complex. Mol Biol Cell *18*, 2503-2510.

Mishima, M., Kaitna, S., and Glotzer, M. (2002). Central spindle assembly and cytokinesis require a kinesin-like protein/RhoGAP complex with microtubule bundling activity. Developmental Cell *2*, 41-54.

Mitchison, T., and Kirschner, M. (1984). Dynamic instability of microtubule growth. Nature *312*, 237-242.

Mitchison, T.J., and Kirschner, M.W. (1985a). Properties of the kinetochore in vitro. I. Microtubule nucleation and tubulin binding. The Journal of Cell Biology *101*, 755-765.

Mitchison, T.J., and Kirschner, M.W. (1985b). Properties of the kinetochore in vitro. II. Microtubule capture and ATP-dependent translocation. The Journal of Cell Biology *101*, 766-777.

Mizuguchi, G., Xiao, H., Wisniewski, J., Smith, M., and Wu, C. (2007). Nonhistone Scm3 and Histones CenH3-H4 Assemble the Core of Centromere-Specific Nucleosomes. Cell *129*, 1153-1164.

Monier, K., Mouradian, S., and Sullivan, K.F. (2007). DNA methylation promotes Aurora-B-driven phosphorylation of histone H3 in chromosomal subdomains. Journal of Cell Science *120*, 101-114.

Montpetit, B. (2006). Sumoylation of the budding yeast kinetochore protein Ndc10 is required for Ndc10 spindle localization and regulation of anaphase spindle elongation. The Journal of Cell Biology *174*, 653-663.

Morrow, C. (2005). Bub1 and aurora B cooperate to maintain BubR1-mediated inhibition of APC/CCdc20. Journal of Cell Science *118*, 3639-3652.

Mountzios, G., Terpos, E., and Dimopoulos, M.A. (2008). Aurora kinases as targets for cancer therapy. Cancer Treat Rev *34*, 175-182.

Murata-Hori, M., and Wang, Y.L. (2002). Both midzone and astral microtubules are involved in the delivery of cytokinesis signals: insights from the mobility of aurora B. The Journal of Cell Biology *159*, 45-53.

Murnion, M.E., Adams, R.R., Callister, D.M., Allis, C.D., Earnshaw, W.C., and Swedlow, J.R. (2001). Chromatin-associated protein phosphatase 1 regulates aurora-B and histone H3 phosphorylation. J Biol Chem *276*, 26656-26665.

Murphy, M.R., Fowlkes, D.M., and Fitzgerald-Hayes, M. (1991). Analysis of centromere function in Saccharomyces cerevisiae using synthetic centromere mutants. Chromosoma *101*, 189-197.

Musacchio, A., and Salmon, E. (2007). The spindle-assembly checkpoint in space and time. Nat Rev Mol Cell Biol *8*, 379-393.

Mythreye, K. (2003). Differential kinetochore protein requirements for establishment versus propagation of centromere activity in Saccharomyces cerevisiae. The Journal of Cell Biology *160*, 833-843.

Nasmyth, K. (2005). How Do so Few Control so Many? Cell *120*, 739-746.

Ng, R., Ness, J., and Carbon, J. (1986). Structural studies on centromeres in the yeast Saccharomyces cerevisiae. Basic Life Sci *40*, 479-492.

Nguyen, H.G., and Ravid, K. (2006). Tetraploidy/aneuploidy and stem cells in cancer promotion: The role of chromosome passenger proteins. J Cell Physiol *208*, 12-22.

Nicklas, R.B., and Koch, C.A. (1969). Chromosome micromanipulation. 3. Spindle fiber tension and the reorientation of mal-oriented chromosomes. The Journal of Cell Biology *43*, 40-50.

Niedenthal, R.K., Sen-Gupta, M., Wilmen, A., and Hegemann, J.H. (1993). Cpf1 protein induced bending of yeast centromere DNA element I. Nucleic Acids Res *21*, 4726-4733.

Norden, C., Mendoza, M., Dobbelaere, J., Kotwaliwale, C.V., Biggins, S., and Barral, Y. (2006). The NoCut pathway links completion of cytokinesis to spindle midzone function to prevent chromosome breakage. Cell *125*, 85-98.

Oegema, K., Desai, A., Rybina, S., Kirkham, M., and Hyman, A. (2001). Functional analysis of kinetochore assembly in Caenorhabditis elegans. J Cell Biol *153*, 1209-1226.

Ohi, R., Sapra, T., Howard, J., and Mitchison, T. (2004). Differentiation of cytoplasmic and meiotic spindle assembly MCAK functions by Aurora B-dependent phosphorylation. Mol Biol Cell *15*, 2895-2906.

Ohzeki, J., Nakano, M., Okada, T., and Masumoto, H. (2002). CENP-B box is required for de novo centromere chromatin assembly on human alphoid DNA. The Journal of Cell Biology *159*, 765-775.

Okada, M., Cheeseman, I., Hori, T., Okawa, K., McLeod, I.X., Yates, J., Desai, A., and Fukagawa, T. (2006). The CENP-H-I complex is required for the efficient incorporation of newly synthesized CENP-A into centromeres. Nat Cell Biol *8*, 446-457.

Ortiz, J., Stemmann, O., Rank, S., and Lechner, J. (1999). A putative protein complex consisting of Ctf19, Mcm21, and Okp1 represents a missing link in the budding yeast kinetochore. Genes & Development *13*, 1140-1155.

Pearson, C., Maddox, P., Zarzar, T.R., Salmon, E., and Bloom, K. (2003). Yeast kinetochores do not stabilize Stu2p-dependent spindle microtubule dynamics. Mol Biol Cell *14*, 4181-4195.

Pereira, G. (2003). Separase Regulates INCENP-Aurora B Anaphase Spindle Function Through Cdc14. Science *302*, 2120-2124.

Peterson, J.B., and Ris, H. (1976). Electron-microscopic study of the spindle and chromosome movement in the yeast Saccharomyces cerevisiae. Journal of Cell Science *22*, 219-242.

Pietrasanta, L.I., Thrower, D., Hsieh, W., Rao, S., Stemmann, O., Lechner, J., Carbon, J., and Hansma, H. (1999). Probing the Saccharomyces cerevisiae centromeric DNA (CEN DNA)-binding factor 3 (CBF3) kinetochore complex by using atomic force microscopy. Proc Natl Acad Sci USA *96*, 3757-3762.

Pinsky, B., and Biggins, S. (2005). The spindle checkpoint: tension versus attachment. Trends in Cell Biology *15*, 486-493.

Pinsky, B., Kotwaliwale, C.V., Tatsutani, S.Y., Breed, C.A., and Biggins, S. (2006a). Glc7/protein phosphatase 1 regulatory subunits can oppose the Ipl1/aurora protein kinase by redistributing Glc7. Mol Cell Biol *26*, 2648-2660.

Pinsky, B., Kung, C., Shokat, K., and Biggins, S. (2006b). The Ipl1-Aurora protein kinase activates the spindle checkpoint by creating unattached kinetochores. Nat Cell Biol *8*, 78-83.

Pinsky, B., Tatsutani, S.Y., Collins, K.A., and Biggins, S. (2003). An Mtw1 complex promotes kinetochore biorientation that is monitored by the Ipl1/Aurora protein kinase. Developmental Cell *5*, 735-745.

Rangasamy, D., Berven, L., Ridgway, P., and Tremethick, D.J. (2003). Pericentric heterochromatin becomes enriched with H2A.Z during early mammalian development. EMBO J *22*, 1599-1607.

Riedel, C., Katis, V., Katou, Y., Mori, S., Itoh, T., Helmhart, W., Gálová, M., Petronczki, M., Gregan, J., Cetin, B.*, et al.* (2006). Protein phosphatase 2A protects centromeric sister chromatid cohesion during meiosis I. Nature *441*, 53-61.

Rieder, C.L., and Alexander, S.P. (1990). Kinetochores are transported poleward along a single astral microtubule during chromosome attachment to the spindle in newt lung cells. The Journal of Cell Biology *110*, 81-95.

Rodrigo-Brenni, M.C., Thomas, S., Bouck, D., and Kaplan, K.B. (2004). Sgt1p and Skp1p modulate the assembly and turnover of CBF3 complexes required for proper kinetochore function. Mol Biol Cell *15*, 3366-3378.

Romano, A. (2003). CSC-1: a subunit of the aurora b kinase complex that binds to the survivin-like protein BIR-1 and the incenp-like protein ICP-1. The Journal of Cell Biology *161*, 229-236.

Rosasco-Nitcher, S., Lan, W., Khorasanizadeh, S., and Stukenberg, P. (2008). Centromeric Aurora-B Activation Requires TD-60, Microtubules, and Substrate Priming Phosphorylation. Science *319*, 469-472.

Ruchaud, S., Carmena, M., and Earnshaw, W. (2007). Chromosomal passengers: conducting cell division. Nat Rev Mol Cell Biol *8*, 798-812.

Sampath, S., Ohi, R., Leismann, O., Salic, A., Pozniakovski, A., and Funabiki, H. (2004). The Chromosomal Passenger Complex Is Required for Chromatin-Induced Microtubule Stabilization and Spindle Assembly. Cell *118*, 187-202.

Sanchez-Perez, I., Renwick, S., Crawley, K., Karig, I., Buck, V., Meadows, J., Franco-Sanchez, A., Fleig, U., Toda, T., and Millar, J. (2005). The DASH

complex and Klp5/Klp6 kinesin coordinate bipolar chromosome attachment in fission yeast. EMBO J *24*, 2931-2943.

Sandall, S., Severin, F., McLeod, I.X., Yates, J., Oegema, K., Hyman, A., and Desai, A. (2006). A Bir1-Sli15 complex connects centromeres to microtubules and is required to sense kinetochore tension. Cell *127*, 1179-1191.

Sasai, K., Katayama, H., Stenoien, D.L., Fujii, S., Honda, R., Kimura, M., Okano, Y., Tatsuka, M., Suzuki, F., Nigg, E.*, et al.* (2004). Aurora-C kinase is a novel chromosomal passenger protein that can complement Aurora-B kinase function in mitotic cells. Cell Motil Cytoskeleton *59*, 249-263.

Sassoon, I., Severin, F.F., Andrews, P.D., Taba, M.R., Kaplan, K.B., Ashford, A.J., Stark, M.J., Sorger, P.K., and Hyman, A.A. (1999). Regulation of Saccharomyces cerevisiae kinetochores by the type 1 phosphatase Glc7p. Genes & Development *13*, 545-555.

Schmidt, M., Budirahardja, Y., Klompmaker, R., and Medema, R. (2005). Ablation of the spindle assembly checkpoint by a compound targeting Mps1. EMBO Rep *6*, 866-872.

Schuh, M., Lehner, C.F., and Heidmann, S. (2007). Incorporation of Drosophila CID/CENP-A and CENP-C into centromeres during early embryonic anaphase. Curr Biol *17*, 237-243.

Schumacher, J.M., Golden, A., and Donovan, P.J. (1998). AIR-2: An Aurora/Ipl1-related protein kinase associated with chromosomes and midbody microtubules is required for polar body extrusion and cytokinesis in Caenorhabditis elegans embryos. The Journal of Cell Biology *143*, 1635-1646.

Sessa, F., Mapelli, M., Ciferri, C., Tarricone, C., Areces, L., Schneider, T., Stukenberg, P., and Musacchio, A. (2005). Mechanism of Aurora B Activation by INCENP and Inhibition by Hesperadin. Molecular Cell *18*, 379-391.

Severin, F., Kaplan, K., Sorger, P., and Hyman, T. (1999). In vitro assays for studying Saccharomyces cerevisiae kinetochore activity. Methods Cell Biol *61*, 145-153.

Severin, F.F., Sorger, P.K., and Hyman, A.A. (1997). Kinetochores distinguish GTP from GDP forms of the microtubule lattice. Nature *388*, 888-891.

Sorger, P.K., Severin, F.F., and Hyman, A.A. (1994). Factors required for the binding of reassembled yeast kinetochores to microtubules in vitro. The Journal of Cell Biology *127*, 995-1008.

Steensgaard, P., Garrè, M., Muradore, I., Transidico, P., Nigg, E., Kitagawa, K., Earnshaw, W., Faretta, M., and Musacchio, A. (2004). Sgt1 is required for human kinetochore assembly. EMBO Rep *5*, 626-631.

Stemmann, O., Neidig, A., Köcher, T., Wilm, M., and Lechner, J. (2002). Hsp90 enables Ctf13p/Skp1p to nucleate the budding yeast kinetochore. Proc Natl Acad Sci USA *99*, 8585-8590.

Stern, B.M., and Murray, A.W. (2001). Lack of tension at kinetochores activates the spindle checkpoint in budding yeast. Curr Biol *11*, 1462-1467.

Stoepel, J., Ottey, M.A., Kurischko, C., Hieter, P., and Luca, F.C. (2005). The mitotic exit network Mob1p-Dbf2p kinase complex localizes to the nucleus and regulates passenger protein localization. Mol Biol Cell *16*, 5465-5479.

Stoler, S., Keith, K.C., Curnick, K.E., and Fitzgerald-Hayes, M. (1995). A mutation in CSE4, an essential gene encoding a novel chromatin-associated protein in yeast, causes chromosome nondisjunction and cell cycle arrest at mitosis. Genes Dev *9*, 573-586.

Stoler, S., Rogers, K., Weitze, S., Morey, L., Fitzgerald-Hayes, M., and Baker, R.E. (2007). Scm3, an essential Saccharomyces cerevisiae centromere protein required for G2/M progression and Cse4 localization. Proc Natl Acad Sci USA *104*, 10571-10576.

Sullivan, B.A., Blower, M.D., and Karpen, G.H. (2001). Determining centromere identity: cyclical stories and forking paths. Nat Rev Genet *2*, 584-596.

Sumara, I., Giménez-Abián, J.F., Gerlich, D., Hirota, T., Kraft, C., de la Torre, C., Ellenberg, J., and Peters, J. (2004). Roles of polo-like kinase 1 in the assembly of functional mitotic spindles. Curr Biol *14*, 1712-1722.

Takahashi, K., Chen, E.S., and Yanagida, M. (2000). Requirement of Mis6 centromere connector for localizing a CENP-A-like protein in fission yeast. Science *288*, 2215-2219.

Takemoto, A., Murayama, A., Katano, M., Urano, T., Furukawa, K., Yokoyama, S., Yanagisawa, J., Hanaoka, F., and Kimura, K. (2007). Analysis of the role of Aurora B on the chromosomal targeting of condensin I. Nucleic Acids Res *35*, 2403-2412.

Tanaka, K., Kitamura, E., Kitamura, Y., and Tanaka, T. (2007). Molecular mechanisms of microtubule-dependent kinetochore transport toward spindle poles. The Journal of Cell Biology *178*, 269-281.

Tanaka, K., Mukae, N., Dewar, H., van Breugel, M., James, E.K., Prescott, A.R., Antony, C., and Tanaka, T. (2005a). Molecular mechanisms of kinetochore capture by spindle microtubules. Nature *434*, 987-994.

Tanaka, T. (2008). Bi-orienting chromosomes: acrobatics on the mitotic spindle. Chromosoma, 13.

Tanaka, T., and Desai, A. (2008). Kinetochore–microtubule interactions: the means to the end. Current Opinion in Cell Biology, 11.

Tanaka, T., Rachidi, N., Janke, C., Pereira, G., Galova, M., Schiebel, E., Stark, M.J., and Nasmyth, K. (2002). Evidence that the Ipl1-Sli15 (Aurora kinase-INCENP) complex promotes chromosome bi-orientation by altering kinetochore-spindle pole connections. Cell *108*, 317-329.

Tanaka, T., Stark, M.J., and Tanaka, K. (2005b). Kinetochore capture and bi-orientation on the mitotic spindle. Nat Rev Mol Cell Biol *6*, 929-942.

Tang, Z., Shu, H., Qi, W., Mahmood, N.A., Mumby, M.C., and Yu, H. (2006). PP2A is required for centromeric localization of Sgo1 and proper chromosome segregation. Developmental Cell *10*, 575-585.

Tarnawski, A., Pai, R., Chiou, S.K., Chai, J., and Chu, E.C. (2005). Rebamipide inhibits gastric cancer growth by targeting survivin and Aurora-B. Biochem Biophys Res Commun *334*, 207-212.

Tatsuka, M., Katayama, H., Ota, T., Tanaka, T., Odashima, S., Suzuki, F., and Terada, Y. (1998). Multinuclearity and increased ploidy caused by overexpression of the aurora- and Ipl1-like midbody-associated protein mitotic kinase in human cancer cells. Cancer Res *58*, 4811-4816.

Terada, Y., Tatsuka, M., Suzuki, F., Yasuda, Y., Fujita, S., and Otsu, M. (1998). AIM-1: a mammalian midbody-associated protein required for cytokinesis. EMBO J *17*, 667-676.

Thomas, S., and Kaplan, K.B. (2007). A Bir1p Sli15p kinetochore passenger complex regulates septin organization during anaphase. Mol Biol Cell *18*, 3820-3834.

Trinkle-Mulcahy, L., Andrews, P.D., Wickramasinghe, S., Sleeman, J., Prescott, A., Lam, Y.W., Lyon, C., Swedlow, J.R., and Lamond, A.I. (2003). Time-lapse imaging reveals dynamic relocalization of PP1gamma throughout the mammalian cell cycle. Mol Biol Cell *14*, 107-117.

Tsai, M., Wiese, C., Cao, K., Martin, O., Donovan, P., Ruderman, J., Prigent, C., and Zheng, Y. (2003). A Ran signalling pathway mediated by the mitotic kinase Aurora A in spindle assembly. Nat Cell Biol *5*, 242-248.

Tulu, U., Fagerstrom, C., Ferenz, N., and Wadsworth, P. (2006). Molecular Requirements for Kinetochore-Associated Microtubule Formation in Mammalian Cells. Current Biology *16*, 536-541.

Uren, A.G., Beilharz, T., O'Connell, M.J., Bugg, S.J., van Driel, R., Vaux, D.L., and Lithgow, T. (1999). Role for yeast inhibitor of apoptosis (IAP)-like proteins in cell division. Proc Natl Acad Sci USA *96*, 10170-10175.

Vader, G., Cruijsen, C.W., van Harn, T., Vromans, M.J., Medema, R., and Lens, S. (2007). The chromosomal passenger complex controls spindle checkpoint function independent from its role in correcting microtubule kinetochore interactions. Mol Biol Cell *18*, 4553-4564.

Vader, G., Kauw, J., Medema, R., and Lens, S. (2006). Survivin mediates targeting of the chromosomal passenger complex to the centromere and midbody. EMBO Rep *7*, 85-92.

Vagnarelli, P., and Earnshaw, W. (2004). Chromosomal passengers: the four-dimensional regulation of mitotic events. Chromosoma *113*, 211-222.

van Breugel, M., Drechsel, D., and Hyman, A. (2003). Stu2p, the budding yeast member of the conserved Dis1/XMAP215 family of microtubule-associated proteins is a plus end-binding microtubule destabilizer. J Cell Biol *161*, 359-369.

Vanoosthuyse, V., and Hardwick, K. (2005). Bub1 and the multilayered inhibition of Cdc20–APC/C in mitosis. Trends in Cell Biology *15*, 231-233.

Vong, Q.P., Cao, K., Li, H.Y., Iglesias, P.A., and Zheng, Y. (2005). Chromosome alignment and segregation regulated by ubiquitination of survivin. Science *310*, 1499-1504.

Wadsworth, P., and Khodjakov, A. (2004). E pluribus unum: towards a universal mechanism for spindle assembly. Trends in Cell Biology *14*, 413-419.

Wang, H., Ramey, V.H., Westermann, S., Leschziner, A.E., Welburn, J.P., Nakajima, Y., Drubin, D., Barnes, G., and Nogales, E. (2007). Architecture of the Dam1 kinetochore ring complex and implications for microtubule-driven assembly and force-coupling mechanisms. Nat Struct Mol Biol.

Washburn, M., Wolters, D., and Yates, J.R. (2001). Large-scale analysis of the yeast proteome by multidimensional protein identification technology. Nat Biotechnol *19*, 242-247.

Weaver, B.A., and Cleveland, D.W. (2007). Aneuploidy: instigator and inhibitor of tumorigenesis. Cancer Res *67*, 10103-10105.

Weaver, B.A., Silk, A.D., Montagna, C., Verdier-Pinard, P., and Cleveland, D.W. (2007). Aneuploidy acts both oncogenically and as a tumor suppressor. Cancer Cell *11*, 25-36.

Wei, R., Al-Bassam, J., and Harrison, S. (2007). The Ndc80/HEC1 complex is a contact point for kinetochore-microtubule attachment. Nat Struct Mol Biol *14*, 54-59.

Westermann, S., Avilasakar, A., Wang, H., Niederstrasser, H., Wong, J., Drubin, D., Nogales, E., and Barnes, G. (2005). Formation of a Dynamic Kinetochore- Microtubule Interface through Assembly of the Dam1 Ring Complex. Molecular Cell *17*, 277-290.

Westermann, S., Drubin, D., and Barnes, G. (2007). Structures and functions of yeast kinetochore complexes. Annu Rev Biochem *76*, 563-591.

Westermann, S., Wang, H., Avila-Sakar, A., Drubin, D., Nogales, E., and Barnes, G. (2006). The Dam1 kinetochore ring complex moves processively on depolymerizing microtubule ends. Nature *440*, 565-569.

Wheatley, S. (2001). INCENP Binds Directly to Tubulin and Requires Dynamic Microtubules to Target to the Cleavage Furrow. Experimental Cell Research *262*, 122-127.

Wheatley, S., Carvalho, A., Vagnarelli, P., and Earnshaw, W. (2001). INCENP is required for proper targeting of Survivin to the centromeres and the anaphase spindle during mitosis. Curr Biol *11*, 886-890.

Widlund, P., Lyssand, J.S., Anderson, S., Niessen, S., Yates, J., and Davis, T. (2006). Phosphorylation of the chromosomal passenger protein Bir1 is required for localization of Ndc10 to the spindle during anaphase and full spindle elongation. Mol Biol Cell *17*, 1065-1074.

Wigge, P.A., Jensen, O.N., Holmes, S., Souès, S., Mann, M., and Kilmartin, J.V. (1998). Analysis of the Saccharomyces spindle pole by matrix-assisted laser desorption/ionization (MALDI) mass spectrometry. The Journal of Cell Biology *141*, 967-977.

Wigge, P.A., and Kilmartin, J.V. (2001). The Ndc80p complex from Saccharomyces cerevisiae contains conserved centromere components and has a function in chromosome segregation. J Cell Biol *152*, 349-360.

Wilson, E.B. *The Cell in Development and Heredity*. MacMillan. 3rd ed. New York, 1928.

Winey, M., Mamay, C.L., O'Toole, E.T., Mastronarde, D.N., Giddings, T.H., McDonald, K.L., and McIntosh, J.R. (1995). Three-dimensional ultrastructural analysis of the Saccharomyces cerevisiae mitotic spindle. J Cell Biol *129*, 1601-1615.

Yan, X., Cao, L., Li, Q., Wu, Y., Zhang, H., Saiyin, H., Liu, X., Zhang, X., Shi, Q., and Yu, L. (2005). Aurora C is directly associated with Survivin and required for cytokinesis. Genes Cells *10*, 617-626.

Yeh, E., Haase, J., Paliulis, L.V., Joglekar, A., Bond, L., Bouck, D., Salmon, E.D., and Bloom, K. (2008). Pericentric chromatin is organized into an intramolecular loop in mitosis. Curr Biol *18*, 81-90.

Yoon, H.J., and Carbon, J. (1999). Participation of Bir1p, a member of the inhibitor of apoptosis family, in yeast chromosome segregation events. Proc Natl Acad Sci U S A *96*, 13208-13213.

Zeitlin, S.G., Shelby, R.D., and Sullivan, K.F. (2001). CENP-A is phosphorylated by Aurora B kinase and plays an unexpected role in completion of cytokinesis. The Journal of Cell Biology *155*, 1147-1157.

Zhang, K., Lin, W., Latham, J., Riefler, G., Schumacher, J., Chan, C., Tatchell, K., Hawke, D., Kobayashi, R., and Dent, S. (2005). The Set1 Methyltransferase Opposes Ipl1 Aurora Kinase Functions in Chromosome Segregation. Cell *122*, 723-734.